



HAL
open science

Cellular characterization of extracellular vesicle uptake and content delivery within acceptor cells

Émeline Bonsergent

► **To cite this version:**

Émeline Bonsergent. Cellular characterization of extracellular vesicle uptake and content delivery within acceptor cells. Cellular Biology. Université Paris Cité, 2021. English. NNT : 2021UNIP5138 . tel-04512912

HAL Id: tel-04512912

<https://theses.hal.science/tel-04512912>

Submitted on 20 Mar 2024

HAL is a multi-disciplinary open access archive for the deposit and dissemination of scientific research documents, whether they are published or not. The documents may come from teaching and research institutions in France or abroad, or from public or private research centers.

L'archive ouverte pluridisciplinaire **HAL**, est destinée au dépôt et à la diffusion de documents scientifiques de niveau recherche, publiés ou non, émanant des établissements d'enseignement et de recherche français ou étrangers, des laboratoires publics ou privés.

Université de Paris

École doctorale Frontières de l'Innovation en Recherche et Éducation –
ED n°474

Immunité et Cancer, Institut Curie, INSERM, U932
Laboratoire Matière et Systèmes Complexes, CNRS, UMR7057

Cellular characterization of extracellular vesicle uptake and content delivery

Par **Émeline BONSERGENT**

Thèse de doctorat de **BIOLOGIE CELLULAIRE ET BIOLOGIE DU
DEVELOPPEMENT**

Dirigée par **Grégory LAVIEU**

Présentée et soutenue publiquement le 30 septembre 2021

Devant un jury composé de :

Julie GAVARD – DR – Université de Nantes – Rapporteur

Cédric DELEVOYE – DR – Sorbonne Université – Rapporteur

Catherine JACKSON – DR – Université de Paris – Examinatrice

Grégory LAVIEU – CR – Université de Paris – Directeur de thèse



TITRE : Caractérisation cellulaire de la prise en charge des vésicules extracellulaires et de la libération cytosolique de leur contenu dans les cellules receveuses

RESUME : Les vésicules extracellulaires (EVs) sont des particules sécrétées par toutes les cellules, qui permettent le transfert de molécules biologiques (protéines, lipides, acides nucléiques) d'une cellule donneuse à une cellule receveuse. Ce rôle de transporteurs les rend intéressantes à la fois à un niveau fondamental pour comprendre leurs implications dans de nombreux processus physio/pathologiques, mais aussi à un niveau thérapeutique puisqu'elles représentent une opportunité de vecteurs pour des thérapies ciblées et personnalisées. Cependant, avant d'atteindre de telles applications, une caractérisation cellulaire et moléculaire de leur prise en charge par les cellules receveuses est nécessaire.

Lors de cette thèse, deux études basées sur des approches *in vitro* et *in cellulo* ont été mises en place pour mieux comprendre ce processus. Des EVs, dont le contenu a été marqué, ont été incubées soit avec des membranes plasmiques purifiées, soit avec des cellules en culture. Le contenu des EVs a été suivi au cours de cette incubation pour quantifier quelle portion de ces vésicules peut être associée aux cellules receveuses, internalisées par celles-ci et principalement quelle quantité de contenu sera libéré dans le cytosol de ces cellules.

Ces méthodologies ont permis d'obtenir une preuve formelle de l'échange intercellulaire de protéines médié par les EVs, ainsi que la première quantification de la prise en charge de ces EVs par des cellules HeLa (1% de prise en charge spontanée en 1 heure), et de la libération de leur contenu dans le cytosol receveur (30% du contenu des vésicules prises en charge). Cette prise en charge ne semble pas dépendre d'un récepteur spécifique. Les EVs peuvent être internalisées dans des compartiments endo/lysosomaux, où s'effectue vraisemblablement la libération du contenu vésiculaire dans le cytosol des cellules receveuses. En effet, cette libération nécessite une acidification des endosomes, la présence de protéines à la surface des EVs et de la membrane receveuse, et probablement une fusion membranaire.

Ces résultats ouvrent la voie pour une caractérisation moléculaire de ce processus, afin d'identifier les acteurs clés de la prise en charge des EVs par les cellules receveuses.

MOTS CLEFS : Vésicules extracellulaires, Trafic intracellulaire, Libération de contenu vésiculaire, Fusion membranaire

TITLE: Cellular characterization of extracellular vesicle uptake and content delivery within acceptor cells

ABSTRACT: Extracellular Vesicles (EVs) are membranous particles secreted by all cells. They are thought to transfer biomolecules (proteins, lipids, nucleic acids) from a donor cell, to an acceptor cell. This implies the involvement of EVs in numerous physio/pathological processes. EVs are also promising vectors for targeted delivery of therapeutics, which could revolutionize cell and gene therapy. However, much remains to be done at the fundamental level to better understand the cellular and molecular mechanisms that govern EV uptake and content delivery.

During this PhD work, two assays were developed based on *in vitro* and *in cellulo* approaches to better understand this process. Extracellular vesicles containing labeled cargoes were isolated and mixed with purified plasma membrane or live cells. The fate of the EV-cargoes was then followed to identify their entry and delivery points within the acceptor cells, in a quantitative manner.

This experimental strategy led to the first quantification of EV uptake (1% spontaneous rate in 1 hour) and content delivery (30% of the uptaken EV content) within HeLa cells. This EV uptake was not a saturable process and EV association with the acceptor cells was inhibited at 4°C. Confocal imaging showed that EVs can be internalized in endo/lysosomal compartments of the acceptor cells. These compartments appeared to correspond to the delivery point of the EV content, as endosomal acidification was required for EV content delivery. The EV content delivery step also required proteins on both EV and acceptor membranes, and was likely to include a membrane fusion event, as the expression of viral entry inhibitors, the IFITM proteins, decreased EV content delivery.

These results pave the way to a detailed molecular characterization of this process, in order to finally identify the key molecular actors of EV uptake and content delivery by acceptor cells.

KEYWORDS: Extracellular vesicles, Intracellular trafficking, Vesicular content release, Membrane fusion

REMERCIEMENTS

La thèse est très loin d'être un parcours solitaire, et au moment de faire le bilan avec cette rédaction, beaucoup de personnes me viennent en tête sans qui le résultat présenté ici serait bien différent. Je souhaite donc remercier du fond du cœur :

. **Julie Gavard, Cédric Delevoye, Catherine Jackson**, membres de mon jury de thèse, pour avoir accepté de participer à ma défense de thèse et d'examiner mon travail. Je remercie aussi Julie Gavard et Cédric Delevoye d'avoir accepté d'être les rapporteurs de cette thèse, et ainsi d'avoir pris le temps de lire ce manuscrit et de l'évaluer. J'ai réellement apprécié les discussions qui ont découlées de leur remarques.

. **La Ligue contre le cancer** pour avoir sélectionné mon dossier et financé ce projet, et ainsi m'avoir permis de réaliser cette thèse ; **l'Université de Paris** et **le CRI** pour m'avoir accueilli au sien de leurs établissements et d'avoir complété ce projet de formations transdisciplinaires ; **l'Institut Curie** et **l'Université de Paris** pour m'avoir accueilli dans leurs locaux pour la réalisation de ces travaux.

. **Olivier Schwartz** et **Cédric Delevoye**, membres de mon comité de thèse, pour votre présence dans ce comité, mais surtout pour nos discussions très intéressantes sur mon projet et votre soutien tout au long de ma thèse.

. **Grégory**, pour ton soutien dans toutes les étapes de ce projet, du M2 à aujourd'hui, et plus encore. Tout d'abord pour avoir accepté d'être mon maître de stage puis directeur de thèse. Pour m'avoir formée, encadrée, encouragée pendant ces quasi 4 années à travailler ensemble. Tu as été un acteur majeur de la réussite de cette thèse, que ce soit pour ton aide expérimentale, l'écriture des demandes de financements, des papiers/revue, la préparation des congrès, l'écriture de cette thèse ... Merci pour ta patience, l'autonomie que tu m'as laissée et la grande confiance que tu m'as apportée.

. **Shéryl**, pour ta confiance dès ton premier stage, ta bonne humeur précieuse et nécessaire, tes blagues et nos délires communs, nos discussions infinies et ton soutien dans cette dernière année. *Je ne suis pas du tout sûre* que la transition de laboratoire aurait été la même sans ta grande aide.

. **Zahra**, pour ton sourire, tes anecdotes incroyables (*yarabi!*), ta spontanéité et ton expertise de thésarde précieuse dans cette dernière année, pour me maintenir *au maximum* la tête sur les épaules.

. **Julia**, pour ton soutien expérimentale et scientifique précieux, ton aide sur ce manuscrit, nos discussions desserts et *ces petites vaches* qui me font tant rire.

. **Youssoupha**, pour m'avoir fait confiance pendant ton stage de L3, pour ta bonne humeur et ton implication dans ton projet.

Merci à tous les membres de l'équipe pour les moments partagés. La création de cette équipe a été une étape enrichissante et nous avons assez vite réussi à trouver nos marques pour travailler ensemble dans une bonne ambiance. Je vous souhaite à tous plein de réussites pour poursuivre cette belle aventure.

. Tous les membres de **MSCMed** pour leur accueil et leur aide lors de l'installation aux Saints-Pères. Merci pour nos discussions en réunion ou au coin du couloir, et pour les moments partagés, notamment avec les **Young Researchers**, malheureusement trop rares avec cette crise sanitaire.

. **Clotilde**, à l'origine de cette thèse en m'accueillant dans son équipe. Merci pour ton soutien, ta présence tout au long de cette thèse et ta bienveillance qui m'ont permis de passer 3 très bonnes années à Curie.

. Mais aussi à tous les membres de son équipe, anciens ou actuels. **Mathilde** et **Eleonora**, pour votre aide à mon arrivée à Curie, pour le soutien que vous m'avez apporté et tous ces moments passés ensemble de Curie à Naples. **Ester**, pour ta gentillesse et ta présence dans tous ces moments que nous avons traversés. **Mercedes** et **Lorena**, pour votre soutien et votre accueil au sein de l'équipe. **Fede**, pour ta bonne humeur et ton sourire qui sont précieux, et pour ta gentillesse et ta bienveillance. **Nathalie** et **Alix**, pour votre aide, nos discussions et ces moments partagés. **Alain**, pour ton aide et ta disponibilité dès que j'ai eu des questions. Ainsi que tous les étudiants qui sont venus passer quelques semaines à nos côtés pour leurs sourires.

. **Anastasia**, pour beaucoup de choses, mais avant tout ta présence pendant ces 3 ans à Curie et après, de ton soutien, et pour toutes ces discussions et ces rires, que ce soit devant un chocolat chaud ou ailleurs.

. **Alice**, pour ta soutient et ton parfait équilibre entre sagesse et folie, **Elisa**, pour ton enthousiasme et ta sincérité, **Yara**, pour ton sourire et ta gentillesse, **Léa**, pour ta bonne humeur et ton expertise déménagement qui m'ont aidée à relativiser, **PE**, pour ta gentillesse et ton énorme patience en tant que voisin, **Marine** pour ta zinzinerie bien sûr (et tout ce qui va avec). Et vous tous pour tous ces moments où nous nous sommes soutenus et où nous avons fait de nos thèses un expérience humaine riche.

. **Yohan, Fra, Hélène, Coline, Mélanie, Yago, Javiera**, pour tous ces moments passés entre étudiants, qui nous ont tirés vers le haut et qui ont ponctué ces quasi 4 années de nombreuses discussions et d'innombrables rires.

. **Marion**, pour nos discussions et ton implication dans le **Green Lab**, qui nous ont permis de commencer à mettre des choses en place et de se regrouper pour partager de bons moments.

. **Sylvia** et **Virginie**, tout d'abord pour vos précieux sourires matinaux qui étaient devenus mes petits rituels en début de journée à Curie, mais aussi pour tout ce que vous faites pour le laboratoire et nous permettre de travailler dans des conditions excellentes.

Tous les membres de l'**U932** pour leurs accueils, sourires, discussions, moments partagés qui ont enrichis ces 3 ans à l'Institut Curie.

. **Julian, Carmen, Tobias**, pour votre confiance, nos échanges et votre aide durant nos collaborations.

. **Anne-Laure, Daniel Henrion, Romain, Cees Otto, Agustin, Afroditi, Manoel**, qui m'ont encadrée pendant mes nombreux stages et m'ont, chacun à leur façon, fait découvrir les différents aspects de la recherche scientifique et encouragée à toujours aller plus loin.

.Mme Le Tilly, Mme Duval, Mr Sire, qui ont dépassé leur fonction de professeurs et m'ont portée vers cette voie de la recherche académique.

.Yohan, pour tout. Ton soutien, tes encouragements, les réveils qui sonnent tôt, ces dimanches à passer par le labo, ces vacances reportées/annulées quand l'échéance arrivait... Être une thésarde n'a pas été simple tous les jours et je me doute que l'accompagner non plus, alors merci de me supporter et de me suivre dans cette folle carrière.

.Maman, Papa, Damien, pour votre soutien et votre présence tout au long de ces études. Pour m'avoir laissée choisir ma voie à chaque étape, en m'aidant et m'encourageant. Les études ont toujours été un plaisir pour moi, jamais une peine, et ce ne peut être dû qu'à votre accompagnement. Merci aussi de vouloir assister à ma défense de thèse, bien que ce ne soit pas votre domaine, je suis heureuse de pouvoir partager ce moment avec vous.

.Ma Famille, de près ou de loin, pour leur présence, leur écoute, leur soutien.

.Manon, pour ton soutien, ta présence à tout moment, ta compréhension quand je l'étais moins, présente, et cette amitié qui nous porte toutes les deux depuis maintenant près de 10 ans ... Merci à toi et à **Alice** pour ces moments de détente si précieux pendant cette thèse.

.Alice, Elisa, Jérphine, Maëlys, pour votre soutien et votre présence pour agrémenter ces 4 ans de voyages, de visios et de rires.

.Cyril, Axel, Alexandrine, Sarah, pour ces chemins croisés et ces discussions, scientifiques ou moins, qui nous ont menés où nous en sommes.

J'espère sincèrement n'avoir oublié personne, et je souhaite d'une manière générale remercier toutes les personnes ayant, de près ou de loin, participé à ce beau parcours qui me mène aujourd'hui à écrire cette thèse. Ils m'ont permis d'évoluer professionnellement bien sûr, mais aussi personnellement en me faisant mûrir et en me donnant confiance. Je m'estime chanceuse d'avoir croisé autant de personnes enrichissantes pendant ces années d'études, et après tous ces mots il ne m'en reste plus qu'un qui ne sera jamais assez écrit :
MERCI !

MAIN ABBREVIATIONS LIST

AF4: Asymmetric flow field-flow fractionation

AFM: Atomic Force Microscopy

ATP: Adenosine TriPhosphate

BMDC: Bone Marrow DC

CATCHR: Complexes Associated with Tethering Containing Helical Rods

COPI: Coat Protein complex I

CRISPR: Clustered Regularly Interspaced Short Palindromic Repeats

DCs: Dendritic cells

DNA: Desoxyribonucleic Acid

EBV: Epstein-Barr virus

ECM: Extracellular matrix

EFF-1: Epithelial Fusion Failure 1

ER: Endoplasmic reticulum

ESCRT: Endosomal sorting complex required for transport

EVs: Extracellular vesicles

FACS: Fluorescent-activated cell sorting

FPV: Fowl plague virus

GFP: Green Fluorescent Protein

HCV: Hepatitis C virus

HERV: Human endogenous retrovirus

HUVEC: Human Umbilical Vascular Endothelial Cell

HIV: Human immunodeficiency virus

HOPS: Homotypic fusion and Protein Sorting complex

HSP: Heat shock protein

HSV1: Herpes Simplex Virus

IF: Immunofluorescence

IFITM: Interferon-Induced Trans-Membrane protein

ILVs: Intraluminal vesicles

MHC: Major histocompatibility complex

MSC: Mesenchymal Stem Cell

MVBs: Multivesicular bodies

miRNA: micro-RNA

mRNA: messenger RNA

NLuc: NanoLuc luciferase

NSF: N-ethylmaleimide sensitive fusion protein

RNA: Ribonucleic Acid

SFV: Semliki Forest virus

SM: Sec1 / Munc18-like protein

SNAPs: Soluble NSF attachment proteins

SNAREs: SNAP receptors

SV40: Simian virus 40

TCR: T cell receptor

VPS: Vacuolar Protein Sorting

VSV-G: Vesicular Stomatitis virus G-protein

VV: Vaccinia virus

WT: Wild Type

TABLE OF CONTENTS

REMERCIEMENTS	7
MAIN ABBREVIATIONS LIST.....	11
TABLE OF CONTENTS.....	13
1. INTRODUCTION.....	15
1.1. EV DISCOVERY AND INITIAL CHARACTERIZATION	16
1.2. EVs: A HETEROGENEOUS POPULATION OF VECTORS	18
1.2.1. <i>Exosomes</i>	18
1.2.2. <i>Ectosomes</i>	19
1.2.3. <i>Other EV nomenclatures</i>	19
1.3. EVs: ENDOGENOUS BIOLOGICAL MESSENGERS	20
1.3.1. <i>EVs as multimodal messengers in numerous physio/ pathological processes</i>	20
1.3.2. <i>Evidences of EV uptake and content delivery</i>	23
1.3.3. <i>First clues in cellular and molecular characterization of EV uptake</i>	26
1.4. VIRUS INTERNALIZATION AND CONTENT DELIVERY.....	28
1.4.1. <i>Plasma membrane content delivery</i>	28
1.4.2. <i>Clathrin-mediated endocytosis</i>	30
1.4.3. <i>Macropinocytosis</i>	31
1.4.4. <i>Caveolin-mediated endocytosis and other internalization pathways</i>	32
1.4.5. <i>How to use virus studies to look at EVs</i>	32
1.5. INTRACELLULAR VESICLES AND CELL-CELL MEMBRANE FUSION MACHINERIES.....	34
1.5.1. <i>Rab proteins: the relay couriers</i>	35
1.5.2. <i>Tethering proteins: the matchmakers</i>	35
1.5.3. <i>SNARE proteins: the main actors of membrane fusion</i>	37
1.5.4. <i>SNARE-associated proteins</i>	39
1.5.5. <i>Other fusion proteins</i>	39
1.6. PHD GOALS.....	41
2. RESULTS	43
2.1. EV CONTENT RELEASE IN CELL-FREE ASSAY	43
2.2. EV UPTAKE AND CONTENT RELEASE IN CELL-BASED ASSAY	55
2.3. KEY RESULTS AND WORKING MODEL	69

3. DISCUSSION	71
3.1. THE IMPORTANCE OF EV-CARGOES TOPOLOGY.....	71
3.2. EV UPTAKE BY HEĻA ACCEPTOR CELLS	72
3.3. EV CONTENT RELEASE WITHIN THE CYTOSOL OF HEĻA ACCEPTOR CELLS	75
3.4. PUTATIVE ROUTES FOR EV ENTRY AND CONTENT RELEASE WITHIN HEĻA CELLS ..	77
3.5. TOWARD EVs AS THERAPEUTIC VECTORS.....	78
ANNEXES	81
ANNEX 1: SUPPLEMENTARY FIGURES OF CELL-FREE ASSAY EXPERIMENTS	81
ANNEX 2: SUPPLEMENTARY FIGURES OF THE CELL-BASED ASSAY EXPERIMENTS	83
ANNEX 3: METHODOLOGICAL REVIEW ON EV UPTAKE AND CONTENT RELEASE STUDY – PREPRINT OF REVIEW COMMISSIONED BY SPRINGER.....	88
REFERENCES	97
ILLUSTRATION TABLE	107
RĒSUMĒ	108

1. INTRODUCTION

Extracellular Vesicles (EVs) are round-shaped lipidic structures, secreted by all cells and acting as endogenous vectors in intercellular communication. They remained quite ignored for decades by biologists, who considered them as cell waste compartments. Fortunately, they now are an important focus in the cell biology field, mainly due to their therapeutic potential. Several studies even determined they were key factors in clinical trials. However, much remains to be done to understand their complex biology. Particularly how EVs are uptaken by acceptor cells, and then how EVs deliver their content within those cells. Tools have been developed to follow the fate of these vesicles upon incubation with acceptor cells to qualitatively assess EV uptake, but the cellular characterization of the EV content delivery process, and a rigorous quantification of this phenomenon, have never been established. This is the core of my PhD work, which is presented below.

In this introduction, I will first cover the history of EV biology, that includes EV discovery and initial characterization of EV compositions and identification of EV sub-populations. Then I will focus on their function as intercellular messengers, with the different evidences already described and the methods used to study their uptake by acceptor cells. Finally, I will briefly highlight similarities with EV and different but related types of vesicles such as viruses or intracellular vesicles, for which the mechanisms involved in the release of their content has been characterized at the molecular level.

1.1. EV discovery and initial characterization

The first description of EV-like structures originates from 1967, with the report of tiny blood components, which could be pelleted by ultracentrifugation (1). These structures were different from intact platelets and seemed to originate from them. However, these particles, named “platelet dust” by the authors, still displayed a coagulant activity, as the intact platelet. A few years later, using electron microscopy, vesicles from cartilage matrix were described as membrane enveloped particles of various sizes (30nm - 1µm) and density (Figure 1A) (2). The detection of those vesicles was correlated with calcification. Both observations already suggested that cell-derived vesicles could possess some proprieties of the donor cells.

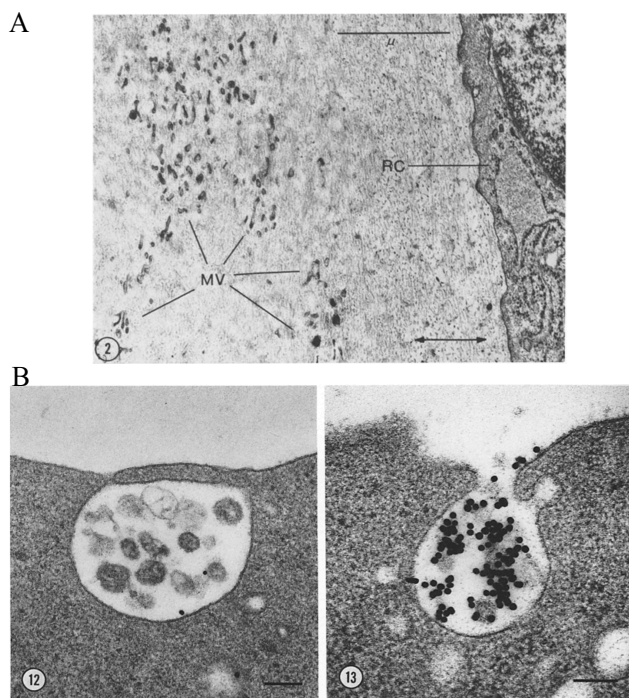


Figure 1: First EV observations

A: First electron micrograph describing extracellular vesicles. “Matrix vesicles (MV) adjacent to a chondrocyte (RC) within the reserve cell zone. [...] The long axis of the tibia is indicated by arrow. x32,000” from Anderson H.C. (2). B: Electron micrographs showing the release of ILVs through the fusion of MVBs with the plasma membrane, leading to exosome secretion. “12: View of an MVE sparsely labeled with AuTf after a 20-min incubation at 37°C. Note the apparent fusion of the MVE and the plasma membrane. This may represent incipient MVE exocytosis. Bar: 100 nm. x 107,000. 13: View of MVE exocytosis in an unfixed reticulocyte. This cell was incubated for 30 min with AuTf, subjected to a 20min chase

with unconjugated transferrin, and then quick-frozen without prior fixation and freeze-substituted. Bar: 200nm. x61,000” from Harding C. et al. (3).

Later, the secretion of some EVs from intracellular compartments was evidenced by electron microscopy, showing intracellular MultiVesicular Bodies (MVBs) fusing with the plasma membrane (Figure 1B) (3, 4). This fusion allows the secretion of the whole MVB content, including IntraLuminal Vesicles (ILVs), to the extracellular environment. These studies performed on reticulocytes suggested that the secretion of these ILVs, also called “exosomes”, were used during the maturation of these cells to get rid of proteins and lipids unrequired in mature cells (5). This explains why, even though the previously described studies linked the vesicles to a functional aspect, they

remained only considered only as “waste vesicles” for years, exclusively limiting them to the disposal of no longer required cellular components.

The first functional assay using EVs came in the late 90s. The authors used B lymphocyte-derived “exosomes”, displaying Major Histocompatibility Complex (**MHC**) class II proteins on their surfaces (6). This study showed that these vesicles, who had a different protein composition than the donor cell plasma membrane, can induce antigen-specific T-cell response when they derived from B lymphocytes preincubated with specific antigens.

Thanks to several studies in the field of immunology, the intercellular messenger ability of these vesicles arose, in particular in anti-tumoral immunity. EVs were indeed described to transfer tumoral antigens from tumor cells to Dendritic Cells (**DCs**). The uptake of the tumoral antigens mediated by EVs allowed DCs to process these antigens, to finally present them to CD8 positive T-cells using their MHC class I (7). These EVs, through the intermediary of the DCs, were then able to trigger CD8 positive T-cell anti-tumoral response and extend the donor cell action.

These studies indicated that at the least, EVs could carry proteins on their membranes, to transduce signals between cells of different origins. To expand their messenger potential, a new EV signal modality was described with the delivery of functional content into acceptor cells. First, it was shown that nucleic acid, specifically messenger Ribonucleic Acid (**mRNA**), could be found and even enriched in EVs (8). The EVs are here carriers to deliver these mRNA within acceptor cells. According to the authors, once transferred to the acceptor cells by means of EVs, these mRNAs could be translated into proteins within the acceptor cells. It was shown a few months later that mRNA, co-isolated with EVs from mouse cells, could be uptaken by human cells, which were then being able to synthesize mouse proteins from the mRNAs they received (9). The same study also evidenced the presence of other nucleic acid in isolated EVs: micro-RNA (**miRNA**). The ability of acceptor cells to synthesize exogenous proteins using EV-associated mRNA was, at that time, the first evidence that EVs could transfer functional soluble molecules from a donor cell to the cytosol of an acceptor cell.

These studies definitely closed the “waste only vesicle” story, and opened a wide-spectrum of research topics about the EVs, whether in physiological and pathological pathways, or for therapeutic purposes. This new interest also motivated the scientific community to better characterize and define these EVs.

1.2. EVs: a heterogeneous population of vectors

It is only in 2011 that the term “extracellular vesicles” appeared in the literature to describe all kinds of vesicles secreted by cells in their extracellular environment (10), although it was previously used to describe only some EV subpopulations. Indeed, secreted EVs are a heterogeneous population of vesicles of different sizes, compositions and secretory origins. They can be isolated from bodily fluids, such as blood (1, 11, 12) and semen (13), or from cell culture media (14), including HeLa cells (15, 16). The number of various isolation methods, together with their history and the fact that they were studied for decades before being really characterized, created a chaos of names relating to the EVs.

The scientific community now consensually agrees to call “extracellular vesicle” all particles secreted by cells, which consists of cellular material surrounded at least by one lipid bilayer, but which is not capable of replication (17). Thus, I will further refer to them only by the term “EVs”, as this study was designed to characterize the uptake of the whole EV population. However, several studies of the EV secretion allowed to identify several of these EV-subpopulations, mainly based on their secretion origin, but also on their composition.

1.2.1. Exosomes

One has to be careful with this nomenclature in the literature. First of all, they should not be confused with the exoribonuclease complex named with the same term (18). Secondly, it was (and might still be) quite widely used to refer to the whole EV population, or at least without proof of any EV subpopulation identity (19).

Exosomes are, as mentioned above, endosomal-derived EVs. They correspond to 30-100nm ILVs that are formed during endosomal maturation, by invagination of the endosomal membrane and budding into internal compartments in the MVBs (20). The formation of these ILVs goes along with the sorting of their content, mainly mediated by post-translational protein modifications and Endosomal Sorting Complex Required for Transport (ESCRT) (21). The historical fate of the MVBs was to fuse with lysosomes, leading to content degradation (22). But for exosomes biogenesis, the ILVs

are finally released in the extracellular milieu through the fusion of MVBs with the plasma membrane (23).

1.2.2. Ectosomes

Ectosomes, also known as microvesicles or microparticles, are plasma-derived EVs. They were named after the exocytosis pathway described in the 90s, ectocytosis (24), describing the shedding of vesicles from the plasma membrane toward the extracellular environment. The biogenesis of those vesicles can occur through plasma membrane protrusion (for instance cilia or filopodia) or directly using known mechanisms such as the ESCRT-dependent budding (25). Their secretion pathway enables bigger vesicle formation than ILVs, producing ectosomes up to 1 μ m (26).

Importantly, the budding mechanisms involved in ectosome secretion are similar to the ones required for some enveloped viruses. This similarity will create a mixed population of particles secreted by infected cells, from native virus to Wild Type (WT) EVs (viral content-free), with intermediate viral content loaded EVs (27). Thus, viral isolation from infected cells will contain EVs and, in the other way around, the EVs from infected cells will be co-isolated with viruses.

1.2.3. Other EV nomenclatures

Across time, different nomenclatures were used to try to define specific EV populations, based on various characteristics.

They could be named after the physiology of secreting cell for instance, like the oncosomes or the apoptosomes. The oncosomes are EVs from tumor cells, which thus contain tumoral cargoes that can interfere with the tumoral progression (28). The apoptosomes, or apoptotic bodies, are generated over dying cell fragmentation (29). They are the biggest existing EVs, sizing up to 5 μ m, but cannot be isolated according to their sizes because they can also be as small as exosomes (50nm).

New generations of EV isolation methods also allowed to identify new populations. For instance the exomeres were recently described using Asymmetric Flow Field-Flow Fractionation (AF4), permitting to isolate these tiny particles of around 35nm (30).

However, exomeres do not seem to have an external membrane, which exclude them from the EV definition.

This heterogeneity of the EV population led to numerous studies, that aimed at characterizing specific EV subpopulations, in order to finally be able to isolate one from the others. But the main message coming from these studies is that EVs share a lot, either in their size, content, density or secretion mechanism actors (25, 31, 32).

Proteomic analyses showed that more than one molecule was required to be able to distinguish one sub-population from another one (32). The EV field has been struggling for decades to characterize them. The most recurrent markers are CD9, a plasma membrane protein assumed to be a plasma membrane-derived EV marker, and CD63, a protein enriched in MVBs and presumed to be an exosome marker. However, immuno-isolation studies highlighted that they can be found on the same kind of EVs (31).

The EVs composition depends on a lot of factors: secreting cells, secretion pathways, condition of secretion, but also from isolation methods (33). In this PhD work, I decided to use a cargo-based approach to follow the EV uptake and content delivery. I focused on Hsp70, a cytosolic chaperone protein that is virtually present in all types of EVs. Using a generic EV cargo enabled me to characterize a delivery process that may be used by more than one EV subpopulation.

1.3. EVs: endogenous biological messengers

The huge interest around EVs is directly linked to their proposed ability to transfer information and cargoes from one cell to another one. With the increasing sensitivity of research tools, they now seem to be involved in pretty much all kinds of intercellular communication at several levels.

1.3.1. EVs as multimodal messengers in numerous physio/pathological processes

To fulfill this messenger purpose, EVs do not necessarily require the release of their content within the cytosol of the acceptor cell, and they can even act without acceptor cell (Figure 2). They can indeed “simply” carry enzymes on their surface, and act

directly in the extracellular environment, by promoting ExtraCellular Matrix (**ECM**) digestion when bearing elastases for instance (34). In this way, EVs can extend the enzymatic activity from the donor cell in distant extracellular media.

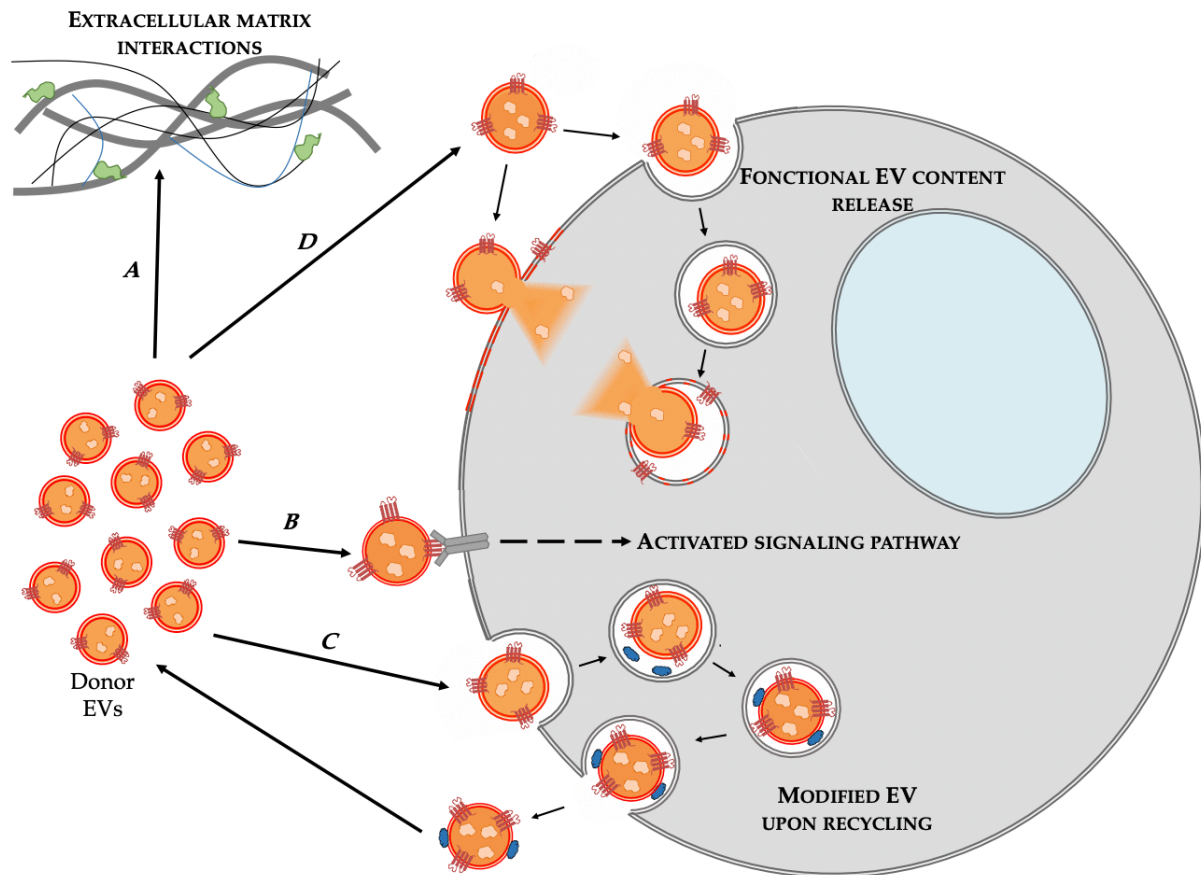


Figure 2: EVs are multimodal intercellular messengers

EVs are involved in intercellular communication by several ways: they can act on extracellular components (A), initiate intracellular signaling pathways if bound to a cell receptor (B), be recycled to gain properties with new associated proteins (C), or release their content within the cytosol of the acceptor cell (D).

The proteins of the EV membrane can also trigger signalization events at the surface of the acceptor cells. The main and pioneer example is the activation of different families of T cells, with the binding of their T Cell Receptor (**TCR**) to MHC-bound peptide on EV surface, from B cell or DC donor cells (6, 35). This EV-mediated antigen presentation can thus extend the action of the antigen presenting cell action far from their initial localization within an organism.

The uptake of an EV is not necessarily the final step of the EV mission. Indeed, EVs can still be recycled in the extracellular environment of its (primary) acceptor cell. In breast cancer biology, fibroblast EVs can be first internalized by tumor acceptor cells,

prior being recycled in the extracellular milieu without reaching the cytosol of these cells. This internalization will lead to the binding of Wnt11 proteins to the EVs. The recycled EVs are then fully equipped to generate a pro-tumoral effect, promoting metastasis formation in other (secondary) acceptor cells (36).

The EV-mediated function which gathers most of the interest remains their ability to deliver functional biological materials within the cytosol of the acceptor cell. As mentioned previously, the functional mRNA transfer has been described in several models, as for instance glioblastoma cell-derived EVs, which were able to induce cell proliferation of endothelial acceptor cells and the expression of pro-angiogenic proteins (37). In homologous communication between glioma cells, the EV-mediated transfer of a growth hormone induces several pathways involved in cell growth and proliferation (28).

More complex systems involving EVs were studied, like a bi-directional EV communication between endothelial cells and adipocytes. In adipose tissues, the endothelial cells can transfer the protein caveolin to adipocytes depleted of this protein, using EVs. The other way around, adipocyte-derived EVs are enriched in signaling molecules, that will benefit to the endothelial cells (38).

The EV-mediated communication between tumor and immune cells raised a lot of interest, but EVs were also described in many physiological and other pathological processes, of which few examples are described hereinafter. EVs play a crucial role in neuron communication, particularly at the synapse. It has been shown in flies that they are involved in the neuromuscular junctions, transferring proteins from the neural cell to the muscle cell, proteins which would be later required for anterograde communication, in that way keeping the neuromuscular synapse dynamic (39).

The EV uptake is described to be involved in a wide range of pathological processes as well. In the Human Immunodeficiency Virus (HIV) infection, EVs can increase the number of target cells by transferring HIV co-receptor CCR5 to deficient acceptor cells (40). Pathogens can also hijack EVs to spread within organisms. As an example, prions can be shed within exosomes of infected cells (41), and transfer the infectious content to the acceptor cells (42). This will lead to spread the infectious disease, caused by the abnormally folded proteins of prions.

My PhD work focused on the EV-mediated transfer of biomolecules, from a donor cell to an acceptor cell. Thus, the main phenomenon to characterize is the delivery of EV

content within the cytosol of the acceptor cells, and the putative internalization and/or fusion step(s) required for this content delivery.

1.3.2. Evidences of EV uptake and content delivery

For clarity purpose, “uptake” and “content delivery” terms will be used separately to define two aspects of the putative fate of the EVs within the acceptor cells. “Uptake” will describe the global process that associates EV content to the acceptor cells, including EV docking on the acceptor membranes, internalization within intracellular compartments and EV content cytosolic release. “Content delivery” will only relate to this final step of EV uptake: the release of their content within the acceptor cell cytosol.

The role of EVs on acceptor cells can be first assessed with functional assays, looking at acceptor cell fitness, behavior and/or metabolism. As discussed above, it can be, for instance, based on immune cell activation (6, 35). Looking at cell proliferation and protein expression allowed to observe that tumor-derived EVs could transform fibroblasts or endothelial cells. Indeed, after incubation with EVs they showed an increase of their survival and proliferation, and an activation of some tumoral signaling pathways (43). These functional assays are ideal to observe EV effects on acceptor cells, but they do not allow any characterization of cellular and molecular mechanisms involved in the EV uptake.

Protein transfer was largely investigated using different read-out to detect EV uptake or content delivery. Flow cytometry experiments are mostly used to follow fluorescent-tagged EV cargo within acceptor cells. ImmunoFluorescence imaging (IF) is also broadly used to follow EV localization within acceptor cells. For both methods, EVs need to be either loaded with a fluorescent cargo (mainly protein or nucleic acids), labelled using lipid dye or fluorescently tagged antibodies. The analyzes of these experiments can provide semi-quantitative information on EV uptake and/or EV content release. But here again establishing the bulk efficiency relative to the initial EV input remains impossible. However, such experiments led to evidence EV function in several models.

For instance, it was used to follow the homologous transfer of Green Fluorescent Protein (GFP)-tagged growth factor, initially isolated with glioma cell-derived EVs, with unlabeled glioma acceptor cells (28). It can also be used to follow transmembrane protein transfer mediated by EVs to acceptor cells initially deficient for this protein

(40). Confocal imaging allowed to follow GFP-CD63 positive EVs upon acceptor cell internalization. It showed that eventually their uptake can be acceptor cell specific, as in that case neuronal labelled EVs bound specific neuronal acceptor cells (44). The combination of IF and flow cytometry, using an imaging flow cytometer, allows the detection of EV internalization (or at least association with acceptor cells) at a single cell level and higher throughput than microscopy. It was exemplified by a study on EV internalization by bladder cells (45).

Table 1: Summary of methods used to study EV uptake

READ OUT METHODS	EV LABELLING	EV UPTAKE STEP	RESULT QUALITY	REFERENCES
Functional assay	Not required	Direct or indirect impact on cell physiology	Qualitative and semi-quantitative	(6–8, 28, 35, 37, 43, 46)
Confocal imaging	Membrane dye or fluorescent EV content	Docking and internalization	Qualitative and semi-quantitative	(28, 44, 46–50)
Flow cytometry	Membrane dye or fluorescent EV content	Global EV uptake; docking or internalization with chemical treatments	Semi-quantitative	(28, 40, 47, 51–53)
Biochemical assays	Enzymatic or blot-detectable EV content	Global EV uptake, docking or content delivery	Semi-quantitative or quantitative	(38, 42, 44, 49, 54)
	Exogenous nucleic acid EV content	Content delivery	Semi-quantitative	(9, 37, 38, 49, 50, 55)

Considering lipid labeling, PKH dyes (from their discoverer Paul Karl Horan (56)) are lipophilic tailed-dyes which were used for instance to visualize the transfer of oligodendrocyte EVs to microglia acceptor cells (46). They were also used in a more complete study, where labelled EV uptake by Human Umbilical Vascular Endothelial Cells (HUVECs) was characterized by flow cytometry and IF, giving clues on the EV uptake processes (47). Dialkylcarbocyanines as DiO or DiI are other lipid dyes used to

follow labelled EVs during incubation with acceptor cells. They were used for instance to compare labelled EV uptake between different acceptor cell lines by flow cytometry (57) or to follow EV internalization with confocal imaging (48). Finally, self-quenching lipidic dye, as R18, can be used to follow fluorescence accumulation when EV membrane is incorporated within the acceptor cell membranes (54). They all share the great advantage to label all membranes (so probably all EVs). However, their use is limited to EV docking, uptake and internalization analyses and the washing steps are crucial to avoid any non-specific bindings. These dyes cannot be used to assess the EV content delivery.

As already pointed out, the first evidence of EV content release within the cytosol of the acceptor cell came with mRNA-containing EV studies, showing that donor mRNA (from different cells/species) could be expressed and lead to specific protein synthesis in the acceptor cells (9, 37). Following the same strategy of heterotypic intercellular communication, other kinds of nucleic acids were described to be transferred from a donor cell to an acceptor cell using EVs, but the quantification of the EV uptake and content release could not be precisely addressed using this strategy. Exogenous mRNA from engineered donor cell lines can however be designed to assess the cytosolic release of EV content (49). Endogenous viral RNA sequences can also be found in EVs and transferred by them, as for Human Endogenous RetroVirus (**HERV**)-K retrotransposon, from medulloblastoma to endothelial cells (55). Finally, apoptotic body-mediated DesoxyriboNucleic Acid (**DNA**) transfer was also evidenced by following Epstein-Barr Virus (**EBV**) DNA (50).

EV uptake can be addressed by looking at long term effects as well, as with prion protein-loaded EVs. After the acceptor cells incubated with these EVs, they were kept for several passages and they still expressed prion proteins, showing that EVs transferred infectious materials (42).

To address content delivery, enzymatic activity can also be used, by expressing a substrate in the donor cells (which will be loaded in EVs) and express the enzyme within the acceptor cells. Then enzymatic activity can only be detected if EV content release occurs, like for instance with a luciferin/luciferaes couple of donor/acceptor cells (51).

Here, we combined both imaging microscopy and biochemical assays to address EV uptake characterization. To ensure the correlation of the EV content fate with the monitored signal, EV cargoes were labelled with either a fluorescent protein or an

enzyme. The topology of these cargoes was validated prior going further in the characterization.

1.3.3. First clues in cellular and molecular characterization of EV uptake

The internalization of EVs by acceptor cells has been described in several models. The combination of lipid dye for confocal imaging and gold particle staining for electron microscopy was used to follow Bone Marrow DC (**BMDC**)-derived EVs internalized in endo/lysosomal compartments of acceptor phagocytes (52).

Chemical treatments also corroborated this EV internalization step within the EV uptake process. For instance, DC-derived EV uptake by tumor acceptor cells is inhibited by Dynasore treatment (inhibition of dynamin GTPase), but not EIPA treatment (inhibition of macropinocytosis), and requires caveolin 1 protein on the acceptor cells. Together, these results suggest that EVs enter the cell using caveolae-mediated endocytosis (48). Importantly, in this study, donor cells were infected with EBV, which could lead to specific EV populations and internalization pathways.

Flow cytometry experiments showed that EV uptake by glioblastoma or epithelial cells is inhibited by heparin treatment in a dose/response manner and thus requires proteoglycans on acceptor cell surfaces (53). This requirement could be linked to the EV composition, as heparan sulfate proteoglycans can be found on EV membrane, even though they are not homogeneously distributed in the EV population. However, its abundance in EV does not affect the different EV subtype uptake. Heparin treatment also inhibited EV internalization by bladder acceptor cells, confirming still proteoglycans involvement in EV uptake (45).

The lipid composition of the acceptor cell membrane matters, as filipin treatment (molecule that binds cholesterol and thus perturbs membrane composition) decreases EV uptake (54). In the same study performed on melanoma cells, EV secreted under an acidic pH was described as increasing EV uptake compared to a physiological pH secretion.

Previous studies also identified proteins involved in the EV uptake process. Using blocking antibodies in an immune cell communication model, some DC membrane proteins and EV proteins were highlighted as molecular actors of the EV uptake:

mostly CD51, CD61 and CD11a as positive regulators of EV internalization and MFG-E8 as a negative regulator (52). When looking at the EV uptake by monocytes, a high level of CD47 protein on EVs seems to protect them from being internalized by monocytes (58). The implication of these adhesion molecules on both sides of the system (acceptor cells and EVs) indicates that EV docking on the acceptor DCs might occur during EV uptake.

To support this hypothesis, *in vivo* experiments in mice identified couples of integrins that could define different affinity of the EVs toward specific acceptor cells, either from lung or liver cells. This would also explain the organotropism of metastasis formation (30).

EV content release was evidenced using the combination of donor/acceptor cells expressing compatible luciferin/luciferase. Using this technique, it was described that EV content release occurred upon fusion or hemifusion of EV membrane with acceptor cell membranes (51). EV membrane fusion with acceptor cell was measured using self-quenching membrane dye, and was dependent on EV proteins (as their pretreatment with paraformaldehyde decreases fusion). Here again caveolae seemed involved, as filipin treatment was also an EV fusion inhibitor.

In vivo relevance was also addressed, looking at EV internalization in mouse cells, after injection of EV in mice. This internalization was detected by imaging experiments, where a luminescence signal was found in spleen and abdominal skin (49). Labeled EVs were here again found in endolysosomal compartments in DCs from different organs (52). A recent study in zebrafish followed the fate of endogenously secreted EVs in the bloodstream of the fishes. The results indicated that EVs were internalized and their content degraded by specific macrophages (59).

These results are encouraging and pave the route for further characterization, but the knowledge on EV uptake and content delivery remains really poor compared to the characterization of viral entry. To summarize, EV internalization by acceptor cells has been confirmed by numerous studies in several models. However, no consensus could be reached from these studies about the internalization pathway, to validate clathrin and/or caveolin dependency/independency. This internalization is, at this time, not described as receptor-dependent as no candidate was validated yet.

Due to the heterogeneity of the EV population, if common protein-dependent binding and/or fusion system exists, it should be linked to common features such as tetraspanins, integrins, or undescribed fusion machinery. It might also rely on their

lipid composition, with the putative role of phosphatidylserine or cholesterol domains. In that case, the process would then be different across EV subpopulations as lipid composition is not a homogeneous feature across the EVs. The characterization of EV uptake and content delivery might lead to the discovery of new cellular and molecular machineries, as it could also highlight already identified pathways used by other kinds of vesicles.

1.4. Virus internalization and content delivery

Viruses are small particles with an EV-like size, shape, composition and density (60). Many types of viruses have been described, and we have a profound knowledge of the various processes that are used by each type of viruses to infect target cells. Since EVs and viruses share many similarities, it is therefore tempting to hypothesize that EVs may use the same mechanisms for uptake and content delivery.

A virus first needs to bind the target cells. Depending on the virus, the binding can rely on a common endocytic receptor, such as the Low Density Lipoprotein (LDL) receptor (61) or the transferrin receptor (62). The viral receptor can also correspond to more specific proteins, often glycoconjugates, like CD4 for HIV or hemagglutinin for Influenza A (63).

Once attached to the target membrane, the virus needs to deliver its content within the acceptor cells to replicate and create new virions. This content release can be done directly at the plasma membrane, or after virus internalization (Figure 3). Below are listed the pathways used by certain viruses to enter acceptor cells, except phagocytosis, which is specific to only few acceptor cells such as macrophages and DCs.

1.4.1. Plasma membrane content delivery

In the case of HIV-1, after binding to its receptor and co-receptor, the envelope protein of HIV-1 (HIV-1 Env) changes its conformation to allow its fusogenic unit to enter into the target membrane. This new conformation will bend the target membrane, up to full fusion with the HIV-1 membrane (64). Thus, HIV can directly release its content with the acceptor cell cytosol after fusion with the plasma membrane. Even though, as HIV, some viruses directly deliver their content by fusing with the plasma membrane,

most of them will first be internalized in endocytic compartments prior to release their contents. To do so, they mainly hijack pathways that the cell uses to uptake extracellular compounds, to access internal cell compartments in the final goal of using the cell for their own replication.



Figure 3: Viral internalization pathways leading to their content delivery

Viruses use different cellular pathways to enter their target cells and perform their replication. They can either enter directly at the plasma membrane like HIV, or enter using clathrin-dependent or caveolin-dependent endocytosis as VSV and SV40 respectively. Finally, they can also enter by macropinocytosis, like VV. Once internalized, they will release their content using the low pH of endo/lysosomal compartments or the ER membrane.

1.4.2. Clathrin-mediated endocytosis

In the 60s, one of the first description of endocytosis defined cortical pits and coated vesicles that were involved in yolk protein uptake by oocytes (65). This work led to a summarizing scheme, representing the first view of the endocytic pathway (Figure 4).

Thanks to advanced technologies, allowing cell culture, protein purification and modification, the LDL uptake studies performed in the late 70s resulted in a comprehensive view of this receptor trafficking pathway. The several articles that described the receptor-mediated endocytosis of LDL, led the authors to suggest a model for general receptor-mediated endocytosis (66). Clathrin-coated vesicles are known to be an intracellular transporter since the late 70s (67). Semliki Forest Virus (SFV) is the first described viral internalization within internal coated vesicles (68), now known as clathrin-coated vesicles. This is the main path for viral internalization, which is also used by Vesicular Stomatitis Virus (VSV) (69) or Hepatitis C Virus (HCV) (70).

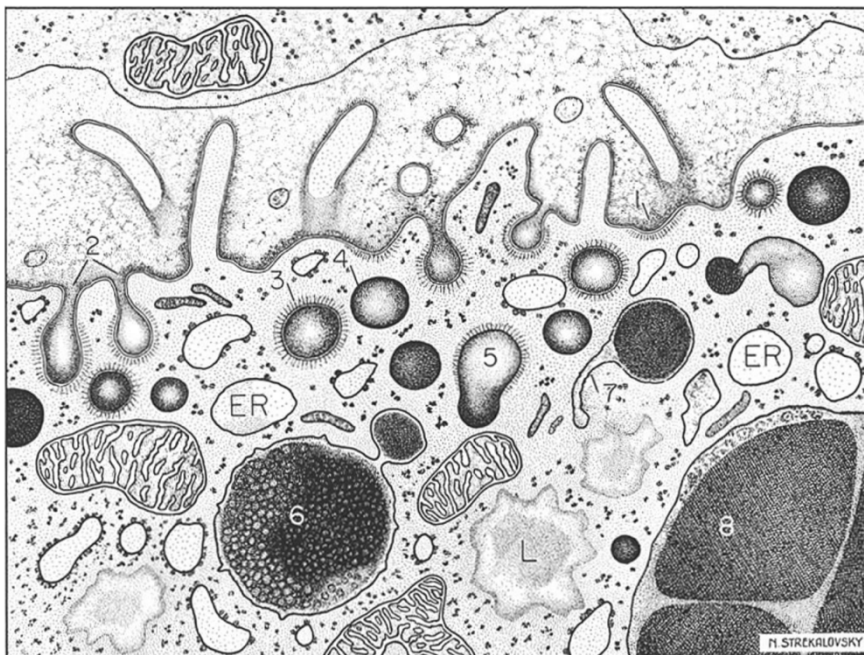


Figure 4: First representation of the endocytic pathway.

Drawing from electron micrographs describing some intracellular compartments (1 to 8) involved in Yolk protein uptake by mosquito oocytes. "This schematic drawing [...] depicts changes and events involving the cortical pits and coated vesicles of the mosquito oocyte. At (1) is shown the first stage of

invagination into the oocyte of the protein-coated plasma membrane from the intercellular space. The fully developed pit (2), by pinching off, forms the coated vesicle (3). These vesicles lose their bristles to form dense spheres of similar size (4) which then fuse with other dense spheres (5). Often a flattened empty sac is attached to the droplet (7). [...] The larger droplets (6) coalesce to form the large crystalline proteid yolk bodies (8) of the oocyte. Other conspicuous and characteristic inclusions and organelles of the oocyte cytoplasm are mitochondria, vesicles of the rough surfaced endoplasmic reticulum (ER), lipid (L) and ribosomes. At the top

of the drawing, microvilli project into the intercellular space fronting on the follicular epithelium. [...] x approximately 60,000." From Roth T.F. and Porte K.R. (65).

Dynamin-2, AP2 and of course clathrin proteins interact to create a membrane-bound cage within the cytosol which will give rise to endocytic vesicles (71, 72). These endocytic vesicles will then deliver their contents within early endosomes, which will then pursue endosomal maturation along which intraluminal pH decreases, from pH6.5 to reach down to pH5. Around pH6, envelope proteins such as VSV-G undergo conformational change (73), which create a more hydrophobic structure. This envelope protein properties will lead to membrane fusion between the virus membrane and the endo/lysosomal membrane (74), releasing viral content within the acceptor cell cytosol.

1.4.3. Macropinocytosis

Macropinocytosis is the pathway that enable uptake of large and numerous objects at once. Its initial step involves a plasma membrane deformation into a thin fold, mediated by actin polymerization. This membrane protrusion then extends into the extracellular milieu, and will possibly extend to fold back on the plasma membrane surface, that way enclosing content from the extracellular milieu (75). The fusion of the extremity of the fold and another region of the plasma membrane will create an intracellular vesicle, called macropinosome, which can reach up to 10 μ m large (76). Eventually, this macropinosome will travel deeper into the cytosol to meet and fuse with specific endo/lysosomal compartments (77, 78).

As macropinosomes are large endocytic vesicles, they are convenient for large viruses to enter, such as Vaccinia Virus (VV) (79). In that case macropinosome will fuse with an endosome which will mature to become a lysosomal compartment. Lysosomes have an appropriate acidic pH for vaccinia virus content release (80). Herpes Simplex Virus 1 (HSV1) is also a large enveloped virus that may enter cells using macropinocytosis, depending on the acceptor cell (81). However, HSV1 might fuse with early endosomes to release its content as endosomal acidification is not required for its content release (82). Macropinosome formation requires PI3-kinase for both VV and HSV1 viruses, and their internalization relies on Na⁺/H⁺ exchangers and p21-activated kinases, which are also involved in membrane fusion (79, 82).

1.4.4. Caveolin-mediated endocytosis and other internalization pathways

Endocytic vesicles can also bud within the cytosol from the plasma membrane in caveolin 1 pits or in lipid rafts. This pathway is used by Simian Virus 40 (**SV40**), that binds the acceptor cells on MHC class I and membrane gangliosides GM1 (83). The latter can be considered as their endocytic receptors and induce membrane curvatures and the formation of endocytic vesicles, called caveolae (84). After membrane fission, these vesicles will be directed and fused to early endosomes, which will mature and form endo-lysosomes (85). Contrary to classical endosomal pathway, the SV40-containing endolysosomes will then be targeted to the Endoplasmic Reticulum (**ER**) where the virus will be released. Once in the ER lumen, the protein folding machinery will allow the virus uncoating that will further lead to the viral content cytosolic release (86). This ER targeting strategy is used by most polioviruses, using different gangliosides isoforms for each step of their uptake (binding, internalization and ER targeting) (83, 87).

Lipid raft-mediated internalization occurs in parallel of previously described pathways for some viruses. Cholesterols are required for every internalization pathway, but dynamin can be necessary (88) or not(89). The endocytic vesicles thus formed can fuse with endo/lysosomal or ER compartments, and the release of the viral content can either happen upon membrane fusion, or membrane lysis/pore formation, as for rotavirus (90).

1.4.5. How to use virus studies to look at EVs

Fortunately, we can take advantage of all the previous viruses-related studies to use similar approaches in the EV uptake and content delivery characterization. For instance, scientists reconstituted viral entry *in vitro*, initially on the Fowl Plague Virus (**FPV**). In one hand, donor endocytic vesicles were isolated from FPV infected cells, in the other hand acceptor endosomes were isolated from Semliki Forest Virus (**SFV**)

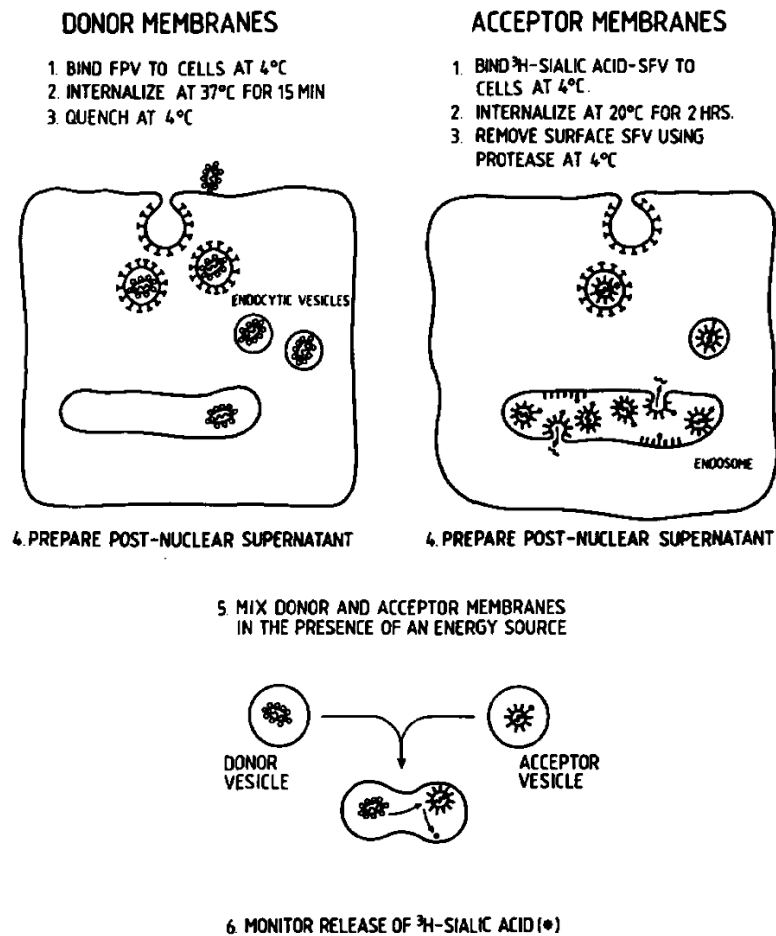


Figure 5: Principle of the first cell-free in vitro content mixing assay

Summary scheme of an in vitro reconstitution of endosomal vesicle fusion. “*Outline of the Cell-Free Assay to Measure an Endocytic Fusion Event*” From Davey *et al.* (91)

infected cells. This second virus will allow the read-out of the content mixing assay, as its sialic acid residues could be cleaved by the FPV neuraminidase (**Figure 5**). This set up allowed for the detection of fusion between donor and acceptor compartments, increased with Adenosine TriPhosphate (ATP), but showed that lysosomes could not fuse at physiological pH (91).

A major step of viral entry characterization is to find the cellular receptor which allows for viral targeting. To do so, virologists used to inhibit endocytosis with low temperature (4°C incubation), to see if the virus could still be associated with the target cells (92). If yes, then a viral receptor(s) was/were present on the acceptor cells membrane and further experiments would identify it/them.

Another virus feature is their capability to target specific cells/tissues (tropism) mediated by their glycoproteins, like EBV for leucocytes and epithelial cells (93) and HIV-1 for immune cells (94), and their intracellular compartments to optimize their

infectivity efficiency. Structural studies finally allowed the identification of specific fusion machineries such as the VSV-G protein. Based on their similar structure and properties, one could hypothesize that EVs could bare similar proteins, and above-mentioned methods should help to identify them.

1.5. Intracellular vesicles and cell-cell membrane fusion machineries

As introduced previously, intracellular trafficking uses complex machineries to transport molecules from one organelle to another one, to secrete or uptake them. This transport system needs membrane fusion to allow a donor vesicle to deliver its content in the acceptor compartment. Hereafter are listed fusion systems used by the cell to fulfill intracellular trafficking, as well as some cell-cell fusion mechanisms (summarized in Figure 6). Both can give clues as to the putative EV membrane fusion mechanisms, since EVs have similar size as intracellular vesicles, but inverted topology, which is indeed the same than the plasma membrane one.

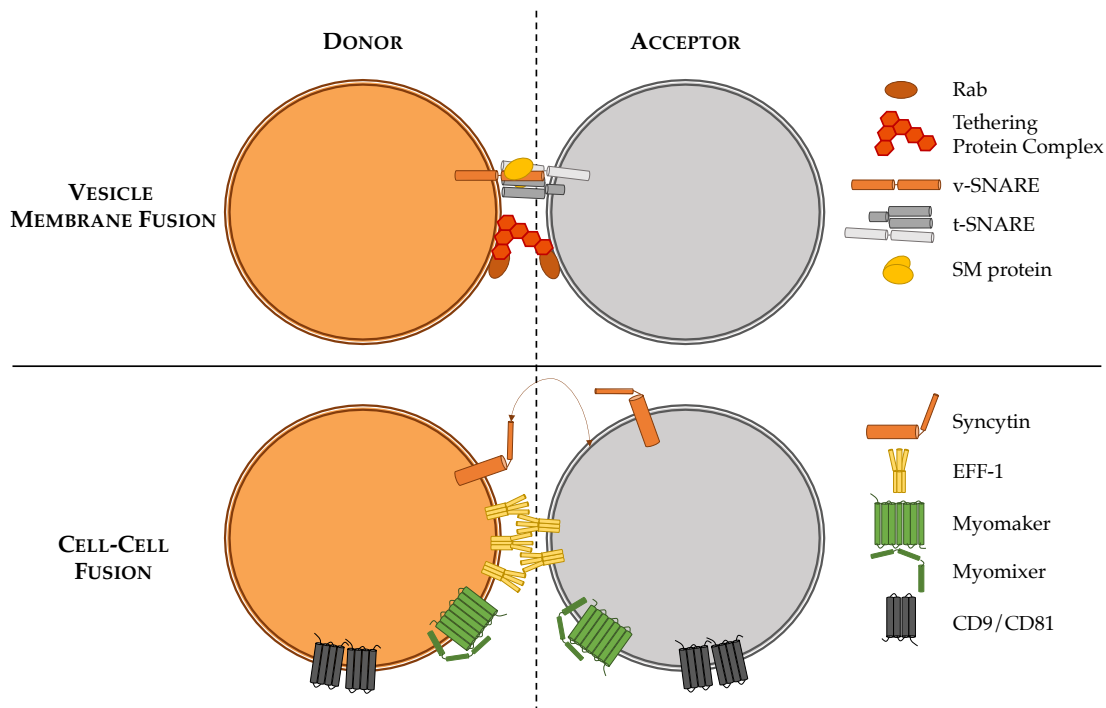


Figure 6: Described fusion systems in eukaryotic cells

Summary of fusion mechanisms displayed by eukaryotic cells to allow intracellular vesicle fusion (upper panel with SNARE complex) or cell-cell fusion during organism development (bottom panel, with syncytin in placental syncytiotrophoblast formation, EFF-1 in *C.elegans* development, Myomaker and myomixer in myotube biogenesis and finally tetraspanin in egg/sperm fusion).

1.5.1. Rab proteins: the relay couriers

Rab proteins belong to the Ras superfamily and there are at least 63 isoforms in human cells (95). Rab proteins were first described in yeast in the 80s, as GTP binding proteins associated with the microtubules and the secretory pathway (96, 97). Soon after, immunofluorescence imaging and electron microscopy showed that Rab proteins colocalized with intracellular membrane compartments, and Rab isoforms seemed to show a differential localization (98). Thus, they are now widely used as an identity markers for intracellular vesicles, as their compartment specificity was extensively characterized (99).

They can be found either bound to GDP, as a cytosolic state, or bound to GTP when they are membrane-associated (100). When activated (Rab-GTP form), they can recruit effector proteins which will either bind another Rab-GDP to coordinate intracellular vesicle trafficking (101), or motor protein to trigger vesicle trafficking among cytoskeleton structure (102).

These effector proteins can also bind tethering proteins to bring two membrane compartments closer and initiate membrane fusion mechanisms.

1.5.2. Tethering proteins: the matchmakers

These proteins allow a specific matching of donor and acceptor compartments to ensure appropriate membrane fusion and content mixing. They consist of several protein complexes that share structural and functional similarity (103, 104). Hereafter are listed some tethering complexes required in intracellular membrane fusions.

The Homotypic fusion and Protein Sorting complex (**HOPS**) is formed by six Vacuolar Protein Sorting (**VPS**) subunits. Two of the VPS subunits can bind GTP-Rab7 proteins (105), which will bridge late endosome with lysosome (

Figure 7) and allow trans-SNARE complex (defined below) to be formed (106). All along the fusion process, the HOPS complex has the crucial role of keeping all fusion actors (proteins and membranes) close enough to each other for the fusion to occur.

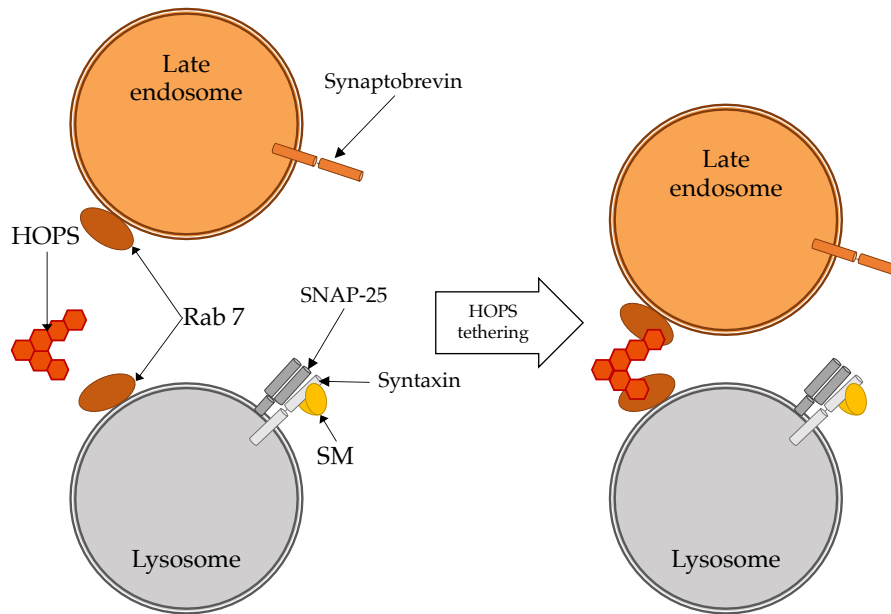


Figure 7: HOPS-mediated tethering of a late endosome and a lysosome

The HOPS complex can bind two Rab7 proteins. As these proteins are both on late endosome and lysosome. Thus, the binding will bring these compartments closer to initiate SNARE-mediated membrane fusion.

Complexes Associated with Tethering Containing Helical Rods (**CATCHR**) are tethering complex involved in intra-Golgi trafficking. They can for instance bind Rab1 and TATA element modulatory factor at the same time, bridging in this way ER-derived vesicles and Golgi membrane respectively (**107**). Finally, the CATCHR complex will bind Rab6 protein, associated to the Golgi membranes, to reinforce the contact site between both membranes, permitting SNARE interactions to occur.

Tethering proteins are not only soluble protein: Golgins, another tetherin family, are anchored to Golgi membranes. A dozen of Golgin were described to be expressed specifically on the different cisternae of the Golgi, to capture the particular vesicles that will deliver their content within the cisterna (**108**). For instance, Golgin-84 and CASP are golgins expressed in the intermediate Golgi cisternae. They can bind to Coat Protein complex I (**COPI**), coating protein of retrograde Golgi vesicle, to attach COPI vesicle to their cisterna membrane (**109**). This proximity will here again initiate SNARE-mediate membrane fusion.

1.5.3. SNARE proteins: the main actors of membrane fusion

One of the first fusion-related proteins characterized is the N-ethylmaleimide-Sensitive Fusion protein (**NSF**), involved in vesicular transport and fusion in the Golgi apparatus (**110**). This soluble cytosolic protein can indeed bind the Golgi membranes with the help of Soluble NSF Attachment Proteins (**SNAPs**) (**111**). This binding to Golgi membrane needed a membrane-associated protein; this is how SNAP REceptors (**SNAREs**) were described for the 1st time in the 90s, in several isoforms, introducing what seemed to be a universal membrane fusion mechanism, with targeting specificity mediated by matching and localization of the different isoforms (**112**). This receptor consists of a complex of three transmembrane proteins (Syntaxin, SNAP-25 and synaptobrevin), displaying a four-helix bundle in the cytosol. This discovery led to

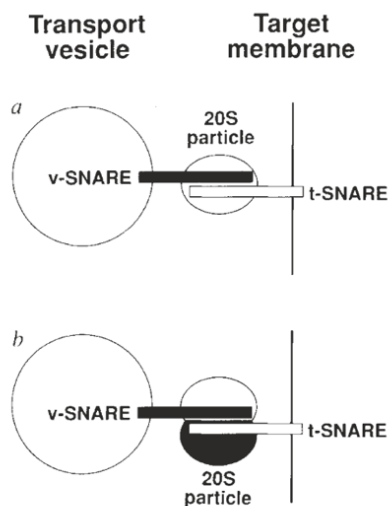


Figure 8: Initial SNARE hypothesis

Schematic views of molecular interactions that allow SNARE-mediated membrane fusion. “Models to explain vesicle targeting based on the finding that SNAREs isolated in 20S fusion particles can originate from either the transport vesicle (v-SNAREs) or from the target membrane (t-SNAREs). A 20S particle (containing NSF and SNAPs) that simultaneously binds a v-SNARE and a t-SNARE (a) would attach a vesicle to its target. Alternatively (b), 20S particles, each capable of binding only one SNARE at a time, could interact to attach vesicle to target, a process that perhaps requires other proteins to assemble together” from Söllner T. et al. (**112**)

what the authors called the “SNARE hypothesis” (with the illustration

Figure 8), where SNAREs can be divided into two subgroups: the transport vesicle SNAREs (v-SNAREs) and the target membrane SNAREs (t-SNAREs), which will specifically combine to allow specific membrane fusion. This specificity was addressed by three complementary studies, showing that only few v-SNARE/t-SNARE combinations led to membrane fusion (**113–115**). The SNARE complex can assemble into 2 conformations: the cis-SNARE, where all the transmembrane domains are inserted in the same membrane, or the trans-SNARE, for which the synaptobrevin form the v-SNARE and the other partner proteins the t-SNARE are on two separated membranes. In the trans-SNARE conformation, the stable combination of t-SNARE and v-SNARE will bring the two membranes closer and exert a force that will lead to

membrane fusion (as illustrated in **Figure 9**) (116). Then the NSF ATPase binds to the SNAP protein to disrupt the SNARE complex, allowing a new cycle of trans SNARE to cis-SNARE fusion process.

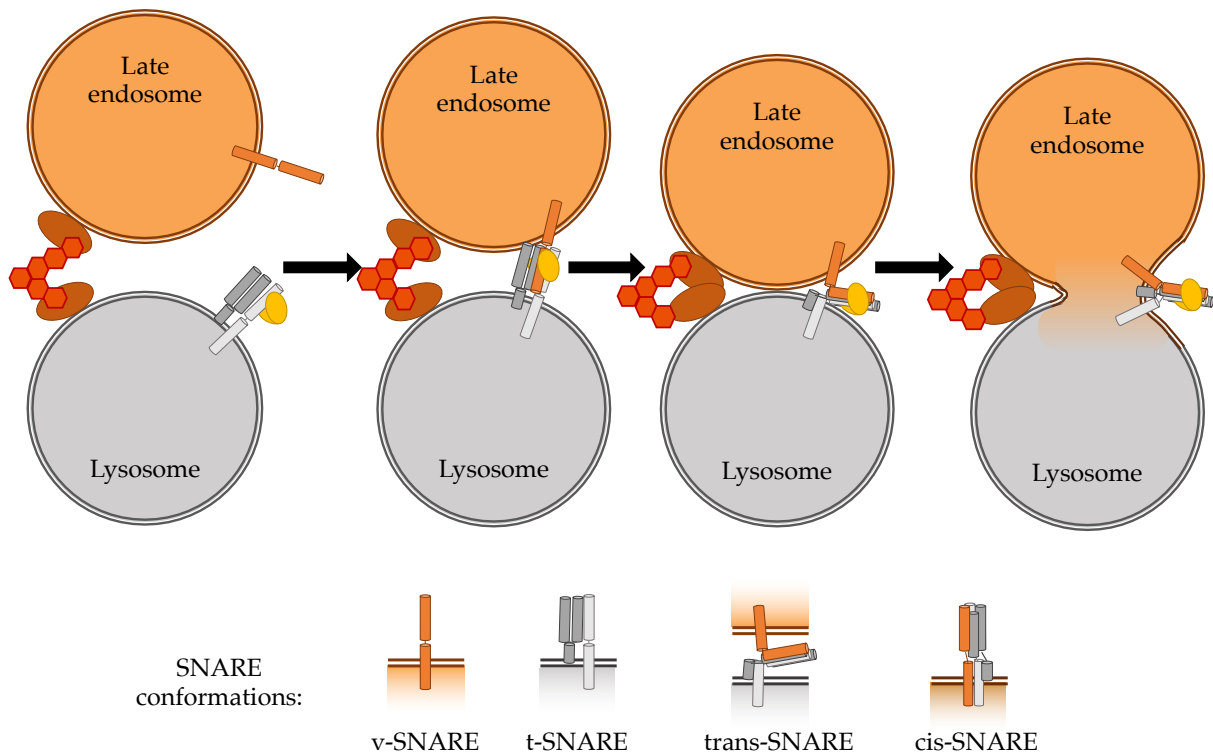


Figure 9: SNARE-mediated vesicle membrane fusion

As consequence of

Figure 7, when late endosome and lysosome are close enough, v-SNARE can bind t-SNARE to create a four-helix bundle (trans-SNARE) reinforced by SM protein (yellow here). Protein interactions will lead to membrane fusion, giving rise at the same time to stable cis-SNARE complex.

This mechanism was first described in the synaptic vesicles content release (112), but we now know that an extended family of SNARE proteins governs most of the fusion mechanisms used by all cell compartments, from ER to Golgi, endocytic vesicles to endolysosomal compartments, secretory vesicles to plasma membrane (117). EVs present an inverted topology compared to the intracellular vesicles. They might use similar mechanism (docking, fusion), but with a different machinery that would act on the luminal side of the membranes.

1.5.4. SNARE-associated proteins

Even though SNARE proteins are sufficient to observe *in vitro* fusion reconstitution between v-SNARE- and t-SNARE-containing compartments (113), in live cells a fourth protein partner is required: Sec1/Munc18-like proteins (SM). These are soluble proteins that bind syntaxin subunits at three different complex stages (syntaxin alone, t-SNARE or trans-SNARE), to coordinate in the membrane fusion (118).

The spontaneous and stable association of SNARE complex needs to be regulated to avoid constant membrane fusion. For instance, the complexin proteins will bind SNARE as a clamp, maintaining the 3 proteins together in cis-SNARE. This conformation avoids NSF to dissociate the complex, thus a new v-SNARE/t-SNARE association (119). It was later observed that complexin clamp could occur at trans-SNARE state, avoiding interaction with SM protein and membrane fusion. This clamp can be removed by the binding of Ca²⁺ ions to synaptotagmin proteins, which will allow these last partners to interact with the SNARE/complexin complex and finally allow membrane fusion (120). This complexin/synaptotagmin OFF/ON fusion system allow “ready-to-fuse” vesicle formation, in neuron for instance, that will fuse and release their content as soon as a Ca²⁺ influx occurs (121).

Importantly, EVs possess an inverted topology compared to the intracellular vesicles using the SNARE fusion machinery. Thus, it is unlikely that this specific fusion machinery is the key factor of the putative EV membrane fusion, but similar fusion complexes might exist as specific EV fusion systems. As they share the same topology than the cell plasma membrane, they might also use proteins and/or lipids involved in cell-cell fusion, including already described/predicted ones as discussed below.

1.5.5. Other fusion proteins

Even though SNAREs are involved in most membrane fusion events, other proteins can mediate specific fusion. They are mainly endogenous viral envelope proteins which were integrated into our genome across evolution.

The first example is the HERV protein family, including syncytin1 and 2 proteins, actors of placenta formation (122). They were both described to display fusogenic

properties leading to syncytia formation mediated by plasma membrane fusion (123, 124). However, little is known concerning the fusion mechanism they mediate. Only syncytin1 structure is described, with a 2-helix coiled coil structure, that can form a stable trimer to bind the syncytin1 target membrane receptor. This binding could trigger protein structural change that will allow the coiled coil trimer to enter in the target membrane to initiate membrane fusion (125). This mechanism is similar to a well characterized fusogenic viral protein: VSV-G protein, which change conformation upon endosomal acidification to initiate membrane fusion (126).

Other tissues require fusion during development, such as muscles. Myoblasts have to go through cell-cell fusion to form polynuclear myotubes. In this process, the plasma membrane protein Myomaker is required for the fusion to occur (127), and can work in synergy with another fusogenic protein, Myomixer (128). The molecular fusion mechanisms involved in myotube formation are still unclear, but downregulation of both protein inhibits membrane fusion, whereas co-expression of Myomaker and Myomixer in fibroblast is sufficient to trigger cell-cell membrane fusion (129).

In *C. elegans*, Epithelial Fusion Failure 1 (**EFF-1**) was identified as necessary for worm development (130), which required cell-cell fusion at several stages. Structural experiment described a similar fusogenic mechanism to the SNARE proteins: EFF-1 are expressed at the plasma-membrane and when homologous extracellular domains bind to form hairpin structures, the plasma membranes are then close enough to initiate membrane fusion (131). Even though this protein is not present in the mammalian genome (132), a hypothesis can be made that similar proteins could exist in mammalian cells.

For instance, CD9 and CD81 tetraspanins were proposed to have a fusogenic effect on sperm-egg membrane fusion (133). It suggested that tetraspanins may create a protein network to connect both membrane extracellular leaflets (134). Interestingly, they may have an opposite effect in myotube formation and mononuclear phagocytes. Down regulation of both CD9 and CD81 proteins in myoblast create an increase of cell-cell fusion, resulting in giant myotubes (135). The same down regulation promotes *in vitro* and *in vivo* fusion between homologous blood monocytes and alveolar macrophages. This evidences at the same time that the inhibitory function of CD9 and CD81 may be mediated by their large extracellular loop (136). Their enrichment in EVs could give them similar fusion regulatory function in the EV content delivery process.

1.6.PhD goals

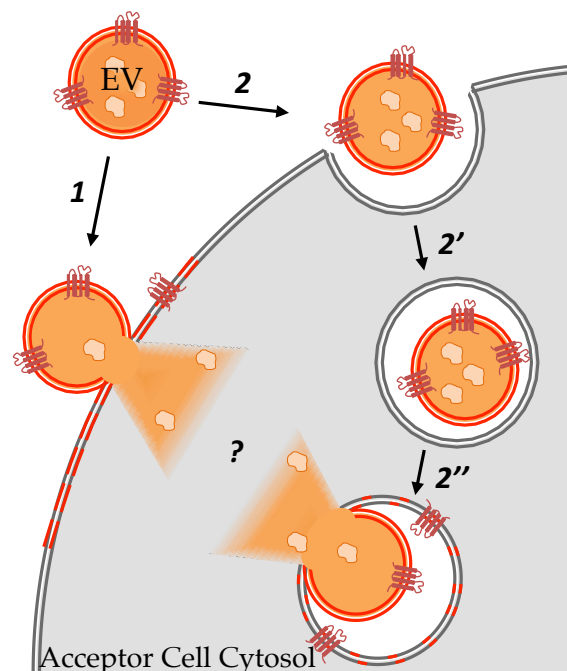
Despite the strong research interest raised by EVs and their possible impact on medicine delivery, EV content delivery within acceptor cells remains poorly characterized. A deeper knowledge of EV content delivery mechanisms is a prerequisite to further develop efficient therapeutics EVs. Plus, this missing knowledge could bring EVs at the level of viruses and liposomes, similar structures for which uptake mechanisms have been known for years.

By analogy with these two lipidic vesicles, at least two hypotheses can be drawn regarding the steps that allow EV content release within the cytosol of acceptor cells (Figure 10). 1) The membrane of the EV can directly fuse with the plasma membrane of the acceptor cell, leading to immediate EV content release. 2) The EV can first be internalized through previously described endocytosis process(es). Then, once directed to its target compartment, the EV could release its content through membrane fusion, using fusion mechanisms that remain to be described. The main goal of this PhD was to characterize EV uptake cellular mechanisms, and to quantify its efficiency.

Figure 10: Hypothetic route for EV content release within acceptor cells

Based on the knowledge on virus and intracellular vesicles trafficking, 2 major hypotheses emerged considering the EV content delivery process within the acceptor cell. Either the EV membrane fuses directly with the plasma membrane of the acceptor cell (1). Or the EV is first internalized in endocytic compartments (2), which will deliver the virus in a specific target compartment (2') where the final EV content release will occur, possibly upon membrane fusion (2'').

To address these points, two assays were developed: a cell-free assay, based on the ones used in virus studies (91), to reconstitute *in vitro* EV content release when EVs were mixed with purified plasma membranes; and a cell-based assay, to follow the fate of EV content in live cells. For both approaches, Heat Shock Protein 70 (HSP70) was used as a generic EV marker (32), to follow the content of the broadest EV population without focusing on a putative specific EV subpopulation. This protein was fused to either a small peptide,



V5, a fluorescent protein, GFP, or an enzyme, the NanoLuc luciferase (**NLuc**), and expressed in donor HeLa cells, which will then secrete labelled EVs.

Once characterized, these EVs were incubated with the acceptor compartments (live cells or plasma membranes), and the fate of their content could be monitored either by western-blot (V5 or GFP tags), confocal imaging (GFP) or enzymatic activity (NLuc). The later display a really high sensitivity (*137*), which allowed quantifying the EV content release within the cytosolic fraction of acceptor cells. This strategy led to the publications of two original papers described in the results section, which highlight some characteristic of EV uptake and delivery within HeLa cells.

2. RESULTS

2.1. EV content release in cell-free assay

This first study was designed to focus on the EV content release step, with its reconstitution *in vitro*. Donor cells were engineered to secrete labelled EVs, containing tagged Hsp70. Once isolated, these EVs were mixed with purified plasma membranes. These membranes were obtained after cell sonication and immune-isolation of plasma membranes from HeLa expressing the CD8-ENLYFQS-GFP chimeric protein.

EV content release was assessed with a protease protection assay. If the protease is added to the EV/plasma membrane mixture, it can only digest proteins which are not protected inside enclosed membranes. Then, tagged Hsp70 should be detectable by western-blot only if protected inside the EVs. If EV content release occurs, then tagged Hsp70 would be digested.

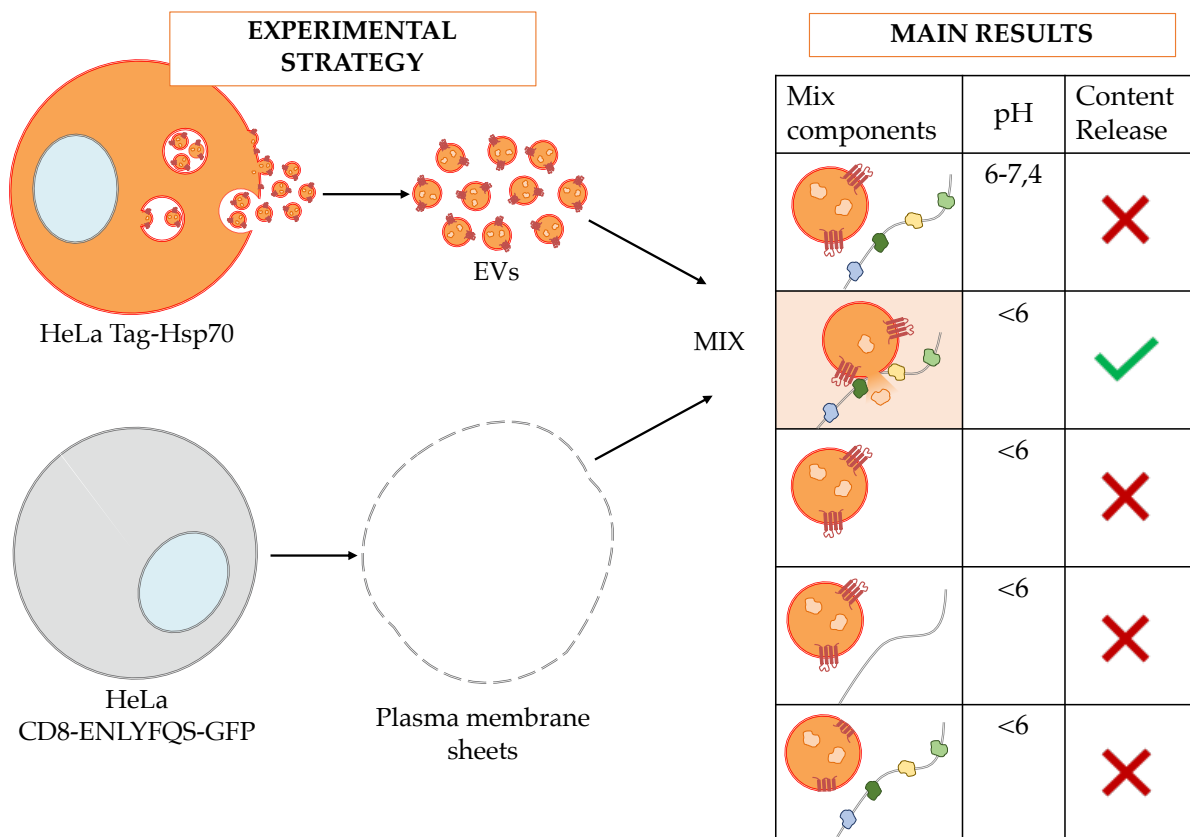


Figure 11: Graphical abstract of EV content release quantification with in cell-free extract

This assay allowed to detect EV content release with plasma membrane sheet as an acceptor membrane, but only upon acidic condition ($\text{pH} \leq 6$). If pH is higher than pH6, no EV content digestion is observed compared to the EVs alone (without plasma membrane). This content release also requires proteins on both EVs and plasma membranes, as pretreatment of one of them with proteinase K abolishes the EV content digestion.

The experimental strategy and the main results are summarized in **Figure 11**, the original article is presented in the following pages, and supplementary information are displayed in **Annex 1**.

Content release of extracellular vesicles in a cell-free extract

Emeline Bonsergent^{1,2} and Gregory Lavieuv¹

¹ INSERM U932, Institut Curie, PSL Research University, Paris, France

² Université Paris Descartes, Paris, France

Correspondence

G. Lavieuv, INSERM U932, Institut Curie, PSL Research University, 26 rue d'Ulm, Paris, 75248, France
E-mail: gregory.lavieuv@curie.fr

(Received 12 March 2019, revised 16 May 2019, accepted 29 May 2019, available online 17 June 2019)

doi:10.1002/1873-3468.13472

Edited by Lukas Alfons Huber

Extracellular vesicles (EVs) transfer molecules from donor to acceptor cells. The EV-content delivery process within the acceptor cell is poorly characterized. We developed a new cell-free assay to assess EV-content release *in vitro*. We found that EV-cytosolic cargoes are released from EVs when isolated vesicles are incubated with purified plasma membrane sheets at acidic pH, a characteristic of the endolysosomal environment. This process is protein dependent. Our results suggest that EV-content delivery occurs within the endo/lysosomes of acceptor cells and is triggered by acidification. This process resembles virus content delivery and may require membrane fusion. The assay presented here will facilitate investigations into the core machinery and mechanisms underlying EV content delivery.

Keywords: endosome; extracellular vesicles; fusion

Extracellular vesicles (EVs) mediate intercellular communication and have been associated with numerous physiological functions [1]. EVs transfer molecules such as nucleic acids and proteins from donor to acceptor cells [2–8]. Functional transfer of cytosolic EV-cargoes such as miRNA, suggest that EVs deliver at least part of their content within the cytosol of the acceptor cells [2]. However, the EV content delivery process is poorly characterized at both cellular and molecular levels. This is not satisfying, especially when considering the high translational impact of EVs.

By analogy with viruses, with which EVs share many physicochemical properties [9], there is at least two possibilities for EVs to deliver their content within the cytosol of the acceptor cells [10]. First, EVs could bind and fuse directly with the plasma membrane of the acceptor cells. Secondly, EVs could enter the acceptor cells through endo-/phago-/pino-cytosis, and then deliver their content through fusion with the endosomal membranes. This indirect pathway often implies that acidification within the endosomes triggers the fusion

reaction. Semliki Forest virus (SFV) uses this indirect pathway, and its fusion machinery is well characterized [11,12]. Importantly, the plasma membrane of the acceptor cell contains all the required physico-chemical properties to fuse with SFV, except one: the acidic pH [13]. pH dependency is therefore a powerful mean to distinguish the two pathways, and a strong indicator for endo/lysosome as the site of delivery.

Briefly, our rather limited knowledge of the EV delivery process can be summarized as follows [14,15]: many EVs are internalized within acceptor cells through multiple endocytic pathways. Most of the internalized EVs are directed to lysosomes, and the efficiency of EV content release into the cytosol is unknown. One study reported direct fusion between EV and the plasma membrane of acceptor cells surrounded by acidic pH [16], which is normally the signature of endosomes, and two other studies reported putative fusion of EV with acceptor cells, without revealing the nature of the target membrane [17,18]. Those disparate and isolated studies fall short when

Abbreviations

DMEM, Dulbecco's modified Eagle's medium; ER, endoplasmic reticulum; EV, extracellular vesicles; SFV, Semliki Forest virus.

compared with seminal work that has been done more than 30 years ago on virus content delivery. For instance, A. Helenius and colleagues clearly demonstrated that SFV could fuse with the plasma membrane and artificial membranes but only at acidic pH [11,13], identified the endosomes as point of delivery [19], and finally identified and characterized the core fusion machinery [20–22].

In an attempt to provide clarity and new insights into the EV content delivery process, we developed a cell-free assay to demonstrate the existence of this event and to characterize the basic governing rules.

We found that EV-cytosolic cargo (contained within EVs) are released from the vesicles when purified EVs are incubated with isolated plasma membrane-derived sheets, and exposed to acidic pH. This process is protein-dependent. Our results suggest that EV content delivery occurs within acidic endo/lysosomes, through a process that might involve membrane fusion.

Materials and methods

Cell culture

HeLa cells (ATCC) were maintained at 37 °C in 5% CO₂ in Dulbecco's modified Eagle's medium (DMEM; Gibco, Grand Island, NY, USA) supplemented with 10% FBS (Gibco). Cells were transfected using lipofectamine 2000 (Invitrogen, Grand Island, NY, USA), following manufacturer instructions. Cells stably expressing GFP-Hsp70 were selected with G418 (Invitrogen).

Plasmids

GFP-Hsp70 construct was purchased from Addgene (#15215; Watertown, MA, USA). V5-Hsp70 construct was obtained by swapping out the GFP sequence, which was replaced by a V5-containing PCR-amplified insert using AgeI/XhoI restriction enzymes (NEB, Ipswich, MA, USA). Note that the V5 insert also contained an Apex encoding sequence that was not used in this study. Template plasmid was purchased from Addgene (#72480). CD8-ENLYFQS-GFP was generated by directed mutagenesis using the quick change site-directed mutagenesis kit (Qiagen, Hilden, Germany) on pC4-CD8-GFP, previously described [23] with the following primer 5'CCCACCATCGCGTCGCAGCCCCTGGAGAATCTTTATTTCCAGGGCTCCCTGCGCCAGAGGCGTGCC3' which introduces a TEVp cleavage sequence (underlined).

EV preparation

Extracellular vesicles were prepared as previously described, through sequential ultracentrifugation protocol with minor modifications [24]. Briefly, confluent GFP-Hsp70- (or V5-Hsp70)-expressing cells were cultured for 24 h in DMEM without FBS. Media was harvested, submitted to 350 *g* centrifugation (10 min, 4 °C). Supernatant was collected and submitted to 2000 *g* centrifugation (30 min, 4 °C). Supernatant was collected and submitted to 10 000 *g* (1 h, 4 °C, 45Ti rotor). Supernatant was collected and centrifuged at 100 000 *g* (1 h30, 4 °C, 45Ti rotor). The latter pellets were washed, resuspended in PBS and centrifuged again at 100 000 *g* (1 h, 4 °C). Pellets were resuspended in 100 µL PBS, and protein concentration was determined using Micro BCA protein assay kit (ThermoScientific, Waltham, MA, USA).

PM sheets preparation

Two days after lipofectamine-based transfection, CD8-ENLYFQS-GFP-expressing HeLa cells were washed in PBS and scrapped. After centrifugation (350 *g*, 4 °C, 5 min), cells were resuspended in 400 µL PBS, prior to being incubated with 100 µL of Protein G-conjugated magnetic beads (Biorad, Hercules, CA, USA) and 2 µL of anti-CD8 antibody (clone Rpa-T8; ebioscience, San Diego, CA, USA) at 4 °C for at least 4 h. Nonattached cells were removed and bead-attached cells were submitted to sonication in 400 µL ice cold PBS using a micro tip sonicator (Ultrasonic Processor, Thomas scientific, Swedesboro, NJ, USA; three pulses of 5 s, 30% duty cycle, output control level 3). Cytoplasm released in the supernatant was discarded, PM remaining attached to the beads were washed three times with 1 m PBS. Bead-attached membranes were resuspended in 100 µL PBS using TEVp (Institut Curie, protein Expression and Purification Core Facility) at 1 µg·mL⁻¹, overnight at 4 °C on rotative wheel. Supernatant containing released-PM sheet was collected and protein concentration was determined using mini BCA protein assay kit.

EV content release assay

Extracellular vesicles were preincubated or not with PM sheets (1 : 1 protein ratio, 5 µg each) at 4 °C for 1 h prior incubation at 25 °C for 1 h. When required, samples were treated with 1% Triton X100. When required we added the 'fusion' buffer (10 mM Na₂HPO₄, 10 mM NaH₂PO₄, 150 mM NaCl, 10 mM 2-(*N*morpholino) ethanesulfonic acid, 10 mM *N*-2-hydroxyethylpiperazine-*N*'9-2-ethanesulfonic acid, adjusted to pH5.5 or required pH) for 1 h or the indicated time at 25 °C. Then samples were

incubated at 4 °C with proteinase K ($2 \mu\text{g}\cdot\text{mL}^{-1}$ except indicated otherwise) for 1 h. Proteinase K was inactivated by adding 0.2 μL of boiled 200 μM PMSF immediately followed by loading buffer (100 °C, 15 min) as previously described [25]. Samples were analyzed by western blot. For pretreatment of EVs and PM sheets by proteinase K (performed as above), the latter was eliminated by addition of 1 mL PBS followed by ultracentrifugation at 100 000 g (40 min, 4 °C, TLA45 rotor). Supernatant was removed before addition of the other components of the content release assay.

Western Blot

Immunoblots were performed as mentioned before [26]. Five microgram of extracted proteins were separated in SDS/PAGE (4–15% miniprotean-TGX stain-free gels; Biorad, Hercules, CA, USA) in the presence of 5% β -mercaptoethanol (except for detection of CD63: no β -mercapto-ethanol in the sample buffer), and then electrotransferred onto PVDF membranes (Biorad, Hercules, CA, USA). After blocking with 5% fat-free milk in PBS-Tween 0.5%, the membranes were incubated with appropriate primary antibodies. Primary antibodies were detected by chemiluminescence using HRP-conjugated secondary antibodies on Chemidoc Touch Imaging system (Biorad, Hercules, CA, USA). Signal Intensity was quantified with IMAGEJ software. We used the following antibodies: anti-GFP (ms, GF28R, 1/2000), anti-V5 (ms, E10/V4RR, 1/200) were from ThermoFisher scientific. Anti-actin (ms, C4, 1/5000) was from Millipore, Burlington, MA, USA. Anti-calnexin (Rb, ab133615, 1/2000) and anti gpp130 (Rb, ab197595, 1/1000) were from Abcam, Cambridge, UK. Anti-integrin $\alpha 6$ (ms, #3750, 1/1000) was from Cell Signaling, Danvers, MA, USA. Anti-CD63 (ms, 556019, 1/1000) and anti-Lamp1 (ms, H4A3, 1/500) were from BD Bioscience, San Jose, CA, USA.

Imaging

CD8-ENLYFQS-GFP-expressing HeLa cells were grown on glass coverslip in 24-well plates. Cells were treated or not with $1 \mu\text{g}\cdot\text{mL}^{-1}$ TEVp at 37 °C for 3 h. Then cells were incubated on ice for 1 h with an antibody raised against the extracellular domain of CD8 (clone Rpa-T8) and an Alexa Fluor 633-coupled secondary antibody to test CD8 cell surface exposure of nonpermeabilized cells. Cells were fixed with 4% PFA and mounted. Images were acquired using a confocal microscope (Leica SP8, Wetzlar, Germany).

For cryo-EM EVs were suspended in 10% gelatin, then placed in cryoprotectant 2.3 M sucrose overnight

at 4 °C. These were transferred to aluminum pins and rapidly frozen in liquid nitrogen. The frozen block was trimmed on an Leica Cryo-EMUC6UltraCut, Wetzlar, Germany and 65 nm thin sections were collected. The frozen sections were thawed and collected on grids prior imaging. Samples were all viewed on FEI Tencai Biotwin TEM at 80Kv. Images were taken using MORADA CCD and ITEM (Olympus, Shinjuku, Tokyo, Japan) software. EM was performed at the Yale Electron Microscopy facility.

Results

Principle of the cell-free assay

To characterize the EV content delivery, we developed a new cell-free system relying on the well-established protease protection assay (Fig 1) [27,25]. The goal was to track the fate of an EV cytosolic cargo that is localized within isolated vesicles. Such a cargo is normally protected from digestion by protease present in the buffer. If/when donor EVs interact with adequate acceptor membrane sheets, in proper conditions, the cargo is released in the buffer and digested by the protease. Our priority was to test PM as putative acceptor membranes, and pH dependency. Thus, this assay required two main components: (a) EVs containing a trackable cytosolic cargo; and (b) plasma membrane sheets in suspension.

Hsp70 is within donor EVs

Hsp70, a cytosolic chaperone, is a long time established EV-associated cargo [24,26,28,29], and is therefore a generic candidate to monitor EV content

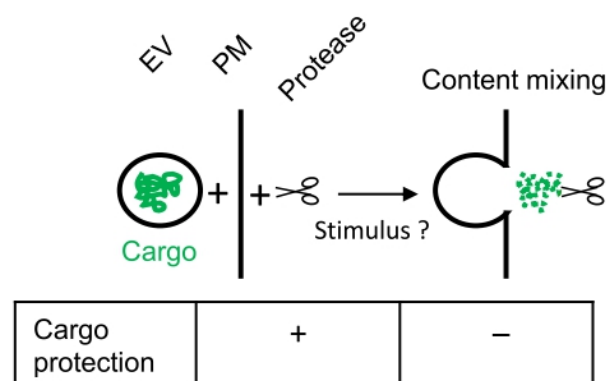


Fig. 1. Principle of the EV content release assay. Purified EVs contain a cargo that is normally protected from protease present in the buffer. Upon proper interaction with PM-derived sheets the EV cargo is expected to be released in the buffer and digested by the protease. Variables such as pH can be adjusted on demand.

release. We generated donor HeLa cells expressing GFP-tagged Hsp70 and isolated EVs from the conditioned medium through established differential ultracentrifugation protocol (Fig 2A). Isolated vesicles contained as expected CD63, a classical EV membrane marker, actin, and GFP-Hsp70 (Fig 2C). As expected calnexin, an endoplasmic reticulum (ER) marker, was absent from the EV fraction. Morphologically, isolated EVs appear as round shape structures, and > 60% of them harboring a size < 100 nm (Fig 1B).

We then tested if GFP-Hsp70 was sensitive to proteinase K digestion. We found that > 95% of GFP-Hsp70 was digested by proteinase K in the presence of detergent, which permeabilized EVs (lane 3 Fig 2D,E). However, less than 20% of GFP-Hsp70 was digested without detergent (lane 2 Fig 2 D,E). This modest digestion suggests the presence of an extracellular free pool of Hsp70, which could be generated through

unconventional secretion [30] or leakage from EVs that were damaged during the isolation procedure. Nevertheless, this demonstrated that most of Hsp70 is within the purified EVs, and constitutes a suitable cargo for the assay. Endogenous actin, and a V5-tagged version of Hsp70 that is used in the second part of this study behaved similarly (Fig. S1).

Purification of plasma membrane sheets as putative acceptor membrane

Assessing EV content release requires access to the luminal face of the acceptor membranes. To control the topology and resuspension of plasma membrane sheets, we engineered a chimeric protein (CD8-ENLYFQS-GFP) that is localized to the plasma membrane and that contains within its proximal luminal domain a specific cleavage site (ENLYFQS)

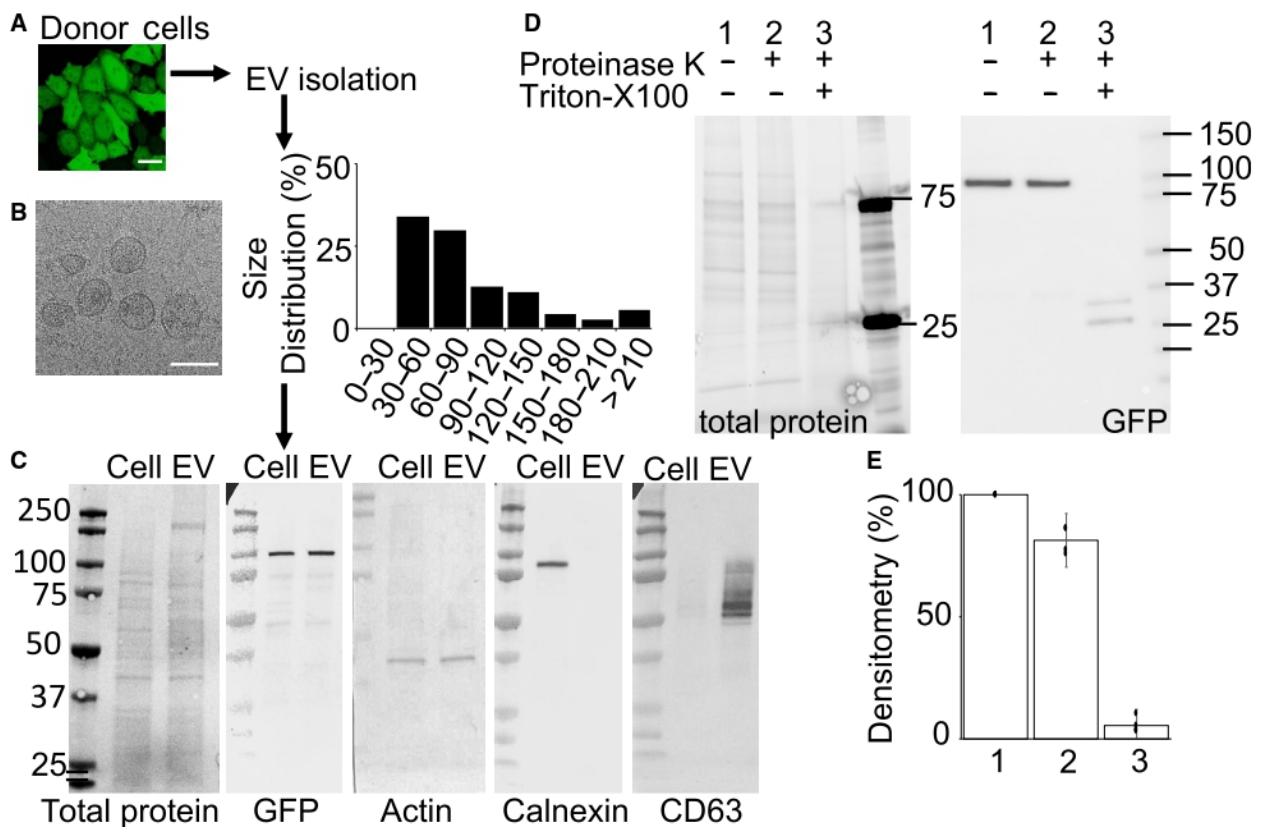


Fig. 2. Characterization of Hsp70-containing EVs. (A) HeLa cells expressing GFP-Hsp70 secrete EVs that are isolated through sequential centrifugations. Bar, 10 μ m. (B) Cryo-electron micrographs showing isolated EVs (100 000 g pellet). Bar, 100 nm. Graph represents the frequency distribution of EVs according to their size (nm). $n = 198$ EVs. (C) Immunoblots showing composition of EVs vs. cell lysate. EVs fractions is depleted of calnexin, an ER marker. (D) EVs were pretreated or not with Triton-X100, and exposed to proteinase K (2 μ g·mL⁻¹, 1 h, 4 °C). After proteinase K neutralization, GFP-Hsp70 protection was assessed by immunoblot. GFP-Hsp70 is within the EVs. (E) Graph represents the densitometry (%) of the GFP-Hsp70. Represented is the mean \pm SD of three experiments. Each experiment is represented by an individual dot.

sensitive to TEVp, a tobacco etch virus-derived protease (Fig. 3A). First, we determined the best conditions to cleave the chimeric protein, by analyzing within the cell lysate accumulation of the cleaved form of the chimeric protein (Fig. 3B). Cleavage was specific since actin remained intact (Fig. 3B). We also analyzed the cell surface labelling using a specific anti-CD8 antibody that only recognizes the most distal luminal portion of the uncleaved CD8-protein (Fig. 3C, red signal) [23,31]. We concluded that TEVp cleaved efficiently and specifically CD8-ENLYFQS-GFP.

We then inserted this cleavage step within a more established sonication-based method to isolate PM

sheets in solution (Fig. 3D) [32]. Briefly, cells expressing CD8-ENLYFQS-GFP were attached on magnetic beads conjugated with the anti-CD8 antibody aforementioned. Sonication was applied on bead-attached cells to unroof them. Released cytoplasm (supernatant fraction) was discarded. Remaining bead-attached PM sheets were subsequently released via action of TEVp. Supernatant containing the resuspended PM sheets was then tested for its content by immunoblotting and compared with the cell lysate (Fig. 3E). Cleaved CD8-ENLYFQS-GFP was found in the PM sheet fraction, as well as integrin, a PM marker. Cytosol (actin), lysosome (Lamp1), and Golgi (Gpp130) markers were virtually absent from the PM sheets preparation. Note

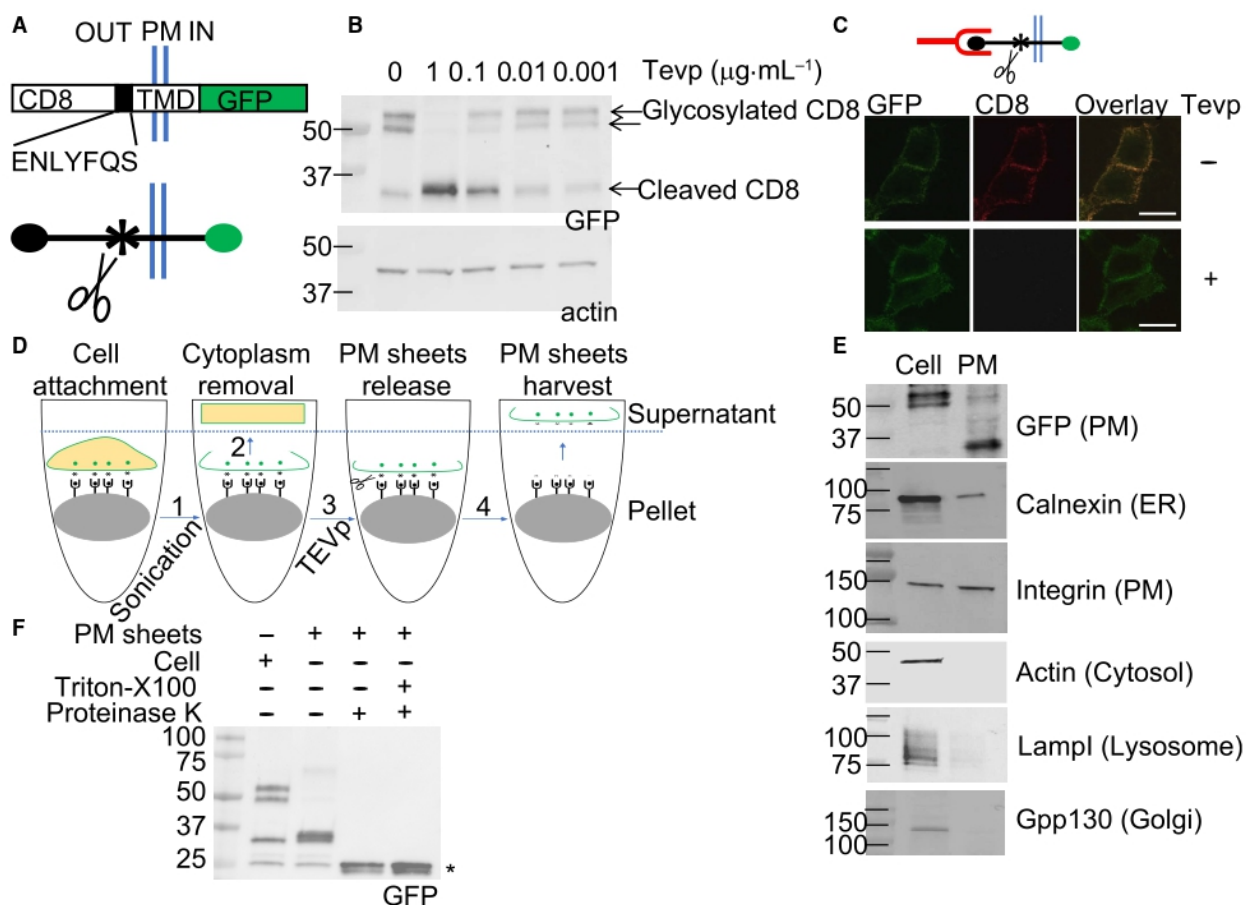


Fig. 3. Characterization of resuspended PM sheets. (A) Scheme representing the chimeric TEVp cleavable CD8-ENLYFQS-GFP, localized at the PM. (B) Immunoblot showing cleavage of CD8-ENLYFQS-GFP by TEVp from cell lysate. (C) Confocal micrograph showing the TEVp-dependent cleavage of CD8-ENLYFQS-GFP at the surface of cells. The red labelled anti-CD8 antibody binds the most distal portion of the luminal CD8-extremity of CD8-ENLYFQS-GFP. (D) Scheme illustrating the PM sheets preparation method. HeLa cells expressing CD8-ENLYFQS-GFP are attached on magnetic beads (gray disc) through the use of the anti-CD8 antibody. Sonication is applied on bead-attached cells to unroof them (1). Supernatant containing released cytoplasm is separated from the bead-attached PM sheets, and discarded (2). Bead-attached PM sheets are subsequently released via action of TEVp (3) and the supernatant containing PM sheets is collected (4, 5). (E) Immunoblot showing the composition of PM sheets vs. cell lysate of untreated cells (input). Equal amount of protein (5 μg) was loaded on the gel. (F) Immunoblot showing the digestion of TEVp-cleaved CD8-ENLYFQS-GFP by proteinase K (2 $\mu\text{g}\cdot\text{mL}^{-1}$, 1 h, 4 °C) whether detergent was added or not to the PM sheets. *, digestion products. PM membrane-derived membranes form open sheets.

that an ER marker (Calnexin) was found in the PM sheet fraction. This is perhaps due to the copious amount of cortical ER that is often associated with plasma membrane [23].

Purified biological membranes are thought to possibly reseal and form closed vesicles when biochemically purified [33]. We assessed if PM sheets prepared with this new method were truly opened layered membranes, using the proteinase K protection assay. If PM sheets reseal, at least half of the GFP signal (emanating from the cytosolic portion of TEVp-digested CD8-ENLYFQS-GFP) should be protected from proteinase K digestion in the absence of detergent. This was not the case. The protein was entirely digested whether detergent was added or not (Fig. 3F).

Altogether, these results established that PM sheets prepared through this method roughly reflect PM composition with opened conformation, which makes of them suitable acceptor membrane candidates.

EV content release is pH dependent

With these two components in hand we proceeded further and assessed EV content release through proteinase K protection of V5- or GFP-tagged Hsp70 (hereafter named Hsp70) in various conditions. Consistent with our previous results, EVs treatment with proteinase K alone led to >80% Hsp70 protection (negative control, lane 2 Fig. 4A,B), whereas adding detergent led to <20% Hsp70 protection (positive control, lane 4 Fig. 4A,B). When EVs and PM sheets were mixed, and then submitted to proteinase K treatment, >80% of the EV cargo was still protected (lane 5, Fig. 4A,B), showing the lack of spontaneous content mixing. Strikingly, exposure to pH 5.5 of the PM sheets/EVs mixture led to <20% Hsp70 protection (lane 6, Fig. 4A,B), synonymous of a massive release of the cargo from EVs. Similar acidic exposure of EVs alone did not lead to significant Hsp70 degradation

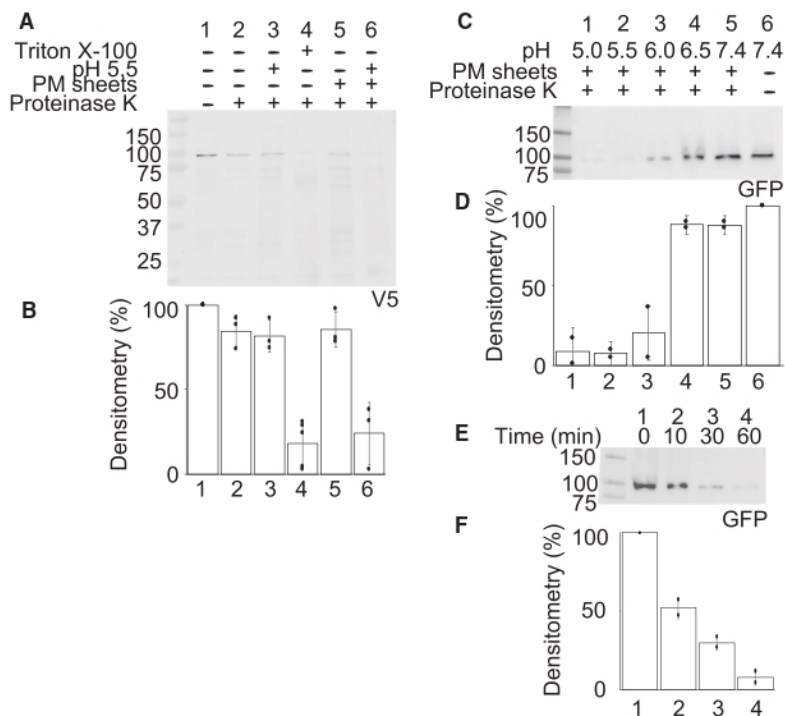


Fig. 4. EV content release is pH dependent. (A) immunoblot showing the status of digestion of V5-tagged Hsp70 (EV cargo) in various conditions. TritonX100, which permeabilized the membrane led to V5-Hsp70 digestion (lane 4, positive control). Hsp70 is digested when EVs are incubated with PM sheets and exposed to pH 5.5 (lane 5). In all other conditions, Hsp70 remains protected. (B) Graph showing the densitometry of the V5 signal. Represented is the mean \pm SD of at least three experiments. Each experiment is represented by a single dot. (C) pH titration. Immunoblot showing the status of GFP-Hsp70 digestion after EVs were incubated or not with PM sheets, exposed at different pH, and treated with proteinase K (except for lane 6, negative control). Content release (i.e. GFP-Hsp70 digestion) is inhibited when pH > 6.0. (D) Graph showing the densitometry of the GFP signal. Represented is the mean \pm SD of two experiments. Each experiment is represented by a single dot. (E) Kinetics. Immunoblot showing the status of GFP-Hsp70 after incubating EVs with PM sheets at pH5.5 for different times, prior treatment with proteinase K. EV cargo release increases with time. (F) Same as in D.

(lane 3 Fig. 4A,B), ruling out a putative pH-dependent side effect on EV membrane integrity. Further, pH titration experiments revealed that EV-content release occurred from pH 5.0 to 6.0, whereas a pH > 6.0 abolished this event (Fig. 4C,D).

We then assessed the kinetics of the reaction and found that > 50% of the EV cargo was released within 10 min of acidic exposure of EV/PM sheets mixture (Fig. 4E,F). Importantly, we also established temperature dependency and showed that EV-content release did not occur at 4 °C (Fig. S2). These results suggest that EV content release is triggered by pH acidification and requires donor EVs and PM-derived acceptor membranes.

EV content release is protein dependent

To assess protein dependency, we pretreated either donor EVs or acceptor PM sheets with proteinase K. After pretreatment, proteinase K was washed out and membranes were recovered by centrifugations. For rigorous comparison we added this additional centrifugation step in the protocol, even in the absence of pretreatment and we again assessed EV content release through proteinase K protection assay. Consistently with previous data, donor EVs released their content only when mixed with PM sheets and exposed to acidic pH (lane 1 and 2, A, B Fig. 5), demonstrating that the additional centrifugation step did not introduced unexpected bias. Strikingly, protein shaving from the surface of either donor EVs or acceptor PM sheets led to > 85% and > 75% Hsp70 protection, respectively (lane 3, 4 Fig. 5A,B). This demonstrates that proteins present at the surface of both EVs and PM-derived membranes are required for EV content release. This seems consistent with previous study reporting protein requirement for EV-internalization, a putative prerequisite for the content delivery event [34].

Discussion

From our results we conclude that EV content delivery requires (a) PM-derived membranes; (b) acidification; and (c) proteins at the surface of both donor EVs and acceptor membranes. This strongly suggests that endo/lysosomes are the main station for EV-content sorting. This is consistent with numerous studies reporting EV internalization through multiple pathways. Because those studies mostly used membrane dyes or markers, they could not assess the cytosolic delivery of EV-cargo, let alone the efficiency of this process. Our study fills this gap.

A caveat of our system is that both faces of the PM sheets are exposed. Although we cannot completely

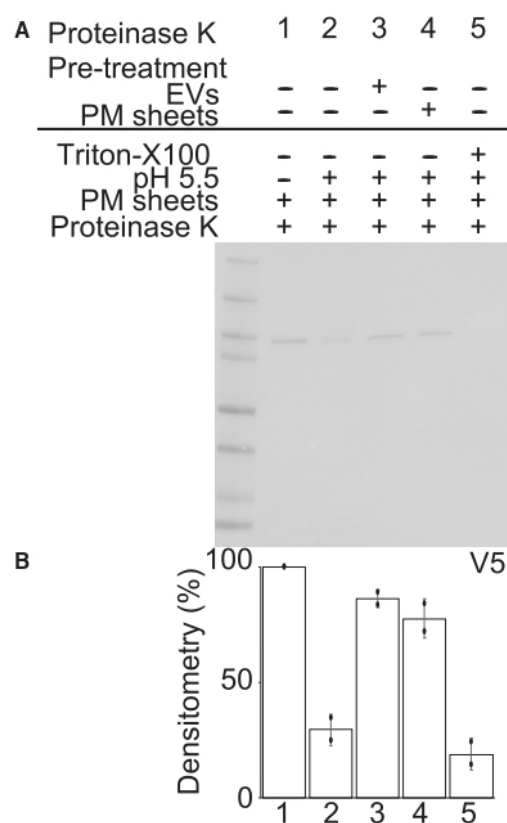


Fig. 5. EV content release is protein dependent. (A) immunoblot showing the status of V5-Hsp70 in various conditions. Pretreatment of either EVs (lane 3) or PM sheets (lane 4) with proteinase K inhibits EVs content release that is normally observed when both components are exposed at pH 5.5 (lane 2). (B) Graph showing the densitometry of V5. Represented is the mean \pm SD of two experiments. Each experiment is represented by a single dot.

rule out that at least a fraction of the EV interacts with the cytosolic face of the PM sheets, this seems very unlikely because (a) such a reaction would be physiologically irrelevant (EVs are within the lumen); (b) in our system, cytosol and energy are not required for EV content release, which suggests that we are indeed measuring a luminal event.

How EVs deliver their cytosolic cargo? Our results suggest that EV content delivery may occur through membrane fusion between EV and late endosome membrane, that is pH- and protein-dependent. Since proteins are required on both EVs and acceptor membranes, the simplest working model would be to consider the formation of a transprotein complex that could be involved in both membranes docking and fusion. Of course, the mechanism could also be more complex, as it is often the case with biological processes.

Another possibility is that within live cells, EVs and their content are first partially digested in endosomes

and then released within the cytosol by escaping from damaged endosomes [35]. Although we cannot rule out this possibility within intact cells, this seems unlikely because our *in vitro* assay does not deal with functional endo/lysosomes.

Remarkably, our *in vitro* EV content release assay is efficient (> 80%) and moderately fast (50% within 10 min). This is roughly comparable to *in vitro* liposome-based reaction recapitulating the SNARE-mediated fusion (50% within 10 min) [36], and slower than the *in vitro* SFV-fusion reaction (> 90% efficiency within 2 min) [11]. Note that both studies had the advantage of using dedicated molecular components (known fusogenic proteins and optimal lipid composition). Interestingly, these two examples of membrane fusion also require proteins, although their respective modes of action differ. On the same line, intraluminal vesicles residing inside multi-vesicular endosomes have been proposed to fuse with the endosomal membrane through a process termed back-fusion [37]. Those vesicles are indeed the source of exosomes, an EV-subtype released from the donor cells, but would also correspond to EVs internalized within the acceptor cells, our model here.

Why then EVs seem so poorly efficient to deliver EV-packaged cytosolic molecules such as cGAMP, when compared to EVs harboring VSV-G, the fusogenic protein of VSV [38]. One clue might come from the fact that the hypothetical fusogenic molecules are present at very low doses within naturally secreted EVs, whereas engineered VSV-G coated EVs (emanating from cells overexpressing VSV-G), harbor a copious amount of the fusogenic protein which favors artificial content delivery. Similar observations have been made with VSV-G pseudotype viruses that were up to 100 times more infectious than WT HIV1 [39], suggesting that as for those viruses, EV-content delivery might be relatively modest.

Those speculations can now be translated into testable hypothesis, for which further development of our assay will be pivotal. This assay will be the ideal companion for cell-based assays to dissect the mechanical aspects of the EV content delivery process. A now famous cell-free assay [40] led to the identification of key molecules governing the secretory pathway, a related aspect of membrane trafficking. The work presented here may be the first step toward the identification of the core machinery required for EV content delivery.

Acknowledgements

GL thanks James. E Rothman for his support when the project was initiated at Yale University and

Clotilde Théry for valuable input during finalization of this work at Institut Curie. GL thanks Graham Morven for the electron microscopy. We thank Ahmed El Marjou and the Protein Expression and Purification Core Facility of Institut Curie for providing recombinant TEVp. EB is a recipient of a PhD fellowship from La ligue contre le Cancer. This work is supported by Fondation ARC (PJA20171206453), Cancéropôle Île-de-France (Emergence 2018) and French National Research Agency (ANR-10-IDEX-0001-02 PSL*, ANR-11-LABX-0043 and ANR-18-CE15-0008).

Author contributions

EB and GL designed and performed experiments, analysed the data, and wrote/edit the manuscript.

References

- 1 Tkach M and Théry C (2016) Communication by extracellular vesicles: where we are and where we need to go. *Cell* **164**, 1226–1232.
- 2 Valadi H, Ekström K, Bossios A, Sjöstrand M, Lee JJ and Lötvall JO (2007) Exosome-mediated transfer of mRNAs and microRNAs is a novel mechanism of genetic exchange between cells. *Nat Cell Biol* **9**, 654–659.
- 3 Skog J, Würdinger T, van Rijn S, Meijer DH, Gainche L, Curry WT, Carter BS, Krichevsky AM, Breakefield XO and Breakefield XO (2008) Glioblastoma microvesicles transport RNA and proteins that promote tumour growth and provide diagnostic biomarkers. *Nat Cell Biol* **10**, 1470–1476.
- 4 Balaj L, Lessard R, Dai L, Cho Y-J, Pomeroy SL, Breakefield XO and Skog J (2011) Tumour microvesicles contain retrotransposon elements and amplified oncogene sequences. *Nat Commun* **2**, 180.
- 5 Kanada M, Bachmann MH, Hardy JW, Frimansson DO, Bronsart L, Wang A, Sylvester MD, Schmidt TL, Kaspar RL, Butte MJ *et al.* (2015) Differential fates of biomolecules delivered to target cells via extracellular vesicles. *Proc Natl Acad Sci* **112**, 201418401.
- 6 Mack M, Kleinschmidt A, Brühl H, Klier C, Nelson PJ, Cihak J, Plachý J, Stangassinger M, Erfle V and Schlöndorff D (2000) Transfer of the chemokine receptor CCR6 between cells by membrane-derived microparticles: a mechanism for cellular human immunodeficiency virus 1 infection. *Nat Med* **6**, 769–775.
- 7 Al-Nedawi K, Meehan B, Micallef J, Lhotak V, May L, Guha A and Rak J (2008) Intercellular transfer of the

- oncogenic receptor EGFRvIII by microvesicles derived from tumour cells. *Nat Cell Biol* **10**, 619–624.
- 8 Korkut C, Li Y, Koles K, Brewer C, Ashley J, Yoshihara M and Budnik V (2013) Regulation of postsynaptic retrograde signaling by presynaptic exosome release. *Neuron* **77**, 1039–1046.
 - 9 Nolte-Hoen E, Cremer T, Gallo RC and Margolis LB (2016) Extracellular vesicles and viruses: are they close relatives? *Proc Natl Acad Sci USA* **113**, 9155–9161.
 - 10 Helenius A (2018) Virus entry: looking back and moving forward. *J Mol Biol* **430**, 1853–1862.
 - 11 White J and Helenius A (1980) pH-dependent fusion between the Semliki Forest virus membrane and liposomes. *Proc Natl Acad Sci USA* **77**, 3273–3277.
 - 12 White JM and Whittaker GR (2016) Fusion of enveloped viruses in endosomes. *Traffic* **17**, 593–614.
 - 13 White J, Kartenbeck J and Helenius A (1980) Fusion of Semliki forest virus with the plasma membrane can be induced by low pH. *J Cell Biol* **87**, 264–272.
 - 14 Mulcahy LA, Pink RC and Carter DRF (2014) Routes and mechanisms of extracellular vesicle uptake. *J Extracell Vesicles* **3**, 24641.
 - 15 Mathieu M, Martin-Jaular L, Lavieu G and Théry C (2019) Specificities of secretion and uptake of exosomes and other extracellular vesicles for cell-to-cell communication. *Nat Cell Biol* **21**, 9–17.
 - 16 Parolini I, Federici C, Raggi C, Lugini L, Palleschi S, De Milito A, Coscia C, Iessi E, Logozzi M, Molinari A *et al.* (2009) Microenvironmental pH is a key factor for exosome traffic in tumor cells. *J Biol Chem* **284**, 34211–34222.
 - 17 Del Conde I, Shrimpton CN, Thiagarajan P and López JA (2005) Tissue-factor-bearing microvesicles arise from lipid rafts and fuse with activated platelets to initiate coagulation. *Blood* **106**, 1604–1611.
 - 18 Montecalvo A, Larregina AT, Shufesky WJ, Beer Stolz D, Sullivan MLG, Karlsson JM, Baty CJ, Gibson GA, Erdos G, Wang Z *et al.* (2012) Mechanism of transfer of functional microRNAs between mouse dendritic cells via exosomes. *Blood* **119**, 756–766.
 - 19 Marsh M, Bolzau E and Helenius A (1983) Penetration of Semliki Forest virus from acidic prelysosomal vacuoles. *Cell* **32**, 931–940.
 - 20 Marsh M, Bolzau E, White J and Helenius A (1983) Interactions of Semliki Forest virus spike glycoprotein rosettes and vesicles with cultured cells. *J Cell Biol* **96**, 455–461.
 - 21 Kondor-Koch C, Burke B and Garoff H (1983) Expression of Semliki Forest virus proteins from cloned complementary DNA. I. The fusion activity of the spike glycoprotein. *J Cell Biol* **97**, 644–651.
 - 22 Kielian MC, Keränen S, Kääriäinen L and Helenius A (1984) Membrane fusion mutants of Semliki Forest virus. *J Cell Biol* **98**, 139–145.
 - 23 Lavieu G, Orci L, Shi L, Geiling M, Ravazzola M, Wieland F, Cosson P and Rothman JE (2010) Induction of cortical endoplasmic reticulum by dimerization of a coatamer-binding peptide anchored to endoplasmic reticulum membranes. *Proc Natl Acad Sci USA* **107**, 6876–6881.
 - 24 Kowal J, Arras G, Colombo M, Jouve M, Morath JP, Primdal-Bengtson B, Dingli F, Loew D, Tkach M and Théry C (2016) Proteomic comparison defines novel markers to characterize heterogeneous populations of extracellular vesicle subtypes. *Proc Natl Acad Sci USA* **113**, E968–E977.
 - 25 Sharma A, Mariappan M, Appathurai S and Hegde RS (2010) *In vitro* dissection of protein translocation into the mammalian endoplasmic reticulum. *Methods Mol Biol (Clifton, N.J.)* **619**, 339–363.
 - 26 Pan BT and Johnstone RM (1983) Fate of the transferrin receptor during maturation of sheep reticulocytes *in vitro*: selective externalization of the receptor. *Cell* **33**, 967–978.
 - 27 Sabatini DD and Blobel G (1970) Controlled proteolysis of nascent polypeptides in rat liver cell fractions. II. Location of the polypeptides in rough microsomes. *J Cell Biol* **45**, 146–157.
 - 28 Mathew A, Bell A and Johnstone RM (1995) Hsp-70 is closely associated with the transferrin receptor in exosomes from maturing reticulocytes. *Biochem J* **308** (Pt 3), 823–830.
 - 29 Jeppesen DK, Fenix AM, Franklin JL, Higginbotham JN, Zhang Q, Zimmerman LJ, Liebler DC, Ping J, Liu Q, Evans R *et al.* (2019) Reassessment of exosome composition. *Cell* **177**, 428–445.e18.
 - 30 Mambula SS and Calderwood SK (2006) Heat shock protein 70 is secreted from tumor cells by a nonclassical pathway involving lysosomal endosomes. *J Immunol (Baltimore, Md. 1950)* **177**, 7849–7857.
 - 31 Lavieu G, Zheng H and Rothman JE (2013) Stapled Golgi cisternae remain in place as cargo passes through the stack. *eLife* **2**, e00558.
 - 32 Wu M, Huang B, Graham M, Raimondi A, Heuser JE, Zhuang X and De Camilli P (2010) Coupling between clathrin-dependent endocytic budding and F-BAR-dependent tubulation in a cell-free system. *Nat Cell Biol* **12**, 902–908.
 - 33 Work T.S. (1979) General methods for the preparation of plasma membranes. In *Laboratory Techniques in Biochemistry and Molecular Biology* (T.S. Work, ed), vol. 7, pp. 45–92. Elsevier, Cambridge, MA.
 - 34 Escrevente C, Keller S, Altevogt P and Costa J (2011) Interaction and uptake of exosomes by ovarian cancer cells. *BMC Cancer* **11**, 108.
 - 35 Skowyra ML, Schlesinger PH, Naismith TV and Hanson PI (2018) Triggered recruitment of ESCRT machinery promotes endolysosomal repair. *Science* **360**, eaar5078.

- 36 Weber T, Zemelman BV, McNew JA, Westermann B, Gmachl M, Parlati F, Söllner TH and Rothman JE (1998) SNAREpins: minimal machinery for membrane fusion. *Cell* **92**, 759–772.
- 37 Bissig C and Gruenberg J (2014) ALIX and the multivesicular endosome: ALIX in Wonderland. *Trends Cell Biol* **24**, 19–25.
- 38 Gentili M, Kowal J, Tkach M, Satoh T, Lahaye X, Conrad C, Boyron M, Lombard B, Durand S, Kroemer G *et al.* (2015) Transmission of innate immune signaling by packaging of cGAMP in viral particles. *Science (New York, N.Y.)* **349**, 1232–1236.
- 39 Aiken C (1997) Pseudotyping human immunodeficiency virus type 1 (HIV-1) by the glycoprotein of vesicular stomatitis virus targets HIV-1 entry to an endocytic pathway and suppresses both the requirement for Nef and the sensitivity to cyclosporin A. *J Virol* **71**, 5871–5877.
- 40 Fries E and Rothman JE (1980) Transport of vesicular stomatitis virus glycoprotein in a cell-free extract. *Proc Natl Acad Sci USA* **77**, 3870–3874.

Supporting information

Additional supporting information may be found online in the Supporting Information section at the end of the article.

Fig. S1. Cargo topology. EVs emanating from HeLa cells expressing V5-Hsp70 were submitted to proteinase K treatment at various concentrations, in the presence or absence of Triton X100. After Proteinase K neutralization, we assessed by immunoblot the protection of overexpressed V5-Hsp70 and endogenous actin, both found in EVs.

Fig. S2. EV-content release is temperature dependent. Immunoblot showing the status of GFP-Hsp70 after proteinase K treatment. After 1 h preincubation at 4 °C, all samples (except lane 4, which remained at 4 °C for an additional hour) were incubated at 25 °C for an additional hour. *, digestion products emanating from GFP-PM sheet (as shown in lane 6) and/or GFP-Hsp70 (as shown in lane 3).

2.2. EV uptake and content release in cell-based assay

In this second study, a cell-based assay was set up to look at the overall EV uptake, from the putative docking to the EV content release using a cell fractionation step. Here again donor cell lines were generated to secrete GFP-Hsp70- or NLuc-Hsp70-containing EVs. These isolated EVs were first characterized, and then incubated with unlabeled acceptor cells, HeLa WT.

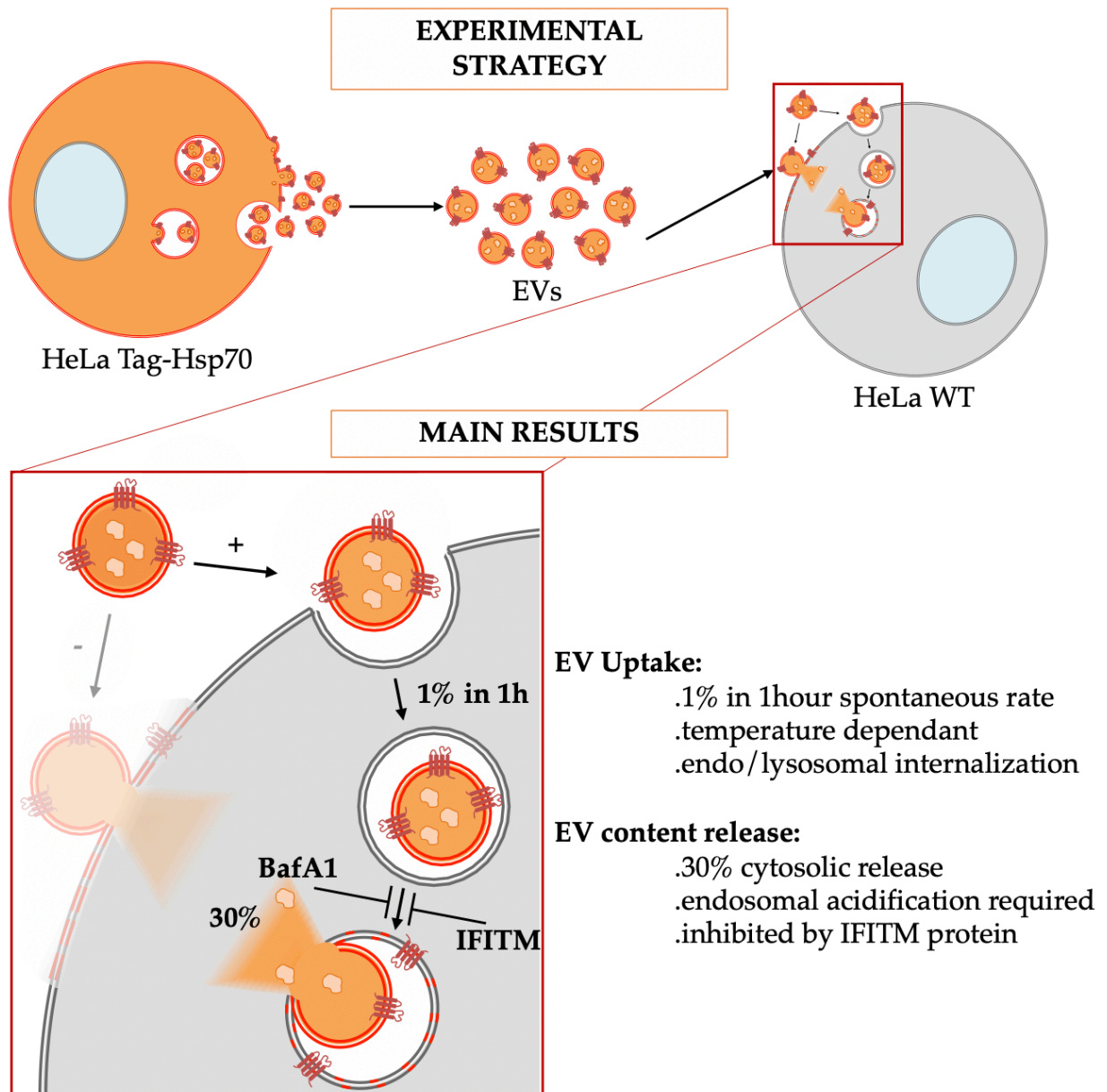


Figure 12: Graphical abstract of the cellular characterization of EV uptake and content delivery within HeLa cells.






Kinetic and dose/response experiments showed that EV uptake is not saturable even at high EV doses (up to 100 μ g/mL) and temperature dependent (no significant EV uptake at 4°C). This strongly suggests that there is no specific EV receptor on HeLa cells. At 37°C, the EV uptake increase overtime, with a spontaneous rate of 1% in one hour.

Upon confocal imaging, EV content colocalized with endosomes and lysosomes of acceptor cells, confirming that at least a part of the EV content is internalized within the acceptor cells.

Cell fractionation was performed on acceptor cells after incubation with NLuc-Hsp70 EVs. Looking at the NLuc activity in the cytosolic fraction of the acceptor cells, EV content release was detected and quantified: 30% of the EV content associated with the acceptor cells was recovered within their cytosol. This cytosolic release requires endosomal acidification, as Bafilomycin A1 inhibits it. Plus, it is likely that a fusion step occurs during the EV content release, as InterFeron-Induced TransMembrane (**IFITM**) protein expression by acceptor cells also decreases EV content release. Indeed, these proteins are known to inhibit viral entry by inhibition of membrane fusion.

This study is the first quantitative characterization of the cellular mechanisms involved in EV uptake and content delivery. The experimental strategy and the main results are summarized in **Figure 12**, the full original article follows and the supplementary figures are presented in **Annex 2**.

Quantitative characterization of extracellular vesicle uptake and content delivery within mammalian cells

Emeline Bonsergent ^{1,2}, Eleonora Grisard¹, Julian Buchrieser ³, Olivier Schwartz³, Clotilde Théry ¹ & Grégoire Lavieau ^{1,2} 

Extracellular vesicles (EVs), including exosomes, are thought to mediate intercellular communication through the transfer of cargoes from donor to acceptor cells. Occurrence of EV-content delivery within acceptor cells has not been unambiguously demonstrated, let alone quantified, and remains debated. Here, we developed a cell-based assay in which EVs containing luciferase- or fluorescent-protein tagged cytosolic cargoes are loaded on unlabeled acceptor cells. Results from dose-responses, kinetics, and temperature-block experiments suggest that EV uptake is a low yield process (~1% spontaneous rate at 1 h). Further characterization of this limited EV uptake, through fractionation of membranes and cytosol, revealed cytosolic release (~30% of the uptaken EVs) in acceptor cells. This release is inhibited by bafilomycin A1 and overexpression of IFITM proteins, which prevent virus entry and fusion. Our results show that EV content release requires endosomal acidification and suggest the involvement of membrane fusion.

¹Institut Curie, PSL Research University, INSERM U932, Paris, France. ²Université de Paris, INSERM, CNRS UMR 7057, Paris, France. ³Institut Pasteur, Virus and Immunity Unit, Department of Virology, CNRS, UMR 3569, Paris, France. ✉email: gregory.lavieau@inserm.fr

Extracellular vesicles, which include exosomes and microvesicles, contain cargoes such as nucleic acids, proteins and lipids¹. As many other vectors of communication, EVs mediate cell–cell communication through activation of receptors located at the surface of acceptor cells². In addition, EVs have been proposed to transfer membrane encapsulated cargoes from donor to acceptor cells^{3–9}, and impact the phenotype of the latter. EVs released by tumor cells are often described as instrumental in affecting tumor surrounding cells to favor their own growth and dissemination^{10,11}.

EVs are internalized by many cell types and through multiple pathways^{1,12}. Endo/lysosomal targeting is often a pre-requisite for the content delivery of viruses, that in several cases is controlled by the acidic endo/lysosomal pH that triggers fusion between virus and endo/lysosomal membranes¹³. Our previous study that used a cell-free system¹⁴, and others¹⁵, suggest that EV-content delivery relies on similar pH-dependent mechanism. However, the true occurrence of EV-content release within acceptor cells remains debated, and has never been rigorously demonstrated, nor quantified. Until now, only EV uptake has been quantitatively assessed¹⁶. In addition, there is no consensus regarding the mode of EV uptake, which could be receptor-dependent or not. For instance, several cell surface molecules have been proposed to play a role in EV capture^{17–21}, but none of them seems required and sufficient. In addition, fate of EV cargoes within the acceptor cells is not characterized. EV cargoes could be released in the cytosol, degraded within lysosome, or re-secreted in the extracellular media through recycling within newly formed EV.

Here, we combined well-established quantitative classical biochemistry with qualitative and quantitative subcellular confocal imaging, to follow the fate of a generic EV cytosolic cargo and measure the actual efficacy of EV capture and content transfer into acceptor cells. Our results suggest that EV-content release requires endosomal acidification and membrane fusion.

Results

Validation of NLuc-Hsp70 as an EV-encapsulated cargo. First, we engineered donor HeLa cells stably expressing NanoLuc luciferase-tagged Hsp70 (hereafter named NLuc-Hsp70). We focused on Hsp70, an established generic EV marker^{22–24}, thus a good candidate for cytosolic release assessment, in contrast with most of the EV markers that are membrane-associated. Importantly, we successfully validated and used this EV cargo in our recent cell-free reconstitution study¹⁴. We used NanoLuc luciferase, a recently engineered luciferase that has superior signal-to-noise ratio, to ensure high sensitivity detection of our assay²⁵. In-gel luciferase activity from lysates of cells that stably expressed NLuc-Hsp70, revealed that the chimeric proteins migrated, as expected, as a unique band corresponding to a >75 kDa protein (Fig. 1a). The absence of detectable partial degradation of NLuc-Hsp70 validated the relevance to monitor NLuc-Hsp70 behavior/fate exclusively through its enzymatic/NLuc activity.

We then isolated EVs released by NLuc-Hsp70 positive donor cells through sequential ultracentrifugation, and compared the luciferase activity between equal protein amount from cell lysate of donor cells and isolated EVs emanating from those cells (Fig. 1b). Enzymatic activities were similar, showing lack of cargo's enrichment within EVs. This is consistent with our previous results¹⁴ and suggests bulk loading of Hsp70 within EVs. As expected, the EV fraction was positive and enriched for classical EV markers such as CD63, CD9, positive for Alix, and negative for Calnexin, an endoplasmic reticulum resident protein generally absent from EVs (Fig. 1c). In addition, and accordingly to the standards for studies of EVs²⁶, isolated vesicles were also

qualitatively validated by electron-microscopy (Supplementary Fig. 1).

Throughout this study, we used the NLuc-CD63 chimeric protein as a control, alongside NLuc-Hsp70. To validate this control, we first performed in-gel luciferase activity on cells transiently expressing NLuc-CD63, which satisfyingly showed lack of significant NLuc-CD63 degradation (Fig. 1a). We also measured luciferase activity in EV and cell lysate and observed on average an enrichment of NLuc-CD63 in the EV fraction (Fig. 1b), consistent with the known enrichment of endogenous CD63.

We then investigated if NLuc-Hsp70 was truly inside EVs, and if the integrity of the EV was not compromised by the isolation procedure. We used a well-established proteinase protection assay, in which cargo contained in a vesicle can only be digested by a proteinase present in the buffer if membranes are disrupted by detergents^{14,27,28}. As a positive control, we used NLuc-CD63, in which the luciferase enzyme was fused to the cytoplasmic N-terminal extremity of the tetraspanin CD63 (inside the vesicle). Both chimeric proteins behave similarly (Fig. 1d): in absence of detergent, roughly 80% of the NLuc activity was recovered for both cargoes (75 ± 5% and 80 ± 11% for NLuc-Hsp70 and NLuc-CD63, respectively). In presence of detergent, NLuc activity dropped to <20% for both cargoes, suggesting that the luciferase was indeed inside the vesicles. This again is consistent with our previous study that used GFP-tagged Hsp70¹⁴.

One possibility is that the NLuc-Hsp70 fraction that is sensitive to proteinase K is not associated with vesicles. To rule out this possibility, we further separated EVs from co-isolated non-vesicular components through floatation into sucrose^{2,29} (Supplementary Fig. 2A). Briefly, 100,000 × g pellets emanating from conditioned media of NLuc-Hsp70- or NLuc-CD63-expressing cells were resuspended in 60% sucrose buffer and overlaid with 2 layers of lower concentrations of sucrose buffer (30%, 0%) followed by overnight centrifugation. Three fractions were collected (top, middle, and bottom, respectively), diluted, subjected to 100,000 × g centrifugation, and pellets were resuspended in PBS. More than 80% of the NLuc activity was found in the middle fraction, where EVs are expected to float, for both NLuc-Hsp70 and NLuc-CD63 cargoes (Supplementary Fig. 2B). Endogenous Alix was also more abundant within the middle fraction (Supplementary Fig. 2C). Middle-fraction EV were then subjected to the protease protection assay (Supplementary Fig. 2D). Consistently with the aforementioned results, in absence of detergent >80% of the NLuc activity was recovered for both cargoes (86 ± 4% and 86 ± 7% for NLuc-Hsp70 and NLuc-CD63, respectively). NLuc activity dropped to <15% in the presence of detergent. Endogenous Alix, tested by immunoblot, showed similar behavior (Supplementary Fig. 2E). Our simplest explanation is that this modest but yet measurable “unexpected” degradation of EV cargo reflects partial damage of EV membranes induced by the isolation procedure.

We concluded that NLuc-Hsp70 is an appropriate cargo to monitor EV uptake and content delivery within acceptor cells.

EV-uptake characterization. We then loaded NLuc-Hsp70-positive EVs on unlabeled acceptor HeLa cells, to assess EV-mediated homotypic cell–cell transport. First, we performed dose–response and kinetic experiments. Luciferase activity recovered in EV-treated acceptor cells increased proportionally to the dose of donor EVs (Fig. 2a). Importantly, saturation could not be reached even at high doses of EVs (100 µg/ml of proteins and higher). Kinetics showed that luciferase activity in acceptor cells increased over time, with a 1% spontaneous rate at 1 h (Fig. 2b).

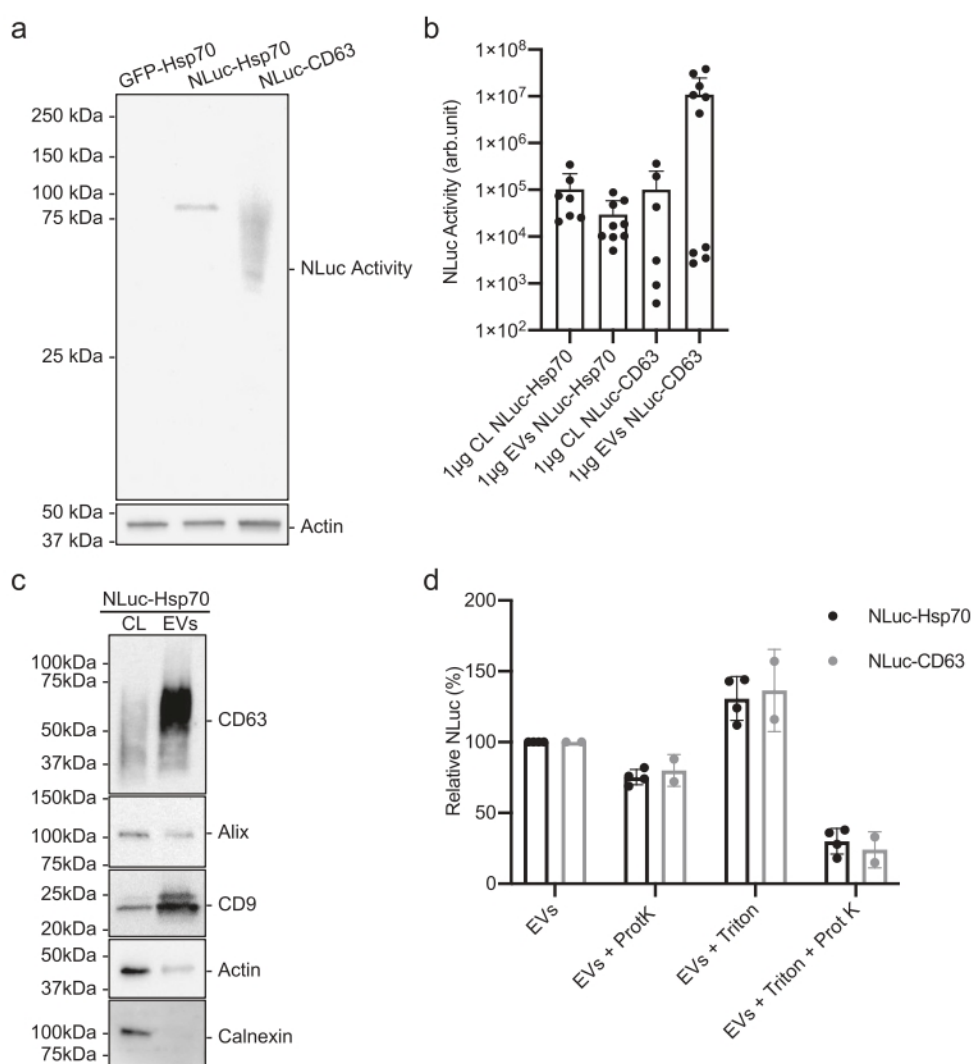


Fig. 1 NLuc-Hsp70 and NLuc-CD63 EV characterization. **a** In-gel detection of NLuc-Hsp70 and NLuc-CD63 activity. Equal protein amount of cell lysates from HeLa GFP-Hsp70 (negative control), stable HeLa NLuc-Hsp70, and transient HeLa NLuc-CD63 (upper gel) were loaded. As a control, actin was tested by immunoblot on the same samples (lower gel). This blot is representative of 2 independent experiments. **b** NLuc activity measurement in 1 μg of cell lysate (CL) or EVs from stable HeLa NLuc-Hsp70 or transient HeLa NLuc-CD63. Each dot is an independent replicate and represents the mean of 2 or 3 technical replicates. From left to right, $n = 7, 9, 6, 10$. Error bars represent standard deviations. **c** Immunoblots of cell lysate (CL) and EVs from stable HeLa NLuc-Hsp70. Equal amounts of protein were loaded to analyze CD9, CD63, Actin, Alix, and calnexin. This blot is representative of three independent experiments. **d** Protease protection assay on NLuc-Hsp70 (black) or NLuc-CD63 (gray) EVs, treated or not with proteinase K and/or detergent. Non-treated EVs were set to 100%. Each dot is an independent replicate and represents the mean of 3 technical replicates, $n = 4$ for NLuc-Hsp70, $n = 2$ for NLuc-CD63. Error bars represent standard deviations.

Importantly, we confirmed those results with EVs isolated through floatation assay (Supplementary Fig. 2F). We measured $1.2 \pm 0.2\%$ uptake for middle-fraction NLuc-Hsp70-EVs, whereas soluble recombinant NLuc was unable to penetrate the acceptor cells ($0.03 \pm 0.01\%$ uptake). These additional control experiments demonstrate that we are indeed following the fate of EV-containing cargoes.

We then used 4 °C temperature block, known to inhibit energy-dependent endocytosis without affecting protein–protein interaction often required for cell surface docking. We reasoned that if EVs were captured at the surface of acceptor cells by a dedicated receptor, NLuc should be detectable even at such a low temperature. The luciferase activity that is normally associated with acceptor cells after EV treatment was virtually absent ($0.4 \pm 0.2\%$) in cells treated at 4 °C for up to 2 h, suggesting very poor, or lack of specific EV binding at the surface of acceptor cells (Fig. 2c).

We then used confocal imaging to monitor the fate of uptaken EVs and performed colocalization experiments between GFP-tagged Hsp70 emanating from donor EVs and endogenous markers for early endosomes (Rab5) and lysosomes (Lamp1) (Fig. 2d). We observed colocalization of GFP with both markers (Fig. 2e, f).

We concluded that EVs are indeed internalized in endo/lysosomal compartments.

EV-content release characterization. We reasoned that if EV-content release occurs, luciferase activity of NLuc-Hsp70 should be measurable within the cytosolic fraction, whereas if EV content remains trapped or degraded inside endo-lysosomal compartments, cytosolic fraction should be negative for luciferase activity (Fig. 3a). To separate cytosolic from membrane fractions we used a detergent-free cell fractionation (Fig. 3b).

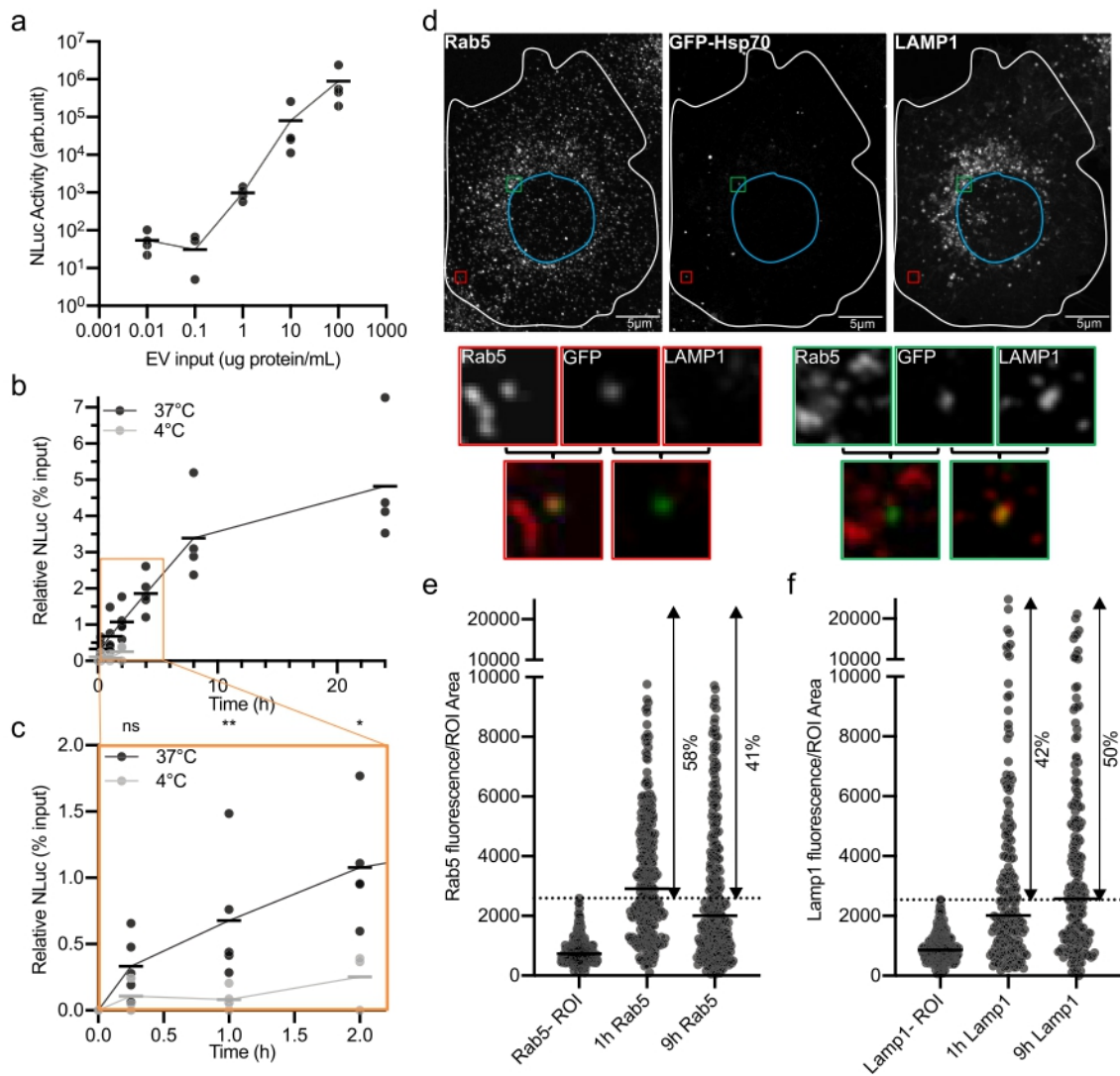
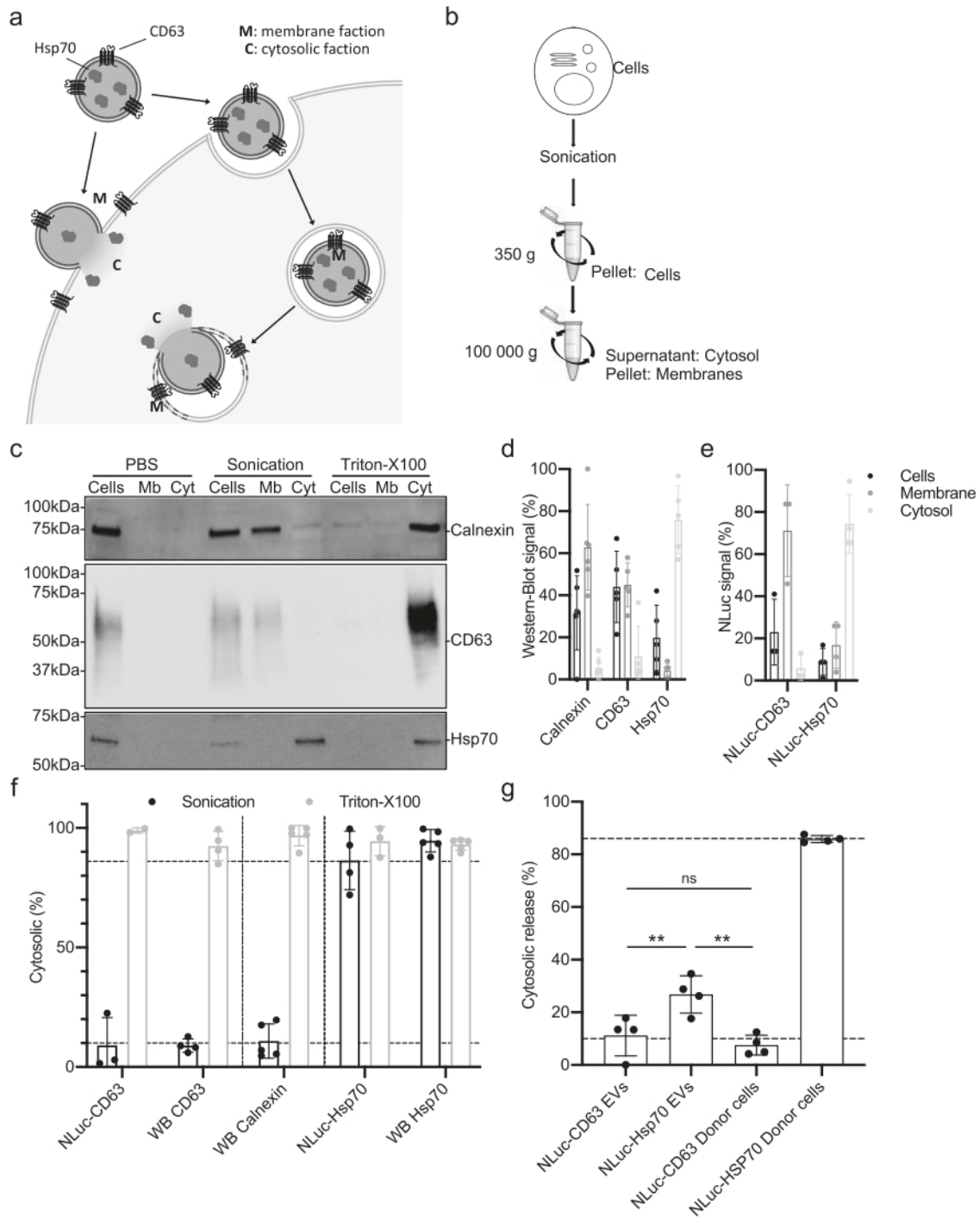


Fig. 2 NLuc-Hsp70 EV uptake by HeLa cells. a Dose-response study. Unlabeled acceptor HeLa WT cells were incubated for 2 h. with different amounts of isolated NLuc-Hsp70 EVs, luciferase activity was assessed at 2 h. One dot is an independent replicate and represents the mean of 2 technical replicates, $n = 4$. **b** Kinetics study. Unlabeled acceptor HeLa WT cells were incubated with isolated NLuc-Hsp70 EVs (1 $\mu\text{g}/\text{ml}$) for different incubation times at 37 °C (black) or 4 °C (gray). Measured EV input (equivalent to the EV dose loaded on cells) was set to 100% to normalize the NLuc activity at each timepoint. Each dot is an independent replicate and represents the mean of 2 technical replicates, $n = 4$. **c** Temperature-dependency study. Orange square, zoom on the 0–2 h timepoints on graph (b), to highlight 4 °C kinetics. Each dot is an independent replicate and represents the mean of 2 technical replicates, $n = 4$. **d** Confocal micrographs showing GFP-Hsp70 EV-content colocalization with either endosomes (Rab5+, red square) or lysosomes (LAMP1+, green square) compartments. Unlabeled acceptor HeLa WT were incubated with GFP-Hsp70 EV for 1 h, then processed for immunofluorescence against Rab5 and LAMP1 prior to being imaged by confocal microscopy. Micrographs are representative of three independent experiments. **e** Quantification of GFP-Hsp70 EV-content colocalization with endosomal and lysosomal compartments. Rab5 fluorescence was measured for each GFP+ dot or negative ROI. Each dot is a GFP+ compartment or Rab5 negative ROI of the same size, $n = 295, 315, 291$ (for each column, left to right order). Dashed line represents the maximum fluorescence of Rab5 negative ROIs. **f** Quantification of GFP-Hsp70 EV-content colocalization with lysosomal compartments. Lamp1 fluorescence was measured for each GFP+ dot or negative ROI. Each dot is a GFP+ compartment or Lamp1 negative ROI of the same size, $n = 193, 196, 195$ (for each column, left to right order). Dashed line represents the maximum fluorescence of Lamp1 negative ROIs.

We first validated our cell fractionation protocol. Briefly, unlabeled HeLa cells were mechanically disrupted and submitted to sequential centrifugation steps to first remove undamaged cells and large debris (350 g) and then separate cytosolic from membrane fractions (100,000 \times g). Supernatant (cytosol) and pellet (membrane) fractions were tested by western blotting for endogenous Hsp70 as a cytosolic marker, CD63 and Calnexin as membrane markers (Fig. 3c). Satisfyingly, >90% of the Hsp70 signal was recovered in the cytosolic fraction, which contains <10% of the CD63 and calnexin, validating our ability to separate membranes and cytosol (Fig. 3c, d, and f). Finally, when samples were exposed to detergent (Triton X-100), all markers

were recovered almost exclusively in the cytosolic fraction, as expected (Fig. 3c, d, and f). Because our delivery assay depends on measurement of luciferase activity, we performed the very same tests in cells expressing NLuc-Hsp70 or NLuc-CD63. Consistent with previous results, cytosolic fraction contained 90% of luciferase activity in NLuc-Hsp70-expressing cells and <10% in NLuc-CD63-expressing cells (Fig. 3e). This validated our method.

We then loaded NLuc-Hsp70- or NLuc-CD63-positive EVs on unlabeled acceptor cells for 1–4 h prior to performing fractionation and measuring luciferase activity in membrane or cytosolic fractions. For NLuc-Hsp70, $27 \pm 7\%$ of the cell-associated luciferase activity that corresponds to the internalized EVs was



recovered in the cytosolic fraction (Fig. 3g). Cytosolic release of NLuc-CD63 originally emanating from donor EVs was $11 \pm 8\%$ (Fig. 3g), consistent with the behavior of NLuc-CD63 within the donor cells (Fig. 3e) that corresponds to background signal). This key data demonstrated that roughly 20–30% of the internalized EVs are capable of releasing their soluble content within the cytosol of acceptor cells (Fig. 3g).

Importantly, treatment of acceptor cells with bafilomycin A1, which inhibits endosome acidification, decreased cytosolic release of NLuc-Hsp70 while general EV uptake was unchanged (Fig. 4a and b). Confocal microscopy that enables the tracking of donor GFP-Hsp70 EVs, revealed an increased number of GFP-Hsp70 foci within the cell (Fig. 4c and d); those GFP foci co-localize with

endosomes (Supplementary Fig. 3A) consistent with EV confinement within neutralized endo/lysosomes.

One possibility is that internalized and partially digested EVs could damage endosomal membrane to trigger EV-content release. To test this hypothesis, we used antibody against endogenous galectin-3, a cytosolic protein that decorates the luminal face of endosomes that have lost their membrane integrity³⁰. As a positive control we used LLOME, known to disrupt endosomal membrane². As expected, LLOME induced galectin-3 foci, whereas internalized EVs did not (Supplementary Fig. 3B). This is consistent with a recent study³¹ and suggests that endosomal escape is not triggered by EV-induced endosomal membrane damage.

Fig. 3 Quantification of the EV-content cytosolic release. **a** Principle of EV-content cytosolic release quantification: signal from EV-content NLuc-CD63 (membrane marker) or NLuc-Hsp70 (cytosolic marker) should be associated with the membrane fraction (Mb), except if content release occurs. Then, only NLuHsp70 should be detected in the cytosolic fraction (C). **b** Scheme representing detergent-free cell fractionation protocol that separates membrane and cytosol fractions. Sonication and differential centrifugation allowed to fractionate the cells in three fractions: intact cell (Cells), membrane (Mb), and cytosolic (Cyt) fractions. **c** Immunoblots showing the distribution of Calnexin (ER luminal protein used to test for organelle integrity), CD63 (membrane marker), and Hsp70 (cytosolic marker) within each fraction emanating from HeLa WT cells that were intact (PBS), mechanically disrupted (Sonication), or detergent-disrupted (Triton-X-100). This blot is representative of four independent experiments. **d** Densitometry analysis of intact cell (black), membrane (dark gray), and cytosolic (light gray) fractions from sonication treatment in (c). From left to right $n=6, 5, 5$. Error bars represent standard deviations. **e** NLuc activity quantification within intact cell (black), membrane (dark gray), and cytosolic (light gray) fractions. Stable HeLa NLuc-Hsp70 cells and transient HeLa NLuc-CD63 cells were submitted to detergent-free fractionation and luciferase activity was measured in each fraction, from left to right $n=3, 4$. Error bars represent standard deviations. **f** Quantification of each marker in the cytosolic fraction from NLuc or western-blot (WB) quantification, after sonication (black) or Triton-X-100 (gray) treatment. Dashed lines represent the full range of experimentally measured maximum and minimal values. Each dot is an independent replicate and represents the mean of two technical replicates, n from 2 to 5. Error bars represent standard deviations. **g** Quantification of the EV-content release: NLuc-CD63 or NLuc-Hsp70 EVs were loaded on unlabeled acceptor HeLa WT cells at 37 °C for 1–4 h, prior to performing the detergent-free cell fractionation protocol and measuring the NLuc activity to determine the % of each marker in the cytosolic fraction. As internal control, we measured the distribution of each marker within the donor cells. Dashed line represents experimental minimum and maximum values established in (e). Each dot is an independent experiment and represents the means of 2 technical replicates, $n=4$. Error bars represent standard deviations. One-way ANOVA was performed with a Turkey's multiple comparison test. Indicated p -values, from left to right: 0.0091, 0.7963, and 0.0019.

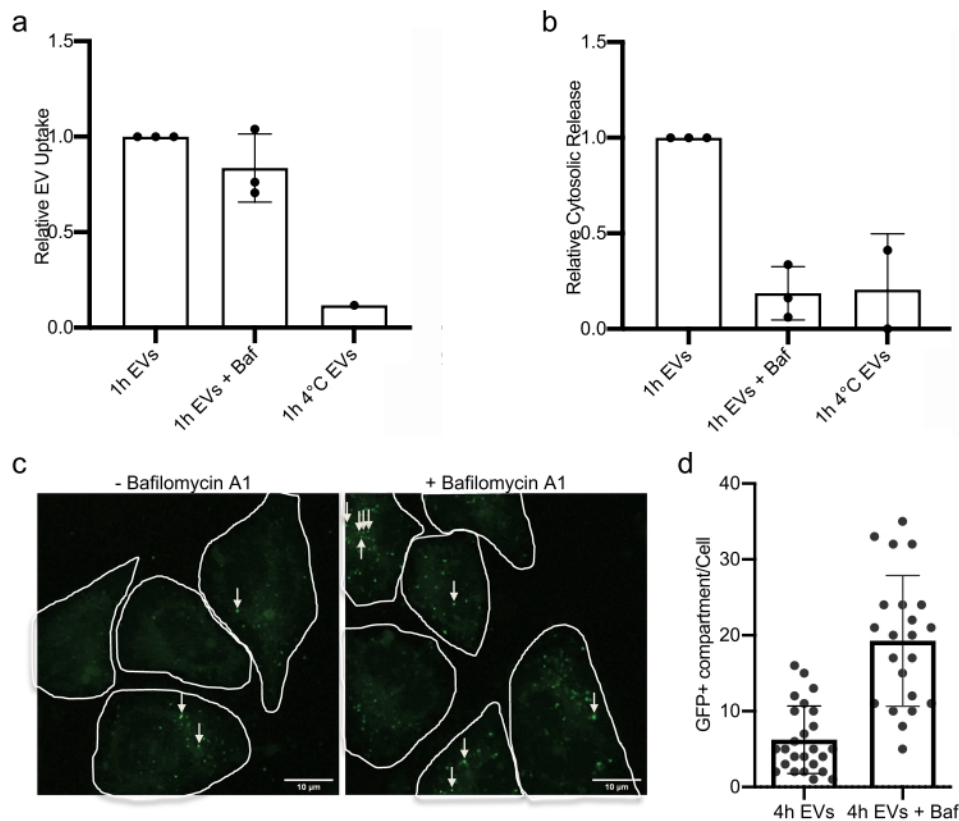


Fig. 4 Endo/lysosomal acidification is required for EV-content delivery. **a** Quantification of NLuc-Hsp70 EV uptake by unlabeled acceptor HeLa WT cells, with or without Bafilomycin A1 (Baf) treatment. Cells were incubated at 4 °C as negative control (no EV uptake). The EV uptake in control condition (non-treated) was set to 1. Each dot is an independent replicate and represents the means of 2 or 3 technical replicates, from left to right $n=3, 3, 1$. Error bars represent standard deviations. **b** Quantification of NLuc-Hsp70 EV-content delivery within unlabeled acceptor HeLa WT cells, with or without Bafilomycin A1 (Baf) treatment. Cells were incubated at 4 °C as negative control (no EV-content release). The cytosolic release from the control condition (non-treated) was set to 1. Baf treatment (loss of endosomal acidification) inhibits the content release. Each dot is an independent replicate and represents the mean of 2 or 3 technical replicates, from left to right $n=3, 3, 2$. Error bars represent standard deviations. **c** Confocal micrographs of HeLa acceptor cells after 4 h incubation with GFP-Hsp70 EVs with or without Baf treatment. White arrows indicate GFP-positive dots. Micrographs representative of three independent experiments. **d** Quantification of the number of GFP-positive dots per cell on unlabeled acceptor HeLa WT cells after 4 h incubation with GFP-Hsp70 EVs with or without Baf treatment. Each dot represents the value of GFP foci number within one acceptor cell, from left to right $n=25, 22$. Error bars represent standard deviations.

IFITM proteins inhibit EV-content release. Aforementioned results and our cell-free study suggest that EV-content release may rely on pH-dependent fusion between EV and endosome membranes. Interestingly, a family of proteins called IFITMs has been shown to broadly inhibit fusion reactions during the processes of virus infection or syncytium formation^{32–34}. We hypothesized that IFITMs may inhibit EV delivery if they used similar fusion mechanism.

We first engineered HEK293T cells that stably expressed flag-tagged IFITM1 and IFITM3. We used these cells because parental HEK293T are IFITMs negative^{33,35}. We focused on IFITM1 known to be localized at the plasma membrane and to some extent at endo/lysosomal compartments, whereas IFITM3 is thought to show the mirrored distribution (endo > PM).

We incubated NLuc-Hsp70 positive EVs on control HEK293T cells or on cells overexpressing Flag-tagged IFITM1 or 3. Remarkably, EV-content delivery was inhibited (>60%) by both IFITM1 and 3, while the luciferase activity was slightly increased within the IFITM-positive acceptor cells (Fig. 5a and b). We confirmed through confocal microscopy that both IFITM proteins were localized at the plasma membrane and internal compartments (i.e., endo/lysosomes), with IFITM3 being more prominent than IFITM1 within those structures (Fig. 5c). We observed GFP-positive EVs within the vicinity of the plasma membrane, and internalized GFP-positive EVs (Fig. 5c). Most of those internalized GFP-positive EVs were positive for IFITM1 (84%) or IFITM3 (92%) (Fig. 5c, d and Supplementary Fig. 4A). Closer analysis of the micrographs revealed that GFP foci either perfectly colocalized with IFITMs positive structures or were engulfed within IFITMs positive structures (Supplementary Fig. 4A). Only few GFP EV were negative for IFITMs (Supplementary Fig. 4A).

This suggests that IFITM1 or IFITM3 may sequester EVs within IFITMs positive endosomes, perhaps by blocking fusion. To test this hypothesis more directly, we used our cell-free assay that reconstitutes the content delivery step¹⁴. In this assay, EVs are incubated with plasma membrane sheets and proteinase K. At acidic pH, EV cargo (GFP-Hsp70) that is normally protected from proteinase digestion is now degraded (Fig. 5e–g samples 1–3). pH-dependent content release was again evidenced when PM sheets purified from parental HEK (IFITM negative) were mixed with EVs (Fig. 5f, g, samples 4, 5). Remarkably, presence of IFITM1 or 3 within the PM sheet abolished EV-content release (Fig. 5f and g, samples 6–9). PM sheet quality was tested and validated by western blot as described previously¹⁴ (Supplementary Fig. 4B, C).

These results validate our hypothesis and suggest that IFITMs inhibit EV-content release by blocking membrane fusion between EV and target membranes.

Discussion

We previously showed in vitro that EV-content release is pH-dependent¹⁴. Here we report that EV uptake and delivery within live cells is a low-yield process, which we quantified for the first time. We estimated that EV internalization occurs at a 1% spontaneous rate at 1 h, with up to 30% of those internalized EVs capable of content delivery. EV uptake is not saturated even at high doses of EV (>100 µg/ml). EV association with acceptor cells is inhibited at low temperature, consistently with previous reports¹⁶. In comparison, receptor-dependent LDL uptake is saturated at lower doses (<10 µg/ml) and LDL association with cell surface is not inhibited at 4 °C³⁶. This suggests that EV uptake is not mediated by a bona fide receptor, at least within the tested cells. However, lack of specific receptors cannot be generalized yet, and it is possible that certain combinations of donor/acceptor

cells that communicate more efficiently through EVs use such receptors to increase EV targeting and capture.

Consistent with previous studies^{12,18,37}, we show that internalized EVs co-localize with endosomes and lysosomes to some extent. Importantly we showed that EV-content release is inhibited by bafilomycin A1 treatment, demonstrating again the pH-dependency of the process.

IFITMs are known to block the entry of several viruses within the cells³⁸. It has been proposed that IFITM1, which is mainly at the plasma membrane, and IFITM3, which is mainly at late endosomes/lysosomes, differently impact viruses that use pH-independent or pH-dependent fusion to deliver their content into the cells³⁹. Based on our results that support acidic endosomes as the point of delivery, and following this simple IFITM/location-based restriction rule, one could have predicted that IFITM3 should be more efficient to perturb EV-content release and might find our IFITM1-related results contradictory. However, in our hands, both overexpressed IFITMs are significantly localized at both PM and internal compartments (i.e., endosomes), although IFITM3 is more abundant within the latter. Importantly, we observed that most of the internalized EVs colocalized with or are sequestered within IFITM1 or IFITM3 positive compartments, where IFITMs may restrict EV-content delivery. Interestingly, careful analysis of the literature on virus restriction entry inhibition by IFITMs revealed that IFITM specificity is not as exclusive as initially proposed^{38,39}. In many cases, most IFITM proteins (including IFITM1) indeed restrict entry of virus that uses pH-dependent entry. Importantly, we independently confirmed with the cell-free assay the negative effect of both IFITM1 and 3 on pH-dependent EV delivery.

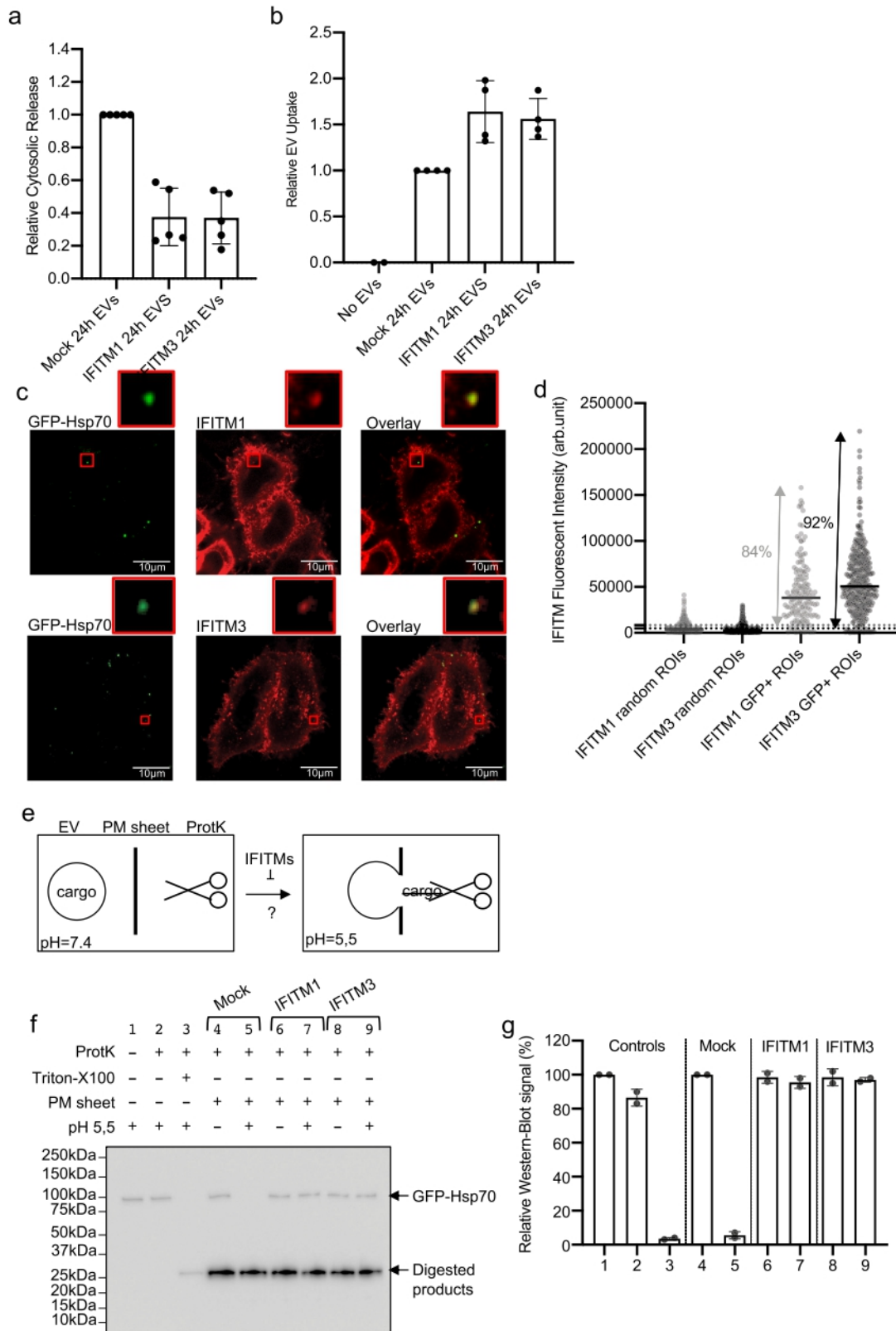
Thus, the simplest interpretation of our data led us to propose that IFITMs (1 and 3) may block fusion between EVs and endosomal membranes. A role for IFITMs as negative regulator of membrane fusion is generally accepted, but the precise mode of action is still obscure³⁹. IFITMs might perturb membrane fluidity, lipid distribution, and size extension of the fusion pore. Further investigation will be required to formally demonstrate that membrane fusion is a pre-requisite for EV-content delivery and clarify the mechanism by which IFITMs perturb such a fusion. For now, we propose that EVs are nonspecifically internalized within the cells, and that endosomal acidification triggers EV-content release, likely through a membrane fusion reaction.

How can such a low-yield process be physiologically relevant?

First, several viruses have similar low potency to enter into the cell, but benefit from the viral replication to amplify the infectivity⁴⁰.

Second, acute spatio-temporal coordination of a 1% yield process may still be compatible with several physiologically relevant functions. For instance, numerous spermatozooids go through the epididymis during their maturation, and it has been shown that RNA contained in EVs emanating from distal part of the epididymis can rescue infertile sperms collected from upstream tissues^{41,42}. It seems conceivable that a 1% efficient EV-mediated RNA transfer into sperms transiting through the epididymis could be sufficient to transmit selective advantage to the few beneficiary acceptor spermatozooids, to the detriment of infertile sperm and allow efficient fecundation.

Third, functions relying on signal amplification may also be compatible with a 1% yield process. EVs have been shown to deliver antigens into dendritic cells capable to activate antigen-specific T-cell response⁴³. Perhaps the delivery of an antigen within a dosage range compatible with the yield reported here, would be sufficient to efficiently presents this antigen at the surface of dendritic cells. These cells could then amplify the response through multiple contacts with numerous T cells⁴⁴, which once activated would trigger an efficient immune-response.



Other aspects of EV-mediated protein transfer that have been reported are more difficult to reconcile with <1% yield process. For instance, EV transport has been proposed to replenish in vivo adipocytes depleted of caveolin⁴⁵. This would surely require a more efficient mechanism involving specific targeting and EV

capture, that is not supported by our results. Perhaps certain tissues/cell combinations^{45,46} are optimized for EV exchange and may help to identify a specific uptake machinery.

Finally, we showed in our system that the rate-limiting step is the uptake process (~1%). The content delivery process

Fig. 5 IFITM proteins inhibit EV-content delivery. **a** Quantification of NLuc-Hsp70 EV-content delivery within Mock HEK cells (control), or HEK cells stably expressing Flag-tagged IFITM1 or IFITM3. NLuc-Hsp70 EVs were loaded on each acceptor cell prior to performing cell fractionation and determining the portion of NLuc-Hsp70 found in the cytosolic fraction. Cytosolic release measured in control (Mock cells) was set to 1. Each dot is an independent replicate and represents the means of 2 or 3 technical replicates, $n = 5$. Error bars represent standard deviations. **b** Quantification of NLuc-Hsp70 EV uptake by control HEK cells (Mock), or stably expressing IFITM1, IFITM3. EV uptake measured in control (Mock) was set to 1. Each dot is an independent replicate and represents the means of 2 or 3 technical replicates, $n = 4$. Error bars represent standard deviations. **c** Confocal micrographs of IFITM1 or IFITM3-HEK acceptor cells after uptake of GFP-Hsp70 EVs. IFITM1 and 3 were detected through their flag-tag (Alexa 546) whereas EV were detected through their GFP signal. Red squares show higher magnification of internalized EVs colocalizing with IFITM1 and 3. Micrographs representative of at least three independent experiments. **d** Quantification of Flag-IFITM1 (light gray) and 3 (dark gray) fluorescent signals in GFP+ ROI versus random ROI on HEK acceptor cells after incubation with GFP-Hsp70 EVs. One dot represents one ROI. $n = 241$ (control IFITM1), 387 (control IFITM3), 166 (GFP+IFITM1), 370 (GFP+IFITM3). Dashed lines represent the average background (random ROI) value plus twofold standard deviation. **e** Scheme illustrating the principle of the cell-free content EV-content release assay. Under acidic pH and in presence of PM sheets, EVs released their content (GFP-Hsp70) in the buffer where the cargo can be digested by proteinase K. The role of IFITM1 and 2 in target PM sheets can be tested following this protocol. **f** Immunoblot showing the resistance of GFP-Hsp70 to proteinase K when EVs are incubated with target PM sheets that contain or not IFITM1 and 3, and that are exposed or not to acidic pH. Digested products of GFP-Hsp70 and GFP-PM sheets (also observable on Supplementary Fig. 3C) show similar profiles. This blot is representative of two independent experiments. **g** Quantification of the GFP-Hsp70 signal (proteinase K resistant) by densitometry analysis. Each dot represents an independent replicate, $n = 2$, control (line 1) was set to 100%. Error bars represent standard deviations.

(~20–30%) is more efficient and suggests that donor and acceptor membranes used here can be further used to attempt to discover the putative pH-dependent fusion machinery.

Methods

Cell culture. HeLa (from ATCC, Virginia, USA) and HEK293T (kindly received from O. Schwartz group, derived from parental HEK293T purchased at ATCC) cells were cultured in DMEM (Gibco, Illinois, USA) complemented with 10% FBS (Gibco, Illinois, USA or Biosera, France), at 37 °C 5% CO₂. HeLa GFP-Hsp70 or NLuc-Hsp70 stable cell lines were selected with geneticin 10 µg/mL (Gibco, Illinois, USA) after lipofectamine-based transfection. HeLa NLuc-CD63 was analyzed 1 day after transient transfection. HEK Mock, IFITM1 or IFITM3 stable cell lines were selected with puromycin 1 µg/mL (Gibco, Illinois, USA), after viral transduction. Except mentioned otherwise, cells were transfected using Lipofectamine 2000 (Invitrogen, Massachusetts, USA), according to manufacturer's protocol.

Plasmids. NLuc-CD63 construct was obtained by removing RFP sequence RFP-CD63 (a gift from Walther Mothes), using AgeI and XhoI restriction enzyme (NEB, Massachusetts, USA). PCR amplified (Supplementary Table 1) NLuc sequence (Promega, Wisconsin, USA) was then inserted using the same enzymes. NLuc-Hsp70 was obtained by replacing GFP sequence from GFP-Hsp70 (15215, Addgene, Massachusetts, USA) by NLuc sequence from NLuc-CD63 plasmid. Here again, AgeI and XhoI were used to digest both plasmids before ligation. CD8-ENLYFQS-GFP, used to generate PM sheets¹⁴.

EV isolation. Donor cells were cultured for 24 h in serum-free DMEM. Conditioned media was harvested and submitted to a 2000 × g centrifugation for 20 min at 4 °C to remove cell debris, and then to a 100,000 × g ultracentrifugation for 1 h 30 min at 4 °C (45 Ti rotor and Optima L-80 ultracentrifuge, Beckman Coulter, California, USA). Note that in initial experiments, intermediate step at 10,000 × g was performed to remove large vesicles and large protein aggregates, but this fraction was virtually depleted of proteins including EV cargo of interest (GFP-Hsp70 and NLuc-Hsp70). We subsequently remove this additional step. The obtained pellet was washed with PBS and centrifuged 1 h at 100,000 × g 4 °C (MLA 80 rotor and Optima MAX-XP ultracentrifuge, Beckman Coulter, California, USA). Pellet was resuspended in 100 µL PBS and either stored at 4 °C (for up to 20 h) or immediately applied on acceptor cells.

For floatation assays, we proceeded as follow²⁸. Briefly, 100,000 × g pellet obtained as aforementioned pellets were resuspended in 1 ml 60% sucrose and deposited in the bottom of the tube. One milliliter of 30% sucrose solution and 1 ml of PBS were sequentially loaded on top of the samples. Samples were centrifuged at 150,000 × g for 16 h at 4 °C (SW55 rotor). One milliliter of each fraction was collected and mixed with 6 ml PBS to dilute sucrose and eliminate its putative interference within our assays. Samples were centrifuged at 150,000 × g for 1 h 30 min (MLA 80 rotor), supernatant containing sucrose was removed and pellets were resuspended in 100 µL PBS prior to further testing for NLuc activity, protease protection assay, or uptake assay.

Western blot and In-Gel NLuc detection. Cells were resuspended in lysis buffer (Tris 50 mM, NaCl 150 mM, Triton-X-100 1%, protease/phosphatase inhibitor (PPI) cocktail (Roche, Switzerland), pH 8) 30 min on ice, then samples were submitted to 20 min 19,000 × g centrifugation. Supernatants (cell lysates) were collected. Protein concentration of cell lysate (CL) and EV samples were obtained using Micro BCA™ Protein Assay kit (Thermo Scientific, Illinois, USA). Samples

were mixed with 4X Laemmli buffer (Bio-Rad, California, USA) 10% β-mercaptoethanol, except for In-Gel, CD63, and CD9 detection (no β-mercaptoethanol) and loaded on 4–15% polyacrylamide gels (Bio-Rad, California, USA). After electrophoresis, proteins were transferred on PVDF membranes using the Trans-Blot Turbo system (Bio-Rad, California, USA). Membranes were blocked in PBS 0.05% Tween20 5% milk, then incubated with 1/1000 primary antibody (α-Actin (MAB1501, Millipore, Germany), α-ALIX (clone3A9, 2171, Cell Signaling, Massachusetts, USA), α-Calnexin (ab133615, Abcam, UK), α-CD63 (clone H5C6, 556019, BD Bioscience, New Jersey, USA), α-CD9 (clone MM2/57, cb1162, Millipore, Germany), α-Hsp70 (ADI-SPA-810-D, Enzo LifeScience, New York, USA), α-FLAG (F3165, Sigma-Aldrich, Missouri, USA), α-GM130 (ab32337, Abcam, UK)) in PBS 0.05% Tween20 5% milk, washed and finally incubated with 1/5000 HRP-coupled secondary antibody (α-mouse or α-rabbit, 115-035-003, Jackson ImmunoResearch, UK) in PBS 0.05% Tween20. Membranes were developed using BM Chemiluminescence Western blotting Substrate (POD) (Roche, Switzerland) and ChemiDoc imager (Bio-Rad, California, USA). For the In-Gel detection of the NLuc, the same procedure was used until the migration of the proteins in the polyacrylamide gel. Then, the gel was handled as recommended by the supplier of the kit Nano-Glo™ In-Gel Detection System (Promega, Wisconsin, USA). For both methods, image analysis and quantification were performed using Image Lab Software (Bio-Rad, California, USA) and ImageJ software.

Proteinase K protection assay. Isolated NLuc-Hsp70 or NLuc-CD63 EV samples were incubated in PBS with or without 0.1% Triton X-100 and 50 µg/mL Proteinase K (AM2542, Ambion, Texas, USA) for 5 h at RT within 96-well plate. Then 20 µL of Nano-Glo™ Live Cell assay reagent (N2011, Promega, Wisconsin, USA) was added on each sample to immediately measure the remaining NLuc activity in each well using iD3 SpectraMax microplate reader (Molecular Devices, California, USA). For Alix resistance assessment by immunoblot, proteinase K was neutralized by adding 0.2 µL of boiled 0.2 µM PMSF immediately followed by loading buffer (100 °C, 15 min)¹⁴.

NLuc EV uptake. Acceptor cells were seeded 24 h before the uptake experiment, at 20,000 cells per well in a 96-well plate. NLuc-Hsp70 EV input was added in serum-free DMEM for a final concentration of 1–10 µg protein/mL, or as specifically indicated. Cells were incubated with EVs at 4 or 37 °C for 0–24 h, or the specifically indicated time. After incubation, cells were washed with PBS and then lysed in the aforementioned lysis buffer, prior to transferring in white 96-well plates. Finally, 50 µL of Nano-Glo™ reagent (Promega, Wisconsin, USA) was added on each well and luminescence activity was read using iD3 SpectraMax microplate reader (Molecular Devices, California, USA) or Centro LB 960 microplate luminometer (Berthold, Germany) (for initial experiments related to Figs. 1b and 2a).

GFP-EV uptake. Acceptor cells were seeded 24 h before the uptake experiment, at 200,000 cells per well in a 24-well plate on the top of coverslips. For HEK cells, we used coverslips coated with poly-L-lysine (P8920, Sigma-Aldrich, Missouri, USA). Acceptor cells were incubated with GFP-Hsp70 EVs (10 µg protein/mL) for 1 h to 24 h at 37 °C. For Galectin3 labeling experiments, cells were treated 30 min with 500 µM LLOME (L7393-500MG, Sigma-Aldrich, Missouri, USA). Then cells were washed with PBS, fixed 15 min RT with PBS 4% Paraformaldehyde and permeabilized 30 min RT in PBS 1% bovine serum albumin (BSA) 0.1% Triton-X-100. Primary antibodies (α-Rab5 (610724, BD Bioscience, New Jersey, USA), α-Lamp1 (GTX62434, GeneTex, California, USA) or α-Galectine3 (14-5301-82, eBioscience, California, USA), or α-FLAG (F3165, Sigma-Aldrich, Missouri, USA)) were incubated ON at 4 °C at 1/100 in PBS 1% BSA 0.1% Triton-X-100. After washes in

PBS, samples were incubated 1 h RT with secondary antibodies (α -mouse or α -rabbit coupled to AlexaFluor (AF) 488, 546, or 647 nm (ThermoFisher, Massachusetts, USA)) at 1/500 in PBS. Once washed, samples were mounted and image using a SP8 confocal microscope (Leica Microsystems, Germany). Image analysis and colocalization quantification were performed using ImageJ software (NIH, Maryland, USA). Briefly, to assess compartment colocalization, the fluorescent signal coming from acceptor cell protein in region of interest (ROI) corresponding to EV surface for Rab5 and Lamp1, or to 5 μm^2 ROI centered on the EV signal.

Acceptor cell fractionation. Acceptor cells were seeded 24 h before the uptake experiment, at 200,000 cells per well in a 24-well plate. The same procedure for NLuc EV uptake above was used for the incubation with NLuc-Hsp70 or NLuc-CD63 EVs. To assess the dependency to endosomal acidification, acceptor cells were treated or not with 200 nM of Bafilomycin A1 (SML1661, Sigma-Aldrich, Missouri, USA) from 30 min before adding EV until the end of the uptake assay. Then acceptor cells were washed with PBS, detached, and collected using PBS 0.5 mM EDTA, and pelleted 10 min at 350 \times g 4 °C and resuspended in PBS 1X PPI. When required Triton-X-100 (positive controls) was added at that stage at 1% final concentration and samples were kept at 4 °C. For detergent-free cell disruption, samples were processed as follows: 5 s vortex, 5 back-and-forth in 30G needle and 5 s sonication (30% duty cycle, output control level 3) with a micro-tip sonicator (Ultrasonic Processor, Thomas Scientific, Swedesboro, NJ, USA).

Sample was then submitted for 10 min, 350 \times g, 4 °C, to pellet the intact cells (resuspended in PBS 1X PPI), then the supernatant was centrifuged 1 h at 100,000 \times g 4 °C to pellet the membranes (resuspended in PBS 1X PPI) and to recover the cytosolic fraction (supernatant). Distribution of the proteins in the different fractions was determined either by western-blot or NLuc activity measurement.

Cell-free EV-content release assay. HEK-derived PM sheets were prepared as follows. Briefly, control HEK cells (Mock) or cell stably expressing Flag-IFITM1 or 3 were transfected with plasmid encoding CD8-ENLYFQS-GFP. Two days after transfection, cells were washed in PBS, detached, and collected. After centrifugation (350 \times g, 4 °C, 5 min), cells were resuspended in 400 μL PBS, prior to being incubated with 100 μL of Protein G-conjugated magnetic beads (Bio-Rad, Hercules, CA, USA) and 2 μL of anti-CD8 antibody (clone Rpa-T8; eBioscience, San Diego, CA, USA) at 4 °C for at least 4 h. Non-attached cells were removed and bead-attached cells were submitted to sonication in 400 μL ice-cold PBS using a micro-tip sonicator (Ultrasonic Processor, Thomas Scientific, Swedesboro, NJ, USA; three pulses of 5 s, 30% duty cycle, output control level 3). Supernatant (cytoplasm) was discarded, PM remaining attached to the beads were washed with PBS. Bead-attached membranes were resuspended in 100 μL PBS using TEVp (Sigma-Aldrich, Missouri, USA) at 1 $\mu\text{g}/\text{mL}$, overnight at 4 °C on rotative wheel. Supernatant containing released-PM sheet was collected and protein concentration was determined using Micro BCA protein assay kit prior to testing PM sheet quality by western blot.

GFP-Hsp70 containing EVs were preincubated or not with HEK-derived PM sheets (1:1 protein ratio) at 4 °C for 1 h prior incubation at 25 °C for 1 h. When required, samples were treated with 1% Triton X-100. When required we added the 'fusion' buffer (10 mM Na_2HPO_4 , 10 mM NaH_2PO_4 , 150 mM NaCl, 10 mM 2-(*N*-morpholino) ethanesulfonic acid, 10 mM *N*-2-hydroxyethylpiperazine-*N* 9-2-ethanesulfonic acid, adjusted to pH 5.5 or required pH) for 1 h at 25 °C. Then samples were incubated at 4 °C with proteinase K (2 $\mu\text{g}/\text{mL}$) for 1 h. Proteinase K was inactivated as for protease protection assay above.

Statistical analysis. First, normality of data was assessed using Shapiro–Wilk test, and Levene's test was used for the homogeneity of variance. When positive, one-way ANOVA was performed (Fig. 3g).

Reporting summary. Further information on research design is available in the Nature Research Reporting Summary linked to this article.

Data availability

The authors declare that the data supporting the findings of this study are available within the Supplementary information files. Further requests should be addressed to the corresponding author. Source data are provided with this paper.

Received: 30 June 2020; Accepted: 3 March 2021;

References

- Mathieu, M., Martin-Jaular, L., Lavieu, G. & Théry, C. Specificities of secretion and uptake of exosomes and other extracellular vesicles for cell-to-cell communication. *Nat. Cell Biol.* **21**, 9–17 (2019).

- Raposo, G. et al. B lymphocytes secrete antigen-presenting vesicles. *J. Exp. Med.* **183**, 1161–1172 (1996).
- Valadi, H. et al. Exosome-mediated transfer of mRNAs and microRNAs is a novel mechanism of genetic exchange between cells. *Nat. Cell Biol.* **9**, 654–659 (2007).
- Skog, J. et al. Glioblastoma microvesicles transport RNA and proteins that promote tumour growth and provide diagnostic biomarkers. *Nat. Cell Biol.* **10**, 1470–1476 (2008).
- Balaj, L. et al. Tumour microvesicles contain retrotransposon elements and amplified oncogene sequences. *Nat. Commun.* **2**, 180 (2011).
- Kanada, M. et al. Differential fates of biomolecules delivered to target cells via extracellular vesicles. *Proc. Natl Acad. Sci. USA* **112**, 201418401 (2015).
- Mack, M. et al. Transfer of the chemokine receptor CCR5 between cells by membrane-derived microparticles: a mechanism for cellular human immunodeficiency virus 1 infection. *Nat. Med.* **6**, 769–775 (2000).
- Al-Nedawi, K. et al. Intercellular transfer of the oncogenic receptor EGFRvIII by microvesicles derived from tumour cells. *Nat. Cell Biol.* **10**, 619–624 (2008).
- Korkut, C. et al. Regulation of postsynaptic retrograde signaling by presynaptic exosome release. *Neuron* **77**, 1039–1046 (2013).
- Becker, A. et al. Extracellular vesicles in cancer: cell-to-cell mediators of metastasis. *Cancer Cell* **30**, 836–848 (2016).
- Kalluri, R. The biology and function of exosomes in cancer. *J. Clin. Investig.* **126**, 1208–1215 (2016).
- Mulcahy, L. A., Pink, R. C. & Carter, D. R. F. Routes and mechanisms of extracellular vesicle uptake. *J. Extracell. Vesicles* **3**, 24641 (2014).
- White, J. M. & Whittaker, G. R. Fusion of enveloped viruses in endosomes. *Traffic* **17**, 593–614 (2016).
- Bonsergent, E. & Lavieu, G. Content release of extracellular vesicles in a cell-free extract. *FEBS Lett.* **593**, 1983–1992 (2019).
- Parolini, I. et al. Microenvironmental pH is a key factor for exosome traffic in tumor cells. *J. Biol. Chem.* **284**, 34211–34222 (2009).
- Toribio, V. et al. Development of a quantitative method to measure EV uptake. *Sci. Rep.* **9**, 10522 (2019).
- Antonyak, M. A. et al. Cancer cell-derived microvesicles induce transformation by transferring tissue transglutaminase and fibronectin to recipient cells. *Proc. Natl Acad. Sci. USA* **108**, 4852–4857 (2011).
- Morelli, A. E. et al. Endocytosis, intracellular sorting, and processing of exosomes by dendritic cells. *Blood* **104**, 3257–3266 (2004).
- Hoshino, A. et al. Tumour exosome integrins determine organotropic metastasis. *Nature* **527**, 329–335 (2015).
- Christianson, H. C., Svensson, K. J., van Kuppevelt, T. H., Li, J.-P. & Belting, M. Cancer cell exosomes depend on cell-surface heparan sulfate proteoglycans for their internalization and functional activity. *Proc. Natl Acad. Sci. USA* **110**, 17380–17385 (2013).
- Miyashita, M. et al. Identification of Tim4 as a phosphatidylserine receptor. *Nature* **450**, 435–439 (2007).
- Pan, B. T. & Johnstone, R. M. Fate of the transferrin receptor during maturation of sheep reticulocytes in vitro: selective externalization of the receptor. *Cell* **33**, 967–978 (1983).
- Mathew, A., Bell, A. & Johnstone, R. M. Hsp-70 is closely associated with the transferrin receptor in exosomes from maturing reticulocytes. *Biochem. J.* **308**, 823–830 (1995).
- Jeppesen, D. K. et al. Reassessment of exosome composition. *Cell* **177**, 428–445.e18 (2019).
- Zhang, L. et al. A novel ultrasensitive bioluminescent receptor-binding assay of INSL3 through chemical conjugation with nanoluciferase. *Biochimie* **95**, 2454–2459 (2013).
- Théry, C. et al. Minimal information for studies of extracellular vesicles 2018 (MISEV2018): a position statement of the International Society for Extracellular Vesicles and update of the MISEV2014 guidelines. *J. Extracell. Vesicles* **7**, 1535750 (2018).
- Sharma, A., Mariappan, M., Appathurai, S. & Hegde, R. S. In vitro dissection of protein translocation into the mammalian endoplasmic reticulum. *Methods Mol. Biol.* **619**, 339–363 (2010).
- Sabatini, D. D. & Blobel, G. Controlled proteolysis of nascent polypeptides in rat liver cell fractions. II. Location of the polypeptides in rough microsomes. *J. Cell Biol.* **45**, 146–157 (1970).
- Shurtleff, M. J., Temoche-Diaz, M. M., Karfilis, K. V., Ri, S. & Schekman, R. Y-box protein 1 is required to sort microRNAs into exosomes in cells and in a cell-free reaction. *Elife* **5**, e19276 (2016).
- Skowrya, M. L., Schlesinger, P. H., Naismith, T. V. & Hanson, P. I. Triggered recruitment of ESCRT machinery promotes endolysosomal repair. *Science* **360**, eaar5078 (2018).
- Joshi, B. S., de Beer, M. A., Giepmans, B. N. G. & Zuhorn, I. S. Endocytosis of extracellular vesicles and release of their cargo from endosomes. *ACS Nano* **14**, 4444–4455 (2020).
- Weidner, J. M. et al. Interferon-induced cell membrane proteins, IFITM3 and tetherin, inhibit vesicular stomatitis virus infection via distinct mechanisms. *J. Virol.* **84**, 12646–12657 (2010).

33. Lu, J., Pan, Q., Rong, L., Liu, S.-L. & Liang, C. The IFITM proteins inhibit HIV-1 infection. *J. Virol.* **85**, 2126–2137 (2011).
34. Buchrieser, J. et al. IFITM proteins inhibit placental syncytiotrophoblast formation and promote fetal demise. *Science* **365**, 176–180 (2019).
35. Tartour, K. et al. IFITM proteins are incorporated onto HIV-1 virion particles and negatively imprint their infectivity. *Retrovirology* **11**, 103 (2014).
36. Goldstein, J. L. & Brown, M. S. Binding and degradation of low density lipoproteins by cultured human fibroblasts. Comparison of cells from a normal subject and from a patient with homozygous familial hypercholesterolemia. *J. Biol. Chem.* **249**, 5153–5162 (1974).
37. Costa Verdera, H., Gitz-Francois, J. J., Schiffelers, R. M. & Vader, P. Cellular uptake of extracellular vesicles is mediated by clathrin-independent endocytosis and macropinocytosis. *J. Control. Release* **266**, 100–108 (2017).
38. Zhao, X., Li, J., Winkler, C. A., An, P. & Guo, J.-T. IFITM Genes, variants, and their roles in the control and pathogenesis of viral infections. *Front. Microbiol.* **9**, 3228 (2019).
39. Bailey, C. C., Zhong, G., Huang, I.-C. & Farzan, M. IFITM-family proteins: the cell's first line of antiviral defense. *Annu. Rev. Virol.* **1**, 261–283 (2014).
40. Aiken, C. Pseudotyping human immunodeficiency virus type 1 (HIV-1) by the glycoprotein of vesicular stomatitis virus targets HIV-1 entry to an endocytic pathway and suppresses both the requirement for Nef and the sensitivity to cyclosporin A. *J. Virol.* **71**, 5871–5877 (1997).
41. Conine, C. C., Sun, F., Song, L., Rivera-Pérez, J. A. & Rando, O. J. Small RNAs gained during epididymal transit of sperm are essential for embryonic development in mice. *Dev. Cell* **46**, 470–480.e3 (2018).
42. Sharma, U. et al. Small RNAs are trafficked from the epididymis to developing mammalian sperm. *Dev. Cell* **46**, 481–494.e6 (2018).
43. Zeelenberg, I. S. et al. Targeting tumor antigens to secreted membrane vesicles in vivo induces efficient antitumor immune responses. *Cancer Res* **68**, 1228–1235 (2008).
44. Bousso, P. & Robey, E. Dynamics of CD8+ T cell priming by dendritic cells in intact lymph nodes. *Nat. Immunol.* **4**, 579–585 (2003).
45. Crewe, C. et al. An endothelial-to-adipocyte extracellular vesicle axis governed by metabolic state. *Cell* **175**, 695–708.e13 (2018).
46. Fitzner, D. et al. Selective transfer of exosomes from oligodendrocytes to microglia by macropinocytosis. *J. Cell Sci.* **124**, 447–458 (2011).

Acknowledgements

We thank Mathieu Maurin for his input on image quantification. We thank Nicolas Manel for his suggestion concerning the IFITMs. We thank Alena Ivanova and Michael Boutros for introducing us to NanoLuc Luciferase. We thank Marine Gros for her help with Galectin3-related experiments. E.B. is a recipient of a PhD fellowship from La ligue contre le Cancer. E.G. is a recipient of a post-doctoral fellowship from Fondation pour la Recherche Médicale (FRM (FRM: SPF20170938694). This work is supported by Fondation ARC (PJA20171206453 and PGA1 RF20180206962), Cancéropole Île-de-France

(Emergence 2018) and French National Research Agency (ANR-10-IDEX-0001-02 PSL*, ANR-11-LABX-0043, and ANR-18-CE15-0008, ANR-19-CE18-002003), and ANR-18-IDEX-0001, IdEx Université de Paris. OS lab is funded by Institut Pasteur, ANRS, Sidaction, the Vaccine Research Institute (ANR-10-LABX-77), Labex IBEID (ANR-10-LABX-62-IBEID), “TIMTAMDEN” ANR-14-CE14-0029, “CHIKV-Viro-Immuno” ANR-14-CE14-0015-01, ANR/FRM Covid support, and the Gilead HIV cure program.

Author contributions

E.B. and G.L. designed, performed, and analyzed the experiments. E.G. and J.B. generated molecular and cellular tools. E.B., E.G., J.B., O.S., C.T., and G.L. wrote or revised the manuscript.

Competing interests

The authors declare no competing interests.

Additional information

Supplementary information The online version contains supplementary material available at <https://doi.org/10.1038/s41467-021-22126-y>.

Correspondence and requests for materials should be addressed to G.L.

Peer review information *Nature Communications* thanks Eva-Maria Krämer-Albers and the other, anonymous, reviewer(s) for their contribution to the peer review of this work. Peer reviewer reports are available.

Reprints and permission information is available at <http://www.nature.com/reprints>

Publisher's note Springer Nature remains neutral with regard to jurisdictional claims in published maps and institutional affiliations.



Open Access This article is licensed under a Creative Commons Attribution 4.0 International License, which permits use, sharing, adaptation, distribution and reproduction in any medium or format, as long as you give appropriate credit to the original author(s) and the source, provide a link to the Creative Commons license, and indicate if changes were made. The images or other third party material in this article are included in the article's Creative Commons license, unless indicated otherwise in a credit line to the material. If material is not included in the article's Creative Commons license and your intended use is not permitted by statutory regulation or exceeds the permitted use, you will need to obtain permission directly from the copyright holder. To view a copy of this license, visit <http://creativecommons.org/licenses/by/4.0/>.

© The Author(s) 2021

2.3. Key results and working model

This PhD work led to the first quantitative characterization of EV uptake and content release within acceptor cells, using complementary cell-free and cell-based assays, with biochemical and imaging approaches. Three main EV uptake steps were assessed: the putative EV docking, internalization and content release. In the end, the project gave rise to the following working model concerning EV uptake by HeLa cells:

0. No evidence of *bona fide* EV receptor was detected in HeLa cells, as the EV uptake process is not saturable and no EV association with the acceptor cells occurs at 4°C.
1. EV uptake, which increases over time, is then probably linked to passive fluid-phase macropinocytosis or other receptor-independent endocytosis.
2. EV can be internalized into endosomes and can be found in lysosomes of HeLa acceptor cells. This result confirmed previous studies, and is consistent with endocytosis as the first step of EV uptake.
3. Endosomal acidification by vacuolar vATPase is required to initiate EV content release within endosomal compartments, which did not trigger endosomal damage.
4. A fusion step, between EV membrane and endosomal membrane, is likely the final step of EV content release within HeLa cytosol, and was inhibited with viral entry restriction factors such as IFITM proteins

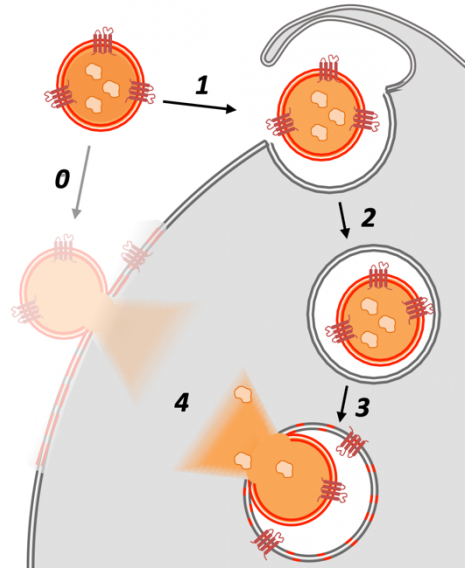


Figure 13: Working model for EV uptake and content delivery within acceptor cells.

All the results seem to describe a fluid phase macropinocytosis leading to an EV content release upon membrane fusion in acidic compartments.

The limiting steps of EV uptake seem to be more associated with the EV entry (1% spontaneous rate in 1 hour). EV delivery efficiency is around 30%, comparable with other membrane trafficking events.

3. DISCUSSION

3.1. The importance of EV-cargoes topology

One of the limitations in the study of EVs is to truly assess the topology of the EV content, to accurately know if the studied cargo is truly within the EV, associated to the EV membrane or if it is actually a contaminant that is only co-isolated with the EVs. In this study, protease protection assays have been performed, as has already been done in numerous cell biology studies (138–140).

For both cell-free and cell-based studies, the protease protection assay was performed using proteinase K treatment. The putative digestion of GFP-Hsp70 was assessed with western-blot analyses, whereas for NLuc-Hsp70 it was with the measurement of its remaining luciferase activity. Both methods showed that around 85% of the EV content is protected within the EV membrane. The unprotected fraction of tagged-Hsp70 could be due to a co-isolation of a free form of this protein. However, this could more probably be linked to a leakage of EV content during the isolation process via ultracentrifugation, which is known to generate some vesicle damage due to shear stress (141). This hypothesis was supported by the similar results obtained for NLuc-CD63, a transmembrane protein.

To exclude that the free form of NLuc-Hsp70 interfered in the EV uptake quantification, soluble recombinant NLuc was incubated with the acceptor cells, and after incubation and washes, no NLuc activity was recovered associated with the acceptor cells (supplementary figure 2, from Annex 2). Together with the protease protection assay, this confirmed that the signal from both GFP-Hsp70 and NLuc-Hsp70 could be used as a reporter of the EV content fate within acceptor cells.

Considering lipid dye-labeled EVs, one has to keep in mind that the washing steps following the labeling are crucial to avoid any free lipid dye association with the acceptor cells. Indeed, any free dye co-isolating with EVs will easily bind any acceptor membrane, increasing the background signal of both IF or FACs analyses. Here again control experiments have to be made to validate the relevance of the signal to follow the EV fate.

Even though the topology assessment is not yet a systematic characterization of EVs in the literature, it should be required for EV uptake studies, even more so for quantitative ones.

3.2. EV uptake by HeLa acceptor cells

The cell-based assay showed that the association of EV content to the acceptor cells, assessed by measuring the NLuc activity linked to the EV content, was not saturable. Even at 100 μ g/mL of EV proteins, no saturation plateau was reached as the NLuc activity associated with acceptor cells proceeded to increase. By comparison, LDL receptor saturation occurs around 20 μ g/mL on rat renal cells (142) and 35 μ g/mL on human fibroblasts (143).

The association of EV content to acceptor cells was also temperature dependent: at 4°C, almost no NLuc signal was detected within the acceptor cells, whereas signal was detectable and increasing over time at 37°C. This is consistent with a previous study showing that EVs seem to drift on the plasma membrane acceptor cell prior to internalization, without stopping at precise spot where receptor binding could have occurred before the internalization (144). Here again opposite results were obtained with LDL receptors (143), hemagglutinin receptor (129) and HIV binding (146), where 4°C incubation could inhibit the internalization of the ligand-receptor complex, but allowed their interaction and binding on the surface of the acceptor cells.

This temperature dependency was already observed in several EV uptake models. PKH-labelled EV uptake by HeLa cells were characterized a few years ago using flow cytometry experiments, showing similar kinetic and a 4°C temperature inhibition (147). However, in this study, EV uptake was described as saturable as it decreased when unlabeled EVs were added to the labelled EVs suspension. The same experimental strategy was also used to show the same temperature block in BMDCs homologous EV-mediated communication (52). This result was also confirmed by other methods: confocal imaging (57) and flow cytometry analysis of EV-mediated miRNA transfer, where pHluorin containing EV displayed similar kinetic with temperature block (51).

This dependency to membrane associated proteins was also assessed in several specific models with blocking antibodies. For instance antibodies against EV-enriched tetraspanins CD9 and CD81 slightly decreased PKH-labelled EV uptake by DCs, as well as the one against the integrin α V β 3 with a stronger effect, whereas anti-MFG-E8 increased it (52). A higher inhibition due to tetraspanin blockage was observed in EV uptake by leukocytes, which seemed to also involve adhesion proteins such as CD11b, CD11c, CD44 and ICAM-1 (148). However, no consensus appeared for all EV populations and/or acceptor cells, and these candidate proteins could be involved in

uptake steps other than docking, for instance by promoting donor EV internalization or fusion.

GFP-Hsp70 labelled EVs gave the same results as NLuc-Hsp70 EVs, as no EV docking on HeLa cells could be observed during confocal experiments. Combining all these experiments, no evidence of a specific EV receptor could emerge. If EV docking occurs during incubation of EVs with HeLa cells, it must be through a weak interaction between EVs and cell surface.

One of the key results of this project is the spontaneous rate of 1% of the initial EV input associated to the acceptor cells after 1 hour of incubation, which increases over time to reach around 5% of the initial EV input after 24h incubation. When looking at the uptake of EV-associated RNA, a study described a kinetic of uptake equivalent to the one described by the cell-based assay experiments, where the amount of retrotransposon coming from EVs and found within the acceptor cell after incubation increased over time, and started to decrease after 24h (55).

The association of EV content with the acceptor cells that increases over time is also pretty similar to fluorescent liposome uptake by HeLa (149). Unfortunately, the fluorescent signal in this study did not allow uptake efficiency calculations. Viral entry efficiency is even more complex to quantify, mainly due to their replication properties. In literature, viral entry and liposome uptake were usually reported using functional assays or reporter systems, which did not allow precise uptake efficiency quantification. And there is a chance that this efficiency would vary a lot depending on virus nature and entry pathway. For instance, pseudotyping HIV virus with VSV-G envelop protein increased over 100 times the infectivity of this virus (150). It might be very interesting to use labelled replication-defective viruses, used as therapeutical treatments like vaccines (151), in parallel with labelled liposomes or labelled EVs to compare uptake and content delivery efficiency of the three vectors.

Even though this EV uptake could be qualified as underperforming, this is actually close to the performance of other extracellular components. For instance, melanoma cells uptake around 1% of an initial LDL input after 4h of incubation, (152), and even lower for ferritin uptake by hepatocytes (153), by applying rough calculations to compare their results with the one obtained with the cell-based assay.

Here, we presented the first quantification of EV uptake efficiency, with an assay that can be easily adapted to other EV sources (to compare EVs coming from different cells or cell physiology) or other EV markers (to focus on specific EV subpopulations). Naturally, NLuc can also be loaded in donor liposomes or replication-defective viruses to compare their vector properties. In addition, other acceptor cells can also be incorporated to the settings to study heterotypic EV-mediated intercellular communication. This would allow to see if, as described with PKH-labelled EVs in microscopy, phagocytes could uptake more than other cells (154). Finally, the NLuc-based assay could be used to investigate the ability of EVs to exchange material between cells from different species, as interspecies EV-mediated transport is still debated (155).

GFP-Hsp70 EVs can be internalized by acceptor cells and reach endosomal and lysosomal compartments. Briefly EV internalization within endo/lysosomal compartments was already observed in several homotypic communication between neural cells (44), BMDCs (52), melanoma cells (54), adrenal gland cells (144) and breast tumor cells (156). DC-derived EVs were also internalized by tumor cells (48).

After EV internalization, endosomal integrity was assessed with galectin 3 staining and confocal imaging. This lectin is a cytosolic molecule with a high affinity for β -galactosides found only on the luminal side of endosomal membrane. Thus endosomal damages would give rise to a binding of galectin 3 to the endosomal membrane, to further recruit ESCRT repair machinery (157). The uptake of exogenous component such as bacteria or cell-penetrating peptide vectors can create such endosomal rupture once the macropinosome or the phagocytic vacuole release its content within acceptor endosomes (158, 159).

GFP-Hsp70 internalization within HeLa cells did not create such endosomal damage, as no galectin 3 foci could be detected within the acceptor cells, compared to LLOME treated cells (positive control, **Annex 2**, supplementary figure 3). Same observation came from incubation of GFP-CD63 EVs with HEK293T acceptor cells (160). Thus, EV internalization in endolysosomal compartments occurs, but do not create endosomal damage that could trigger EV content release.

3.3. EV content release within the cytosol of HeLa acceptor cells

The addition of a cell fractionation step to the cell-based assay led to the first quantification of EV content release within the acceptor cell cytosol. Indeed, 30% of the EV content associated with the acceptor cells were found in their cytosol, showing that EV content release occurs in HeLa cells, in a fairly efficient way.

This EV content release happened with only purified plasma membranes in the cell-free assay. Besides, proteins are required on both EV membranes and purified plasma membranes for the EV content release to occur: pretreatment of one of them by proteinase K blocked the content release. Another study addressed the point of proteins implicated in the EV uptake by using paraformaldehyde pretreatment of EVs to make them unattainable for other molecular interactions. This pretreatment decreased uptake by 25% (54).

Proteins are surely required for EV uptake and content release on both membrane components. Interestingly, this requirement did not seem to be essential for the EV docking, but thus for the following steps. More systematic studies focusing on proteins involved in the EV uptake should unveiled the molecular mechanisms for this uptake. For instance, the cell-based assay could be upgraded to allow high-throughput screening using phage-displayed nanobodies or Clustered Regularly Interspaced Short Palindromic Repeats (**CRISPR**) edition-based approaches.

The first evidence of EV content release was provided by the cell-free assay, where EV content mixed with purified plasma membranes became sensitive to proteinase K digestion when environmental pH decreased under pH6. Then in the cell-based assay, Bafilomycin A1 (endosomal acidification inhibitor) suppressed EV content release within the cytosol of the acceptor cells. Thus, in both assays EV content release could be measured only upon acidic conditions.

Bafilomycin A1 decreased oligodendrocyte EV uptake by microglia (46) and EV communication between DCs (51). Acidic condition was also linked to an EV uptake increase in melanoma cell communication, with a higher EV uptake at pH6 compared to pH7,4 (54). Bafilomycin A1 target, the vacuolar ATPase responsible for endosomal acidification, seemed then to be involved in EV uptake, and more precisely at the EV content release step. This result points to content release pathways used by some viruses such as VSV or VV, where endocytic compartments from different

internalization origins fuse with endo/lysosomal compartments, where the virus will eventually release its content through low-pH-induced membrane fusion (80, 161). The pH titration performed with the cell-free assay showed that pH should be under pH6 to allow EV content delivery, which indicated that it should occur in late endosomes as for VSV fusion machinery **Figure 3**. The final step of EV content release could then involve fusion with acidic compartments membranes.

To address the question of this putative membrane fusion, IFITM proteins were expressed in the acceptor cells. These proteins are extensively studied in virology, as one of their main properties is to inhibit the entry of a broad spectrum of viruses, including HIV-1, HCV, and VSV to a lower extent (162). Even though the mechanisms allowing this viral restriction is not fully characterized, the first indications suggested that IFITM proteins could act on the fusion step of the viral entry. Indeed, restricted viruses accumulate in intracellular compartments instead of releasing their genome within the cytosol (163). Plus, the different IFITM isoforms, which are expressed at different cell localizations (IFITM1 at the plasma membrane, IFITM3 mostly in endosomal compartments) presented different spectra of viral restriction (164).

Two hypotheses exist considering the molecular mechanisms involved in this likely membrane fusion inhibition. Either IFITM proteins modify endolysosomal content properties to block viral fusion, mainly the proteolytic function of some of these compartments (165), but the acidification remains unaltered (163). Or they modify the endolysosomal membrane properties, changing its curvature and fluidity. More evidence supported this second option, with a decrease of membrane fluidity observed by fluorescent imaging (166), and the enrichment of cholesterol in IFITM-expressing cells (167). This membrane modification could be linked to a possible oligomerization of IFITM proteins identified using immunoprecipitation (168). Their inhibitory effect on fusion was finally supported by their ability to inhibit syncytin 1 fusogenic properties in cell-cell fusion assays (169).

Once over-expressed in the acceptor membranes or cells of the cell-free and cell-based assays respectively, IFITM1 and IFITM3 both significantly decreased EV content release compared to Mock-transfected acceptor compartments. This could be explained by the accumulation of EV content within IFITM positive compartments of the acceptor cells (**Annex 2**, supplementary figure 4). Even though EV content delivery upon membrane

fusion needs further mechanistical characterization, these results strongly suggested that such a fusion could be involved.

A recent paper studied EV content release using a split NLuc, with one part expressed in the donor cells (loaded in EVs) and the other one expressed in the acceptor cells. However, they could only detect EV content release using the fusogenic protein VSV-G coated on EVs (170). Given the results of my work, one should expect really low signal when looking at EV content release, so the absence of any content release in this study might be due to a lack of sensitivity. Moreover, as discussed earlier, using the same "VSV-G coating" strategy with HIV virus increased the infectivity by a factor 100 (150).

EV content release upon membrane fusion was already suggested in DC-DC cell communication using dilution of self-quenching lipid dye within acceptor membrane (51). *In vitro* reconstitution of EV membrane fusion with isolated putative acceptor membranes was also detected using Atomic Force Microscopy (AFM) (171). Our two assays support this membrane fusion hypothesis; however, the involved machinery remains now to be described to finally validate that EV content release requires such a fusion step.

3.4. Putative routes for EV entry and content release within HeLa cells

To summarize, the two developed assays showed that 1) EV uptake by HeLa cells does not seem to require any specific receptor, 2) EVs are internalized in endo/lysosomal compartments, 3) EV content release occurs only upon endosomal acidification, 4) membrane fusion might be the final step of the EV content delivery process within HeLa cells.

Altogether, these findings raise the profile of a passive endocytosis-mediated EV internalization, that will target EVs to endo/lysosomal compartments for the final EV content release step to occur upon acidic condition and probably through membrane fusion.

In other epithelial cell models, the use of chemical inhibitors already allowed the identification of some molecular actors that could be involved in the EV uptake by these cells such as actin (47, 147, 172), heparan sulfate proteoglycans (45, 147), Na⁺/H⁺ exchangers and transient receptor potential cation channels (147, 172), cholesterol (47, 155, 171), glycosphingolipid (173), LDL and phosphoinositide 3-kinase (147).

Clathrin inhibition decreased fluorescent-labelled EV uptake, suggesting that clathrin-mediated endocytosis might be also at least partially involved in the full EV uptake process (172). The same clathrin lattices inhibitor was used on HeLa and did not decrease EV uptake at all, a non-significant increase could even be observed (147). However, the concentration used on HeLa was three times lower than in the previous study, which used the recommended concentration. Clathrin inhibition would also block some receptor recycling inhibition, that may have an impact on EV uptake independently of clathrin-dependent internalization.

Using silencing RNA strategy on acceptor cells, some proteins involved in caveolae-dependent and independent endocytosis were identify as molecular actors of EV uptake and content release within endothelial cells (174).

These results underlined molecules involved in multiple endocytosis pathways, without focusing on a specific one. The most likely to happen is macropinocytosis as suggested by another study on HeLa cells (147). Macropinocytosis was already highlighted for oligodendrocyte EV uptake by microglia acceptor cells, using various chemical inhibitors (46). However, we cannot exclude that other endocytic pathways are involved as suggested by some studies. The internalization pathways might vary depending on the acceptor cell identity and physiology. Based on the literature and this work, macropinocytosis might be the main entry pathway, putatively completed by caveolin- or clathrin- dependent endocytosis.

Indeed, EV endocytosis seems to be a passive fluid-phase uptake, which fits with 1) no specific receptor, 2) low efficiency uptake, 3) EV internalization in endolysosomal compartment. Regarding EV content release in HeLa cells, it seems to occur in acidic endo/lysosomal compartment and is likely to involve a fusion step, which remained to be further characterized. Once the key molecular actors are identified, EV uptake and content delivery could be modulated for fundamental purposes, but also therapeutic one with an elevated vector potential.

3.5. Toward EVs as therapeutic vectors

The vectorial potential of EV attracted so much of scientific interest that they are already used in clinical trials. Some already gave positive results in phase I clinical trials, using autologous ascite-derived EVs combined with GM-CSF treatment against colorectal cancer(175), or autologous DC-derived EVs against melanoma (176) or non-small cell

lung cancer(177). For this pathology it even reached complete phase II clinical trial (178), even though results are not fully satisfying they obtained natural killer cell activation in patients.

Umbilical cord Mesenchymal Stem Cell (MSC)-derived EVs were also used in phase I clinical trial in patients with chronic kidney disease, showing satisfying safety results and promising inflammatory immune reaction (179). MSC-derived EVs are of emerging therapeutical interest as they were described to have an ambivalent effect on tumor progression (180), and ability to target immune cells (181).

Other EVs are currently used in several clinical trials (182), as various as prospective clinical trial against acne scars using adipose tissue stem cell-derived EVs with laser treatment (183) or prospective clinical trial using allogeneic BM-MSC-derived EVs against severe Corona virus disease-19 (184).

There is no doubt that cellular and molecular characterization of EV content delivery within various acceptor cells would be crucial to increase the efficiency of EV-based therapeutics, and should accelerate the clinical trial to validate these treatments. Their endogenous origin and their capability to be produced from patient cells are really promising toward personalized and tissue-specific new generation medicines (185).

ANNEXES

Annex 1: Supplementary figures of cell-free assay experiments

Supplementary figure 1

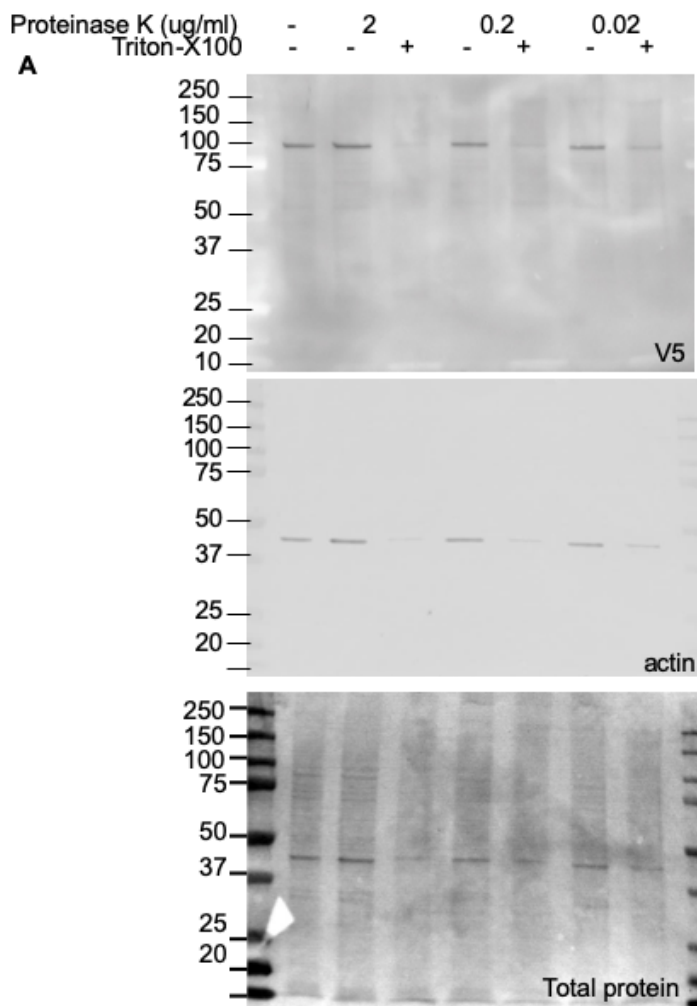


Fig. S1. Cargo topology. EVs emanating for HeLa cells expressing V5-Hsp70 were submitted to proteinase K treatment at various concentrations, in the presence or absence of Triton X100. After Proteinase K neutralization, we assessed by immunoblot the protection of overexpressed V5-Hsp70 and endogenous actin, both found in EVs.

Supplementary figure 2

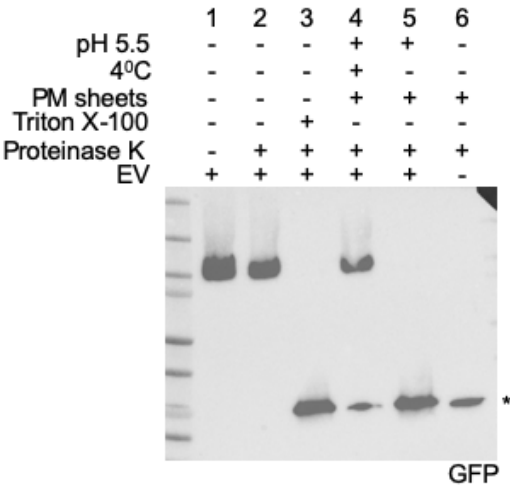
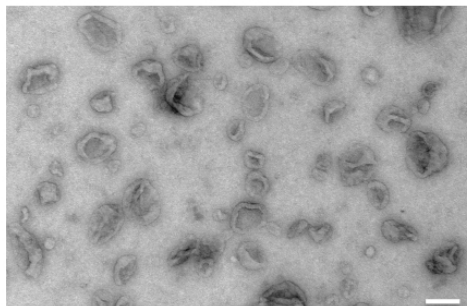


Fig. S2. EV-content release is temperature dependent. Immunoblot showing the status of GFP-Hsp70 after proteinase K treatment. After 1 h preincubation at 4 °C, all samples (except lane 4, which remained at 4 °C for an additional hour) were incubated at 25 °C for an additional hour. *, digestion products emanating from GFP-PM sheet (as shown in lane 6) and/or GFP-Hsp70 (as shown in lane 3).

Annex 2: Supplementary figures of the cell-based assay experiments

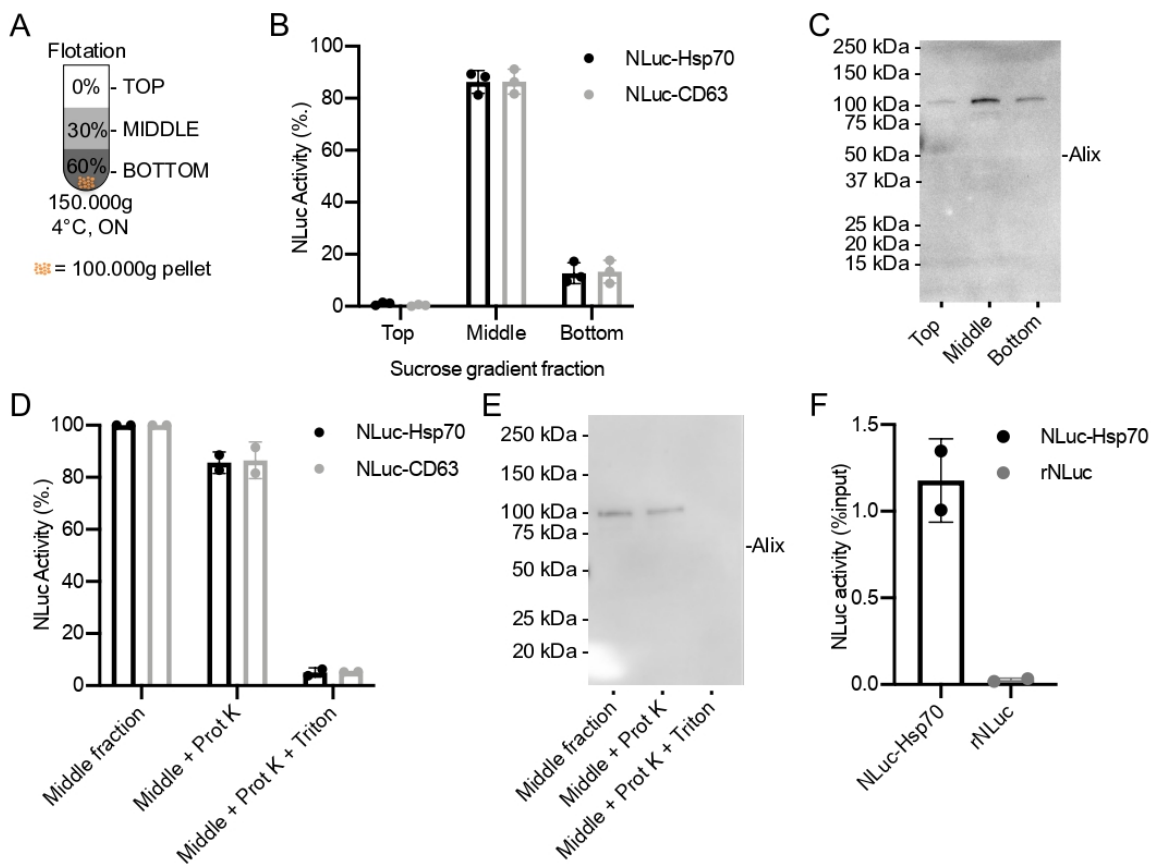
Supplementary Figure 1



Supplementary Figure 1: EM observation of Isolated Evs.

EVs were isolated through sequential centrifugation and processed for Electron Microscopy. Bar, 100 nm.

Supplementary Figure 2



Supplementary Figure 2: NLuc-Hsp70 and NLuc-CD63 EV characterization using sucrose gradient

A: Scheme of the EV isolation through floatation assay.

B: NLuc activity distribution in sucrose fractions after isolation of EVs emanating from NLuc-Hsp70 (black) and NLuc-CD63 (grey) HeLa cells. NLuc activity was measured in each fraction of the sucrose gradient. Sum of the NLuc activity of the 3 fractions was set to 100%. Each dot is an independent replicate and represents the mean of 2 technical replicates, n=3. Error bars represent standard deviations.

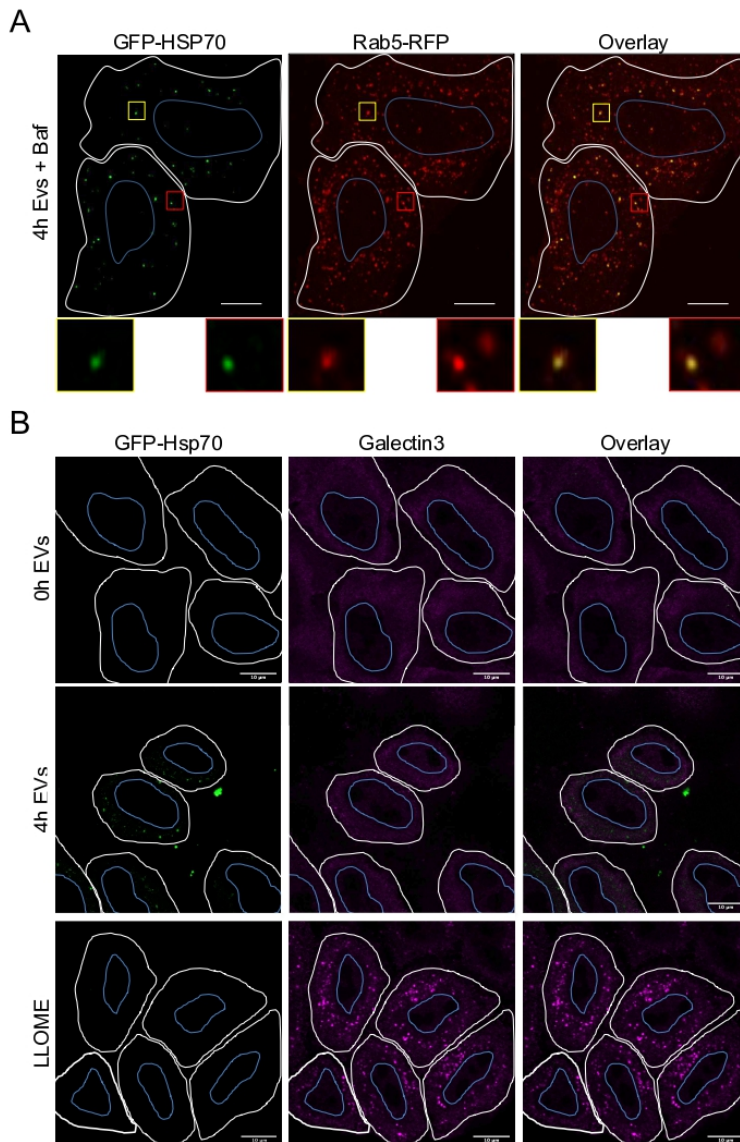
C: Alix distribution in sucrose fractions. Immunoblot of the 3 collected fractions from sucrose gradient were tested for Alix. Equal volume was loaded for each fraction. This blot is representative of 2 independent experiments.

D: Protease-protection assay on the 30% sucrose-EVs (middle fraction) emanating from NLuc-Hsp70 (black) or NLuc-CD63 (grey) HeLa cells. Middle fraction-EV were treated or not with proteinase K, with or without detergent. NLuc activity from nontreated sample (control) was set to 100%. Each dot is an independent replicate and represents the mean of 2 technical replicates, n=2. Error bars represent standard deviations.

E: Protease protection assay on Alix, on middle-fraction EVs emanating from NLuc-Hsp70 or HeLa cells. Presence of Alix was tested by Immunoblot. This blot is representative of 2 independent experiments.

F: Uptake of middle fraction-EVs from NLuc-Hsp70 cells. Isolated floating NLuc-Hsp70 EVs (black) or recombinant soluble NLuc (rNLuc, grey) were incubated with unlabeled HeLa WT acceptor cells for 1h. NLuc activity associated with acceptor cells was measured after incubation. NLuc activity for EV or rNLuc initial input were set to 100% uptake. Each dot is an independent replicate and represents the mean of 2 technical replicates, n=2. Error bars represent standard deviations.

Supplementary Figure 3



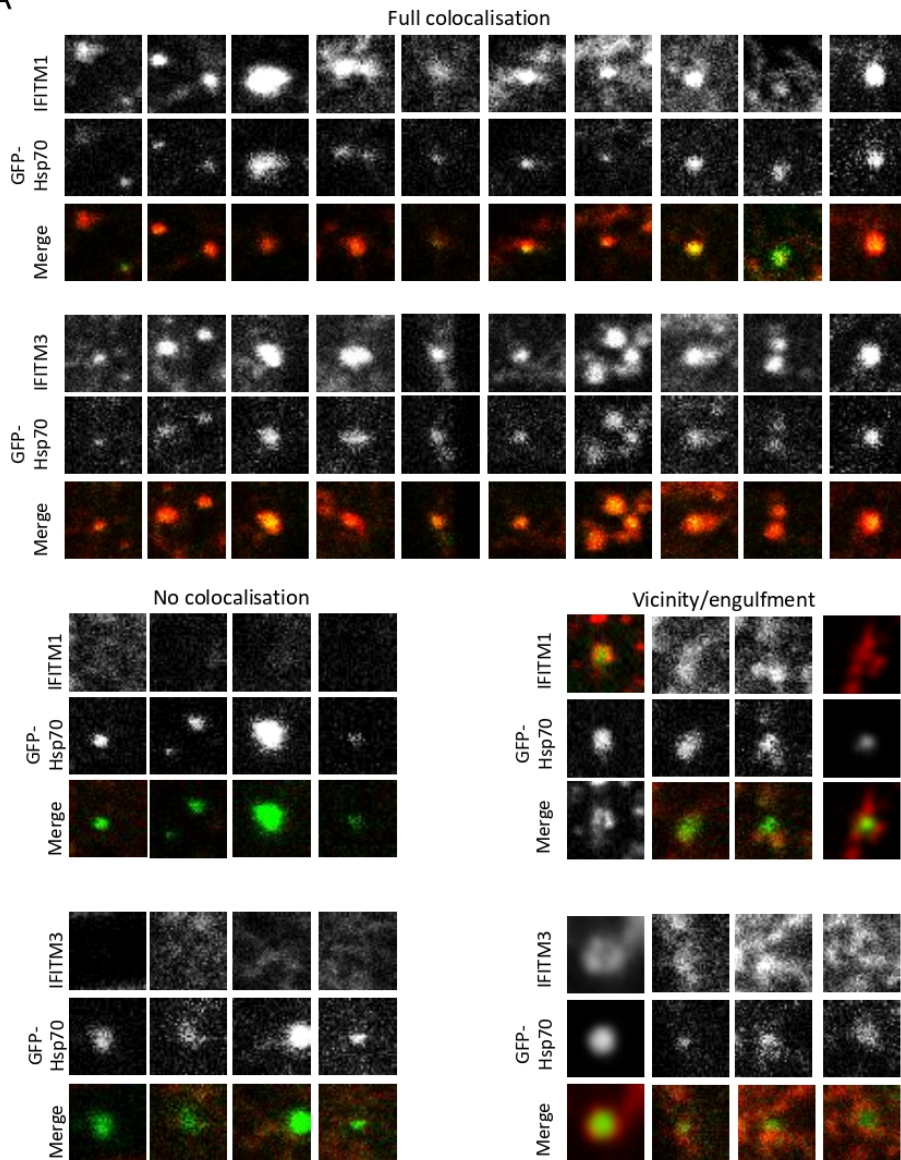
Supplementary Figure 3: Endo/lysosomal acidification is required for EV content delivery

A: BafilomycinA1 treatment confined EV content in endosomal compartments. GFP-Hsp70 EVs were loaded for 4 hours on unlabeled HeLa WT acceptor cells, treated with BafilomycinA1. Cells were immuno-labeled against Rab5. Micrographs representative of 2 independent experiments. Barre, 10 μm

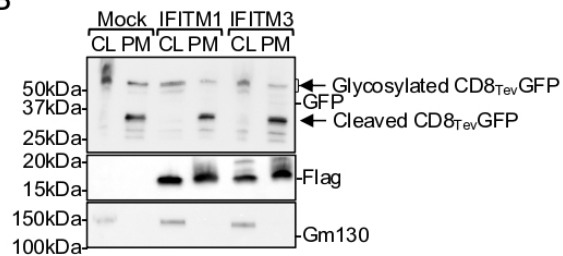
B: Endosomal integrity after incubation with GFP-Hsp70 EV. Isolated GFP-Hsp70 EVs, were loaded for 4 hours on unlabeled HeLa WT acceptor cells, which were fixed and immuno-labeled against Galectin3. Cells were treated 30min with 500mM LLOME as positive control for endosomal damage. Micrographs representative of 3 independent experiments. Barre, 10 μm

Supplementary Figure 4

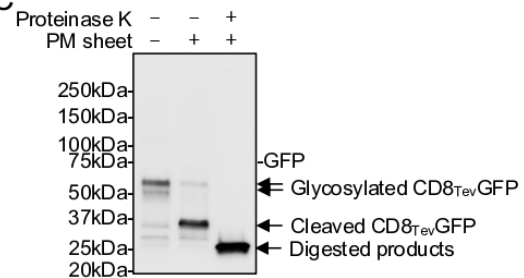
A



B



C



Supplementary Figure 4: IFITM proteins inhibit EV content delivery

A: Micrographs showing GFP positive ROIs where IFITM fluorescent signals fully colocalize, or where GFP foci are engulfed in IFITM positive structures. In few cases (<8-16 %, for IFITM3 and 1, respectively) GFP foci do not colocalize with IFITM positive objects. Micrographs representative of 2 independent experiments.

B: Immunoblots of cell lysate (CL) or purified plasma membranes (PM) from HEK cells expressing CD8_{Tev}GFP alone (mock), or with IFITM1-Flag or IFITM3-Flag proteins. Samples were tested for Flag, GFP, and Gm130 proteins. This blot is representative of 2 independent experiments.

C: Immunoblots of CL of PM from HEK cells expressing CD8_{Tev}GFP treated or not with proteinase K, which generates GFP-positive digested products observed in Figure 6.F(lower bands). This blot is representative of 2 independent experiments.

Supplementary Table 1

Primer name	Primer sequence
F-CD63-AgeI-NLuc	5'-ATTACTACCGGTATGGTCTTCACACTCGAAGATTC-3'
R-CD63-XhoI-NLuc	5'-ATTACT CTCGAG CGCCAGAATGCGTTCGCACAG-3'

Supplementary Table 1: Primer sequence for NLuc cloning

Primers were designed to amplify NLuc sequence with restriction sites that will allow ligation within acceptor Hsp70 or CD63 plasmids.

Annex 3: Methodological review on EV uptake and content release study – preprint of review commissioned by Springer

QUANTITATIVE MEASUREMENT OF EXTRACELLULAR VESICLE CONTENT DELIVERY WITHIN ACCEPTOR CELLS

Émeline BONSERGENT¹, Shéryl BUI¹, Grégory LAVIEU^{1*}.

¹Université de Paris, INSERM, CNRS UMR7057, Paris, France.

45 rue des Saints-Pères, UFR Sciences Fondamentales et Biomédicales, P335B. 75006, Paris,
FRANCE

*Correspondence to gregory.lavieu@inserm.fr

Abstract:

Extracellular vesicles (EVs), including exosomes and microvesicles, are thought to transport bioactive molecules from donor to acceptor cells. Although EV uptake has been qualitatively assessed through subcellular imaging, EV-content delivery has been rarely addressed due to a lack of adequate methods. Here we present a sensitive bulk assay to quantitatively measure EV uptake and content delivery in mammalian cell. In this assay, EVs containing a NanoLuc luciferase-tagged cargo are mixed with unlabeled acceptor cells. Cell fractionation separates membrane and cytosolic fractions, and luciferase activity is measured within each fraction to determine the percentage of cytosolic release. This assay can be used to further decipher cellular and molecular mechanisms that regulate the EV delivery process, or to quantitatively test specific pairs of donor-acceptor cells.

Key Words:

Extracellular Vesicles, Exosomes, Microvesicles, Uptake, Content Release, Fusion

Running Title:

Assessment of EV Uptake and Delivery

1. Introduction

Extracellular vesicles (EVs) are emerging vectors in intercellular cellular communication. They transfer biomolecules such as proteins, lipid and nucleotides from donor to acceptor cells (1–3). While EVs are thought to contribute to many physiological functions and diseases, the EV delivery process remains mysterious. Cellular aspects of the process are only superficially apprehended, and the molecular machinery that govern the EV content release remains a black box (4). Previous studies assessed EV uptake, mainly relying on fluorescent labelling of EV membrane or cargo and tracking their fates in acceptor cells using fluorescence-activated cell sorting (FACS) or sub-cellular imaging (5). These methods, however, do not allow to assess EV content delivery.

We developed a cargo-based approach in which a generic EV cargo, Hsp70, is tagged with the NanoLuc luciferase (NLuc) to track its fate within acceptor cells (6). Briefly, we generated donor cells stably expressing NLuc-Hsp70, isolated EVs by sequential centrifugation. Here we start right after the EV isolation, which has been extensively described (7). Then we assessed the topology of the cargo through a proteinase protection assay, incubated NLuc-Hsp70 positive EVs with unlabeled acceptor cells, and eventually measured luminescence within the membrane and cytosolic fractions of the acceptor cells (Figure 1). This method is flexible and adaptable to many cellular models and cargoes.

2. Materials

2.1 Common materials

1. Donor cell lines expressing the EV cargo of interest tagged with the NLuc reporter. In our studies, we use NLuc-Hsp70, a model for EV cytosolic cargos, and NLuc-CD63, a model for EV membrane cargos. To generate new plasmids, a NLuc template can be purchased from Promega. We use HeLa cells as both the donor and acceptor cells, but the current protocol can be adapted to any cargo or cell of interest.

2. PBS: 138 mM NaCl, 8 mM Na₂HPO₄, 3 mM KCl, 1.5 mM KH₂PO₄, pH 7.4.

3. Triton X-100 solution: PBS containing 50 μM of Triton-X100. Keep at 4 °C.

4. MicroBCA kit for protein quantification.

5. Plate Reader/Luminometer.

6. 96-well opaque white plates and clear-bottom white plates.

2.2 Protease protection assay

1. Proteinase K stock solution: 1 mg/mL proteinase K in ultra-pure water. Weight 1 mg of lyophilized proteinase K and dissolve it in 1 mL of ultra-pure water. Store single-use aliquots at -80 °C.

2. PBS PI: PBS containing 1x protease inhibitor cocktail. Reconstitute a protease inhibitor cocktail to a 1x solution in PBS. Use fresh dilution for each experiment.

3. Triton 1% solution: PBS PI containing 5 µM of Triton X-100. Dilute Triton X-100 stock solution with PBS PI to reach a 1% Triton X-100 solution. Use fresh dilution for each experiment.

4. Nonlytic NLuc reagent: we use the Nano-Glo™ Live Cell assay reagent from Promega.

2.3 Uptake and Content delivery Assays

1. Fetal bovine serum (FBS)-free or EV-depleted cell culture media.

3. Lytic NLuc reagent: we use the Nano-Glo® Luciferase Assay System from Promega.

3. EDTA solution: PBS with 0.5 mM EDTA. Dilute EDTA in PBS to reach a concentration of 0.5 mM. Store at 4 °C.

4. 30 G needles adapted on 1 mL syringes.

5. Micro-tip sonicator.

3. Methods

3.1. Assessment of cargo's topology

Isolated EVs (see Note 1) emanating from donor cells expressing putative NLuc-tagged EV cargo are treated with a protease with or without detergents. In absence of detergents, a cargo inside EVs is expected to be protected from protease degradation.

1. Prepare four aliquots (1 µg equivalent proteins into 10 µL of PBS) for each EV preparation to test the following conditions, with 2-3 technical replicates per condition. Sample A: EVs alone. Sample B: EVs + Triton X-100, to rule out effect of Triton X-100 on NLuc activities (see Note 2). Sample C: EVs + proteinase K, to assess the amount of unprotected cargo. Sample D: EVs + Triton X-100 + proteinase K, to assess the total amount of EV-associated NLuc cargo (samples preparation is summarized in table 1 and detailed in step 2-4 below). All samples are loaded on a 96 opaque white well-plate and must be kept on ice, except when mentioned otherwise.

2. Add 10 µL of Triton 1% solution for samples B and D. Add 10 µL of PBS for samples A and C.

3. Dilute proteinase K stock solution (1 mg/mL) within ice-cold PBS PI to 100 µg/mL (see Note 3).
4. Add 50 µL of the diluted proteinase K solution to samples C and D. The final volume of each well should be 100 µL, supplemented with ice-cold PBS PI when required.
5. Incubate at room temperature for five hours (see Note 2).
6. Add 20 µL of nonlytic NLuc reagent to each well.
7. Read NLuc activities immediately using a luminometer.
8. Compare the readings of samples C and D to determine whether the EV cargo is inside the vesicles. A cargo located inside the vesicle is expected to be proteinase K resistant in absence of detergent.

3.2. EV Uptake assay

EV containing NLuc-cargo are incubated with acceptor cells. The EV uptake assay measures the NLuc activity that remains associated with acceptor cells, after donor EVs washout. EV uptake does not discriminate between EVs docked at the cell surface, EVs internalized within the endo/lysosomal compartments, or EV cargo delivered within the cytosol of acceptor cells.

1. Seed acceptor cells in a clear-bottom white plate to reach around 80-90% confluency by the end of the assay (day 1 for short kinetics or day 2 for long kinetics) (see Note 4).
2. 24 hours later, replace the media with FBS-free media or EV-depleted media according to acceptor cell compatibility/sensitivity. If not possible, experiments can be performed in complete media but FBS-derived EVs may interfere with the NLuc-positive EVs.
3. Add EV input (1 µg equivalent protein into 10 µL of PBS) in each well and incubate for the desired time. We highly recommend performing kinetics (from 1 to 24 hours) and dose responses in initial attempts.
4. Wash 3 times with ice-cold PBS.
5. Add 50 µL of PBS to each well.
6. Add EV input in empty wells (replicates recommended). Dilute EV input in ice-cold PBS to reach a total of 50 µL.
7. If using the Nano-Glo® Luciferase Assay System (Lytic NLuc kit), dilute 1 µL of NLuc-substrate in 50 µL of buffer for each well, and add it to the top of each sample.
8. Read NLuc activities with a luminometer.

9. Subtract backgrounds using signals from acceptor cells not receiving any labelled EVs. EV uptake can be quantified as follows:

$$Uptake (\%input) = \frac{(acceptor\ cells\ signal - background) \times 100}{input\ signal - background}$$

3.3. EV content release assay

After incubation with NLuc-EVs, acceptor cells are mechanically disrupted to separate membrane and cytosolic fractions. This allows us to acutely measure EV-cargo delivery into the cytosol of acceptor cells.

1. Seed acceptor cells to reach around 80-90% confluency by the end of the assay (day 1 for short kinetics or day 2 for long kinetics). Seed at least 100 000 cells in a 24 well-plate to collect enough cells for the cell fractionation step.
2. Proceed as for the EV uptake assay describe in 3.2 until step 6.
3. After PBS wash, add the EDTA solution to adherent cells (300 μ L per well for a 24-well plate) and incubate at room temperature for 10 minutes to detach the cells.
4. Collect the detached cells in 1.5 mL microtubes and centrifuge at 500 g for 10 min 4°C. Cells in suspension can be directly collected using low-speed centrifugation. From this step, all samples should remain on ice or at 4 °C.
5. Remove the supernatant and resuspend the cell pellet in 200 μ L of PBS PI.
6. Vortex the sample for 5 minutes.
7. Pass each sample through a 30 G needle attached to a 1 mL syringe for 5 times.
8. Sonicate the samples (5 seconds at 30% duty cycle, output control level 3 if using the Ultrasonic Processor of Thomas scientific) (see Note 5).
9. Centrifuge the samples at 350 g for 10 minutes at 4 °C to collect the remaining intact cells.
10. Transfer the supernatant to a new microtube and resuspend the pellet (intact cells) in 200 μ L of PBS PI and store on ice to assess the percentage of intact cells.
11. Centrifuge the supernatant at 100.000 g for 1 hour at 4°C to separate membrane fractions (pellet) from cytosolic fractions (supernatant). Resuspend the membrane fraction in 200 μ L of PBS PI.
12. Transfer each sample to a 96-well white plate to measure luminescence activities within each fraction and initial EV input.
13. Calculate the percentage of cytosolic release using the following formula:

$$\text{Cytosolic release (\%)} = \frac{\text{Cytosol signal} \times 100}{(\text{Membrane signal} + \text{Cytosol signal})}$$

4. Notes

1. Here we start right after the EV isolation, which has been extensively described (7). we highly recommend to assess the quality of the EV samples, following MISEV recommendations (8), especially to quantify the protein concentrations of EV samples.
2. Ensure that the NLuc activity within the EV input is at least 1000x above the background. If not, we recommend increasing the input of donor cells. For HeLa cells expressing NLuc-Hsp70, we recommend starting with at least 200 x 10⁶ cells and collecting conditioned media after 24 hours, when isolating EVs through sequential ultracentrifugation.
3. For the protease protection assay, we noticed that the amount and type of detergent affect the NLuc activity (6). We therefore highly recommend systematically assessing the effects of detergents. In our hands, 0.1% Triton X-100 works well. Similarly, the concentration, time and temperature of incubation with the proteinase K need optimization, and the parameters mentioned above are only indicative. Our indicated protocol should be considered as a starting point and may benefit from optimization.
4. We mostly used white-wall plates with clear bottoms, which enable us to visually check the cells during the culture. A white tape is stuck to the bottom just before reading the luminescence on the plate reader, to avoid any leakage of luminescence signal. The EV uptake efficiency is low, around 1% in our cell model. We highly recommend separating the samples for measurements of EV uptake and EV input, which shows low and high NLuc activities, respectively, to avoid cross-contamination between adjacent wells.
5. The cell disruption/fractionation procedure needs to be set up or optimized with each sonicator device. We recommend starting by assessing the behaviors of several cargo models (e.g., Hsp70 as a soluble cargo and CD63 as a membrane cargo) in different fractions using western blotting for endogenous proteins or luminescent signals for NLuc-tagged cargoes (6). Intact cell samples should be used to calculate the overall EV uptake (sum of the 3 fractions) and to estimate cell fractionation efficiency.

5. Acknowledgments.

This work is supported by ANR-18-IDEX-0001, IdEx Université de Paris, ANR-19-CE18-002001, and ANR-20-CE15-002102. E.B is supported by a PhD fellowship from La Ligue contre le cancer. S.B is supported by a PhD fellowship from PSL-University.

Figures and Tables

Conditions	A: EVs alone	B: Triton	C: Protease K	D: Triton + Prot. K
Sample (μL)	10	10	10	10
Triton 1x solution (μL)	-	10	-	10
PBS PPI solution (μL)	90	80	40	30
Proteinase K solution at 0.1 mg/mL (μL)	-	-	50	50

Table 1. Summary of sample preparation to perform protease protection assay on NLuc EV cargo.

EV Uptake Assay

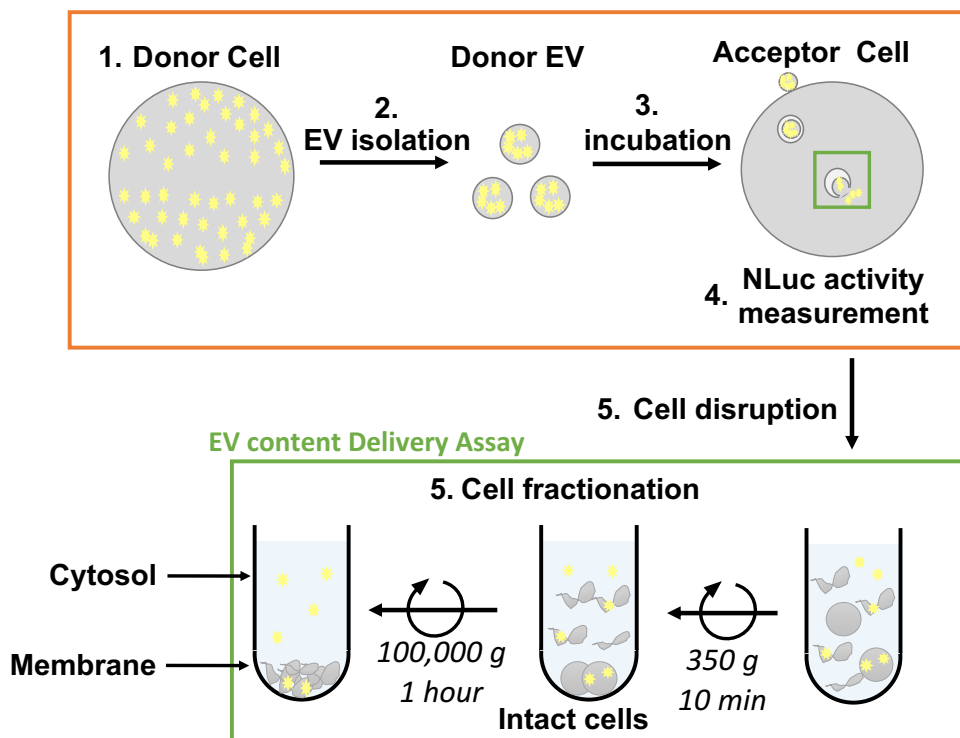


Figure 1. EV Uptake and EV Content Delivery assays. Donor cells expressing Nluc-EV cargo release EVs (1) that are isolated (2). EVs are incubated on unlabeled acceptor cells (3). After EV removal, luminescence can be measured within the acceptor cells (4) to quantify the amount EV that i) are docked at the plasma membrane, ii) are internalized within endo/lysosomal compartments, iii) have release their Nluc-cargo within the cytosol of the acceptor cells (EV Uptake assay in orange). Alternatively, acceptor cells can be further processed for mechanical disruption (5) and cell fractionation (6) to separate cytosolic and membrane fractions, in which Nluc-activity can be measured to determine the % of cytosolic release (EV content delivery in green).

References

1. Valadi H, Ekström K, Bossios A, et al (2007) Exosome-mediated transfer of mRNAs and microRNAs is a novel mechanism of genetic exchange between cells. *Nat Cell Biol* 9:654–659
2. Balaj L, Lessard R, Dai L, et al (2011) Tumour microvesicles contain retrotransposon elements and amplified oncogene sequences. *Nat Commun* 2
3. Skog J, Würdinger T, Rijn S van, et al (2008) Glioblastoma microvesicles transport RNA and proteins that promote tumour growth and provide diagnostic biomarkers. *Nat Cell Biol* 10:1470–1476
4. Mathieu M, Martin-Jaulat L, Lavieu G, et al (2019) Specificities of secretion and uptake of exosomes and other extracellular vesicles for cell-to-cell communication. *Nat Cell Biol* 21:9–17
5. Costa Verdera H, Gitz-Francois JJ, Schiffelers RM, et al (2017) Cellular uptake of extracellular vesicles is mediated by clathrin-independent endocytosis and macropinocytosis. *J Control Release* 266:100–108
6. Bonsergent E, Grisard E, Buchrieser J, et al (2021) Quantitative characterization of extracellular vesicle uptake and content delivery within mammalian cells. *Nat Commun* 12:1864
7. Théry C, Clayton A, Amigorena S, et al (2006) Isolation and Characterization of Exosomes from Cell Culture Supernatants. *Curr Protoc Cell Biol* 30:3.22:3.22.1–3.22.29
8. Théry C, Witwer KW, Aikawa E, et al (2018) Minimal information for studies of extracellular vesicles 2018 (MISEV2018): a position statement of the International Society for Extracellular Vesicles and update of the MISEV2014 guidelines. *J Extracell Vesicles* 7

REFERENCES

1. Wolf P (1967) The nature and significance of platelet products in human plasma. *Br J Haematol* 13:269–288
2. Anderson HC (1969) Vesicles associated with calcification in the matrix of epiphyseal cartilage. *J Cell Biol* 41:59–72
3. Harding C, Heuser J, and Stahl P (1983) Receptor-mediated endocytosis of transferrin and recycling of the transferrin receptor in rat reticulocytes. *J Cell Biol* 97:329–339
4. Pan B-T, Teng K, Wu C, et al (1985) Electron Microscopic Evidence for Externalization of the Transferrin Receptor in Vesicular Form in Sheep Reticulocytes. *J Cell Biol* 101:942–948
5. Johnstone RM, Adam M, Hammond JR, et al (1987) Vesicle formation during reticulocyte maturation. Association of plasma membrane activities with released vesicles (exosomes). *J Biol Chem* 262:9412–9420
6. Raposo G, Nijman HW, Stoorvogel W, et al (1996) B lymphocytes secrete antigen-presenting vesicles. *J Exp Med* 183:1161–1172
7. Wolfers J, Lozier A, Raposo G, et al (2001) Tumor-derived exosomes are a source of shared tumor rejection antigens for CTL cross-priming. *Nat Med* 7:297–303
8. Ratajczak J, Miekus K, Kucia M, et al (2006) Embryonic stem cell-derived microvesicles reprogram hematopoietic progenitors: Evidence for horizontal transfer of mRNA and protein delivery. *Leukemia* 20:847–856
9. Valadi H, Ekström K, Bossios A, et al (2007) Exosome-mediated transfer of mRNAs and microRNAs is a novel mechanism of genetic exchange between cells. *Nat Cell Biol* 9:654–659
10. György B, Szabó TG, Pásztói M, et al (2011) Membrane vesicles, current state-of-the-art: Emerging role of extracellular vesicles. *Cell Mol Life Sci* 68:2667–2688
11. Crawford N (1971) The presence of contractile proteins in platelet microparticles isolated from human and animal platelet-free plasma. *Br J Haematol* 21:53–69
12. George JN, Thoi LL, McManus LM, et al (1982) Isolation of human platelet membrane microparticles from plasma and serum. *Blood* 60:834–40
13. Stegmayr B and Ronquist G (1982) Promotive effect on human sperm progressive motility by prostasomes. *Urol Res* 10:253–7
14. Trams EG, Lauter CJ, Salem N, et al (1981) Exfoliation of membrane ecto-enzymes in the form of micro-vesicles. *Biochim Biophys Acta* 645:63–70
15. Kassis S, Lauter CJ, Stojanov M, et al (1986) Exfoliation of the β -adrenergic receptor and the regulatory components of adenylate cyclase by cultured rat glioma C6 cells. *Biochim Biophys Acta - Mol Cell Res* 886:474–482
16. Gutwein P, Stoeck A, Riedle S, et al (2005) Cleavage of L1 in exosomes and apoptotic membrane vesicles released from ovarian carcinoma cells. *Clin Cancer Res* 11:2492–501
17. Théry C, Witwer KW, Aikawa E, et al (2018) Minimal information for studies of extracellular vesicles 2018 (MISEV2018): a position statement of the International Society for Extracellular Vesicles and update of the MISEV2014 guidelines. *J Extracell vesicles* 7:1535750
18. Mitchell P, Petfalski E, Shevchenko A, et al (1997) The exosome: a conserved eukaryotic RNA processing complex containing multiple 3'→5' exoribonucleases. *Cell* 91:457–66
19. Witwer KW and Théry C (2019) Extracellular vesicles or exosomes? On primacy, precision, and popularity influencing a choice of nomenclature. *J Extracell vesicles* 8:1648167
20. Niel G Van, D'Angelo G, and Raposo G (2018) Shedding light on the cell biology of extracellular vesicles. *Nat Rev Mol Cell Biol* 19:213–228

21. Russell MRG, Nickerson DP, and Odorizzi G (2006) Molecular mechanisms of late endosome morphology, identity and sorting. *Curr Opin Cell Biol* 18:422–8
22. Dunn WA (1994) Autophagy and related mechanisms of lysosome-mediated protein degradation. *Trends Cell Biol* 4:139–143
23. Ostrowski M, Carmo NB, Krumeich S, et al (2010) Rab27a and Rab27b control different steps of the exosome secretion pathway. *Nat Cell Biol* 12:19–30
24. Stein JM and Luzio JP (1991) Ectocytosis caused by sublytic autologous complement attack on human neutrophils. The sorting of endogenous plasma-membrane proteins and lipids into shed vesicles. *Biochem J* 274 (Pt 2:381–6
25. Mathieu M, Martin-Jaular L, Lavieu G, et al (2019) Specificities of secretion and uptake of exosomes and other extracellular vesicles for cell-to-cell communication. *Nat Cell Biol* 21:9–17
26. Ratajczak J, Wysoczynski M, Hayek F, et al (2006) Membrane-derived microvesicles: important and underappreciated mediators of cell-to-cell communication. *Leukemia* 20:1487–95
27. Gluschankof P, Mondor I, Gelderblom HR, et al (1997) Cell Membrane Vesicles Are a Major Contaminant of Gradient-Enriched Human Immunodeficiency Virus Type-1 Preparations. *Virology* 230:125–133
28. Al-Nedawi K, Meehan B, Micallef J, et al (2008) Intercellular transfer of the oncogenic receptor EGFRvIII by microvesicles derived from tumour cells. *Nat Cell Biol* 10:619–624
29. Kerr JF, Wyllie AH, and Currie AR (1972) Apoptosis: a basic biological phenomenon with wide-ranging implications in tissue kinetics. *Br J Cancer* 26:239–57
30. Zhang H, Freitas D, Kim HS, et al (2018) Identification of distinct nanoparticles and subsets of extracellular vesicles by asymmetric flow field-flow fractionation. *Nat Cell Biol* 20:332–343
31. Mathieu M, Névo N, Jouve M, et al (2020) Specificities of exosome versus small ectosome secretion revealed by live intracellular tracking and synchronized extracellular vesicle release of CD9 and CD63. 2020.10.27.323766
32. Kowal J, Arras G, Colombo M, et al (2016) Proteomic comparison defines novel markers to characterize heterogeneous populations of extracellular vesicle subtypes. *Proc Natl Acad Sci U S A* 113:E968–E977
33. Zaborowski MP, Balaj L, Breakefield XO, et al (2015) Extracellular Vesicles: Composition, Biological Relevance, and Methods of Study. *Bioscience* 65:783–797
34. Genschmer KR, Russell DW, Lal C, et al (2019) Activated PMN Exosomes: Pathogenic Entities Causing Matrix Destruction and Disease in the Lung. *Cell* 176:113-126.e15
35. Tkach M, Kowal J, Zucchetti AE, et al (2017) Qualitative differences in T-cell activation by dendritic cell-derived extracellular vesicle subtypes. *EMBO J* 36:3012–3028
36. Luga V, Zhang L, Vitoria-Petit AM, et al (2012) Exosomes mediate stromal mobilization of autocrine Wnt-PCP signaling in breast cancer cell migration. *Cell* 151:1542–56
37. Skog J, Würdinger T, Rijn S van, et al (2008) Glioblastoma microvesicles transport RNA and proteins that promote tumour growth and provide diagnostic biomarkers. *Nat Cell Biol* 10:1470–6
38. Crewe C, Joffin N, Rutkowski JM, et al (2018) An Endothelial-to-Adipocyte Extracellular Vesicle Axis Governed by Metabolic State. *Cell* 175:695-708.e13
39. Korkut C, Li Y, Koles K, et al (2013) Regulation of Postsynaptic Retrograde Signaling by Presynaptic Exosome Release. *Neuron* 77:1039–1046
40. Mack M, Kleinschmidt A, Brühl H, et al (2000) Transfer of the chemokine receptor CCR5 between cells by membrane- derived microparticles: A mechanism for cellular human immunodeficiency virus 1 infection. *Nat Med* 6:769–775

41. Fevrier B, Vilette D, Archer F, et al (2004) Cells release prions in association with exosomes. *Proc Natl Acad Sci U S A* 101:9683–9688
42. Vella LJ, Sharples RA, Lawson VA, et al (2007) Packaging of prions into exosomes is associated with a novel pathway of PrP processing. *J Pathol* 211:582–590
43. Antonyak MA, Li B, Boroughs LK, et al (2011) Cancer cell-derived microvesicles induce transformation by transferring tissue transglutaminase and fibronectin to recipient cells. *Proc Natl Acad Sci U S A* 108:4852–4857
44. Chivet M, Javalet C, Laulagnier K, et al (2014) Exosomes secreted by cortical neurons upon glutamatergic synapse activation specifically interact with neurons. *J Extracell Vesicles* 3:1–10
45. Franzen CA, Simms PE, Huis AF Van, et al (2014) Characterization of uptake and internalization of exosomes by bladder cancer cells. *Biomed Res Int* 2014:619829
46. Fitzner D, Schnaars M, Rossum D Van, et al (2011) Selective transfer of exosomes from oligodendrocytes to microglia by macropinocytosis. *J Cell Sci* 124:447–458
47. Svensson KJ, Christianson HC, Wittrup A, et al (2013) Exosome uptake depends on ERK1/2-heat shock protein 27 signaling and lipid Raft-mediated endocytosis negatively regulated by caveolin-1. *J Biol Chem* 288:17713–24
48. Nanbo A, Kawanishi E, Yoshida R, et al (2013) Exosomes Derived from Epstein-Barr Virus-Infected Cells Are Internalized via Caveola-Dependent Endocytosis and Promote Phenotypic Modulation in Target Cells. *J Virol* 87:10334–10347
49. Kanada M, Bachmann MH, Hardy JW, et al (2015) Differential fates of biomolecules delivered to target cells via extracellular vesicles. *Proc Natl Acad Sci U S A* 112:E1433–42
50. Holmgren L, Szeles A, Rajnavö E, et al (1999) Horizontal Transfer of DNA by the Uptake of Apoptotic Bodies. *Blood* 93:3956–3963
51. Montecalvo A, Larregina AT, Shufesky WJ, et al (2012) Mechanism of transfer of functional microRNAs between mouse dendritic cells via exosomes. *Blood* 119:756–66
52. Morelli AE, Larregina AT, Shufesky WJ, et al (2004) Endocytosis, intracellular sorting, and processing of exosomes by dendritic cells. *Blood* 104:3257–66
53. Christianson HC, Svensson KJ, Kuppevelt TH van, et al (2013) Cancer cell exosomes depend on cell-surface heparan sulfate proteoglycans for their internalization and functional activity. *Proc Natl Acad Sci* 110:17380–17385
54. Parolini I, Federici C, Raggi C, et al (2009) Microenvironmental pH is a key factor for exosome traffic in tumor cells. *J Biol Chem* 284:34211–22
55. Balaj L, Lessard R, Dai L, et al (2011) Tumour microvesicles contain retrotransposon elements and amplified oncogene sequences. *Nat Commun* 2:180
56. MJ M, PS M, BD J, et al (1988) In vivo labeling of resident peritoneal macrophages. *J Leukoc Biol* 43:387–397
57. Horibe S, Tanahashi T, Kawauchi S, et al (2018) Mechanism of recipient cell-dependent differences in exosome uptake. *BMC Cancer* 18:47
58. Kamerkar S, LeBleu VS, Sugimoto H, et al (2017) Exosomes facilitate therapeutic targeting of oncogenic KRAS in pancreatic cancer. *Nature* 546:498–503
59. Verweij FJ, Revenu C, Arras G, et al (2019) Live Tracking of Inter-organ Communication by Endogenous Exosomes In Vivo. *Dev Cell* 48:573–589.e4
60. Nolte-'t Hoen E, Cremer T, Gallo RC, et al (2016) Extracellular vesicles and viruses: Are they close relatives? *Proc Natl Acad Sci U S A* 113:9155–61
61. Finkelshtein D, Werman A, Novick D, et al (2013) LDL receptor and its family members serve as the cellular receptors for vesicular stomatitis virus. *Proc Natl Acad Sci U S A* 110:7306–11

62. Martin DN and Uprichard SL (2013) Identification of transferrin receptor 1 as a hepatitis C virus entry factor. *Proc Natl Acad Sci* 110:10777–10782
63. Olofsson S and Bergström T (2005) Glycoconjugate glycans as viral receptors. *Ann Med* 37:154–72
64. Chen B (2019) Molecular Mechanism of HIV-1 Entry. *Trends Microbiol* 27:878–891
65. Roth TF and Porter KR (1964) YOLK PROTEIN UPTAKE IN THE OOCYTE OF THE MOSQUITO *AEDES AEGYPTI*. L. *J Cell Biol* 20:313–32
66. Brown MS and Goldstein JL (1979) Receptor-mediated endocytosis: insights from the lipoprotein receptor system. *Proc Natl Acad Sci U S A* 76:3330–7
67. Pearse BM (1976) Clathrin: a unique protein associated with intracellular transfer of membrane by coated vesicles. *Proc Natl Acad Sci U S A* 73:1255–9
68. Helenius A, Kartenbeck J, Simons K, et al (1980) ON THE ENTRY OF SEMLIKI FOREST VIRUS INTO BHK-21 CELLS. 84:404–420
69. Dahlberg JE (1974) Quantitative Electron Microscopic Analysis of the Penetration of VSV into L Cells. *Virology* 68:250–262
70. Helle F and Dubuisson J (2007) Hepatitis C virus entry into host cells. *Cell Mol Life Sci* 2007 651 65:100–112
71. Johannsdottir HK, Mancini R, Kartenbeck J, et al (2009) Host Cell Factors and Functions Involved in Vesicular Stomatitis Virus Entry. *J Virol* 83:440–453
72. Cureton DK, Massol RH, Saffarian S, et al (2009) Vesicular stomatitis virus enters cells through vesicles incompletely coated with clathrin that depend upon actin for internalization. *PLoS Pathog* 5:e1000394
73. Carneiro FA, Ferradosa AS, and Poian AT Da (2001) Low pH-induced Conformational Changes in Vesicular Stomatitis Virus Glycoprotein Involve Dramatic Structure Reorganization. *J Biol Chem* 276:62–67
74. Durrer P, Gaudin Y, Ruigrok RWH, et al (1995) Photolabeling Identifies a Putative Fusion Domain in the Envelope Glycoprotein of Rabies and Vesicular Stomatitis Viruses. *J Biol Chem* 270:17575–17581
75. FAWCETT DW (1965) SURFACE SPECIALIZATIONS OF ABSORBING CELLS. *J Histochem Cytochem* 13:75–91
76. Swanson JA and Watts C (1995) Macropinocytosis. *Trends Cell Biol* 5:424–428
77. Racoosin EL and Swanson JA (1993) Macropinosome maturation and fusion with tubular lysosomes in macrophages. *J Cell Biol* 121:1011–20
78. Hewlett LJ, Prescott AR, and Watts C (1994) The coated pit and macropinocytic pathways serve distinct endosome populations. *J Cell Biol* 124:689–703
79. Mercer J and Helenius A (2008) Vaccinia virus uses macropinocytosis and apoptotic mimicry to enter host cells. *Science* 320:531–5
80. Townsley AC, Weisberg AS, Wagenaar TR, et al (2006) Vaccinia virus entry into cells via a low-pH-dependent endosomal pathway. *J Virol* 80:8899–908
81. Garner JA (2003) Herpes simplex virion entry into and intracellular transport within mammalian cells. *Adv Drug Deliv Rev* 55:1497–513
82. Devadas D, Koithan T, Diestel R, et al (2014) Herpes Simplex Virus Internalization into Epithelial Cells Requires Na⁺/H⁺ Exchangers and p21-Activated Kinases but neither Clathrin- nor Caveolin-Mediated Endocytosis. *J Virol* 88:13378–13395
83. Tsai B, Gilbert JM, Stehle T, et al (2003) Gangliosides are receptors for murine polyoma virus and SV40. *EMBO J* 22:4346–4355

84. Ewers H, Römer W, Smith AE, et al (2009) GM1 structure determines SV40-induced membrane invagination and infection. *Nat Cell Biol* 2010 12:11–18
85. Engel S, Heger T, Mancini R, et al (2011) Role of Endosomes in Simian Virus 40 Entry and Infection. *J Virol* 85:4198–4211
86. Schelhaas M, Malmström J, Pelkmans L, et al (2007) Simian Virus 40 depends on ER protein folding and quality control factors for entry into host cells. *Cell* 131:516–29
87. Qian M, Cai D, Verhey KJ, et al (2009) A lipid receptor sorts polyomavirus from the endolysosome to the endoplasmic reticulum to cause infection. *PLoS Pathog* 5:e1000465
88. Kojic LD, Joshi B, Lajoie P, et al (2007) Raft-dependent Endocytosis of Autocrine Motility Factor Is Phosphatidylinositol 3-Kinase-dependent in Breast Carcinoma Cells. *J Biol Chem* 282:29305–29313
89. Sabharanjak S, Sharma P, Parton RG, et al (2002) GPI-Anchored Proteins Are Delivered to Recycling Endosomes via a Distinct cdc42-Regulated, Clathrin-Independent Pinocytic Pathway. *Dev Cell* 2:411–423
90. Shivakumar P, Mourya R, and Bezerra JA (2014) Perforin and granzymes work in synergy to mediate cholangiocyte injury in experimental biliary atresia. *J Hepatol* 60:370–6
91. Davey J, Hurlley SM, and Warren' G (1985) Reconstitution of an Endocytic Fusion Event in a Cell-Free System. *Cell* 43:643–652
92. Larrick JW, Enns C, Raubitschek A, et al (1985) Receptor-mediated endocytosis of human transferrin and its cell surface receptor. *J Cell Physiol* 124:283–287
93. Jiang R, Scott RS, and Hutt-Fletcher LM (2006) Epstein-Barr Virus Shed in Saliva Is High in B-Cell-Tropic Glycoprotein gp42. *J Virol* 80:7281–7283
94. Feng Y, Broder CC, Kennedy PE, et al (1996) HIV-1 entry cofactor: Functional cDNA cloning of a seven-transmembrane, G protein-coupled receptor. *Science* (80-) 272:872–877
95. Colicelli J (2004) Human RAS superfamily proteins and related GTPases. *Sci STKE* 2004:RE13
96. Schmitt HD, Wagner P, Pfaff E, et al (1986) The ras-related YPT1 gene product in yeast: A GTP-binding protein that might be involved in microtubule organization. *Cell* 47:401–412
97. Segev N, Mulholland J, and Botstein D (1988) The yeast GTP-binding YPT1 protein and a mammalian counterpart are associated with the secretion machinery. *Cell* 52:915–924
98. Chavrier P, Parton RG, Hauri HP, et al (1990) Localization of Low Molecular Weight GTP Binding Proteins to Exocytic and Endocytic Compartments. *Cell* 62:317–329
99. Bhui T and Roy JK (2014) Rab proteins: The key regulators of intracellular vesicle transport. *Exp Cell Res* 328:1–19
100. Martinez O and Goud B (1998) Rab proteins. *Biochim Biophys Acta - Mol Cell Res* 1404:101–112
101. Vitale G, Rybin V, Christoforidis S, et al (1998) Distinct Rab-binding domains mediate the interaction of Rabaptin-5 with GTP-bound rab4 and rab5. *EMBO J* 17:1941–1951
102. Seabra MC and Coudrier E (2004) Rab GTPases and myosin motors in organelle motility. *Traffic* 5:393–9
103. Chou H-T, Dukovski D, Chambers MG, et al (2016) CATCHR, HOPS and CORVET tethering complexes share a similar architecture. *Nat Struct Mol Biol* 2016 238 23:761–763
104. Kuhlee A, Raunser S, and Ungermann C (2015) Functional homologies in vesicle tethering. *FEBS Lett* 589:2487–97
105. Rink J, Ghigo E, Kalaidzidis Y, et al (2005) Rab Conversion as a Mechanism of Progression from Early to Late Endosomes. *Cell* 122:735–749
106. Guerra F and Bucci C (2016) Multiple Roles of the Small GTPase Rab7. 5

107. Saraste J (2016) Spatial and Functional Aspects of ER-Golgi Rabs and Tethers. *Front cell Dev Biol* 4:28
108. Wong M and Munro S (2014) The specificity of vesicle traffic to the Golgi is encoded in the golgin coiled-coil proteins Europe PMC Funders Group. *Science* (80-) 346:1256898
109. Malsam J, Satoh A, Pelletier L, et al (2005) Golgin tethers define subpopulations of COPI vesicles. *Science* 307:1095–8
110. Malhotra V, Orci L, Glick BS, et al (1988) Role of an N-ethylmaleimide-sensitive transport component in promoting fusion of transport vesicles with cisternae of the Golgi stack. *Cell* 54:221–7
111. Clary D O, Griff IC, and Rothman' JE (1990) SNAPs, a Family of NSF Attachment Proteins Involved in Intracellular Membrane Fusion in Animals and Yeast. *Cell* 61:709–721
112. Söllner T, Whiteheart SW, Brunner M, et al (1993) SNAP receptors implicated in vesicle targeting and fusion. *Nature* 362:318–24
113. Parlati F, McNew JA, Fukuda R, et al (2000) Topological restriction of SNARE-dependent membrane fusion. *Nature* 407:194–8
114. Fukuda R, McNew JA, Weber T, et al (2000) Functional architecture of an intracellular membrane t-SNARE. *Nature* 407:198–202
115. McNew JA, Parlati F, Fukuda R, et al (2000) Compartmental specificity of cellular membrane fusion encoded in SNARE proteins. *Nature* 407:153–9
116. Hayashi T, McMahon H, Yamasaki S, et al (1994) Synaptic vesicle membrane fusion complex: Action of clostridial neurotoxins on assembly. *EMBO J* 13:5051–5061
117. Wang T, Li L, and Hong W (2017) SNARE proteins in membrane trafficking. *Traffic* 18:767–775
118. Südhof TC and Rothman JE (2009) Membrane fusion: grappling with SNARE and SM proteins. *Science* 323:474–7
119. Giraudo CG, Eng WS, Melia TJ, et al (2006) A clamping mechanism involved in SNARE-dependent exocytosis. *Science* 313:676–80
120. Rothman JE, Krishnakumar SS, Grushin K, et al (2017) Hypothesis-butressed rings assemble, clamp, and release SNAREpins for synaptic transmission. *FEBS Lett* 591:3459–3480
121. Pang ZP, Shin O-H, Meyer AC, et al (2006) A gain-of-function mutation in synaptotagmin-1 reveals a critical role of Ca²⁺-dependent soluble N-ethylmaleimide-sensitive factor attachment protein receptor complex binding in synaptic exocytosis. *J Neurosci* 26:12556–65
122. Lavielle C, Cornelis G, Dupressoir A, et al (2013) Paleovirology of “syncytins”, retroviral env genes exapted for a role in placentation. *Philos Trans R Soc Lond B Biol Sci* 368:20120507
123. Blond J-L, Lavillette D, Cheynet V, et al (2000) An Envelope Glycoprotein of the Human Endogenous Retrovirus HERV-W Is Expressed in the Human Placenta and Fuses Cells Expressing the Type D Mammalian Retrovirus Receptor. *J Virol* 74:3321–3329
124. Blaise S, Parseval N de, Bénit L, et al (2003) Genomewide screening for fusogenic human endogenous retrovirus envelopes identifies syncytin 2, a gene conserved on primate evolution. *Proc Natl Acad Sci U S A* 100:13013–8
125. Gong R, Peng X, Kang S, et al (2005) Structural characterization of the fusion core in syncytin, envelope protein of human endogenous retrovirus family W. *Biochem Biophys Res Commun* 331:1193–1200
126. Gruenberg JE and Howell KE (1986) Reconstitution of vesicle fusions occurring in endocytosis with a cell-free system. *EMBO J* 5:3091–3101
127. Millay DP, O'Rourke JR, Sutherland LB, et al (2013) Myomaker is a membrane activator of myoblast fusion and muscle formation. *Nature* 499:301–5

128. Bi P, Ramirez-Martinez A, Li H, et al (2017) Control of muscle formation by the fusogenic micropeptide myomixer. *Science* 356:323–327
129. Quinn ME, Goh Q, Kurosaka M, et al (2017) Myomerger induces fusion of non-fusogenic cells and is required for skeletal muscle development. *Nat Commun* 8:15665
130. Mohler WA, Shemer G, Campo JJ Del, et al (2002) The Type I Membrane Protein EFF-1 Is Essential for Developmental Cell Fusion. *Dev Cell* 2:355–362
131. Pérez-Vargas J, Krey T, Valansi C, et al (2014) Structural basis of eukaryotic cell-cell fusion. *Cell* 157:407–419
132. Avinoam O, Fridman K, Valansi C, et al (2011) Conserved eukaryotic fusogens can fuse viral envelopes to cells. *Science* 332:589–92
133. Rubinstein E, Ziyat A, Prenant M, et al (2006) Reduced fertility of female mice lacking CD81. *Dev Biol* 290:351–358
134. Frolikova M, Manaskova-Postlerova P, Cerny J, et al (2018) CD9 and CD81 Interactions and Their Structural Modelling in Sperm Prior to Fertilization. *Int J Mol Sci* 19
135. Charrin S, Latil M, Soave S, et al (2013) Normal muscle regeneration requires tight control of muscle cell fusion by tetraspanins CD9 and CD81. *Nat Commun* 4:1674
136. Takeda Y, Tachibana I, Miyado K, et al (2003) Tetraspanins CD9 and CD81 function to prevent the fusion of mononuclear phagocytes. *J Cell Biol* 161:945–956
137. Zhang L, Song G, Xu T, et al (2013) A novel ultrasensitive bioluminescent receptor-binding assay of INSL3 through chemical conjugation with nanoluciferase. *Biochimie* 95:2454–2459
138. Gould SJ, Kalish JE, Morrell JC, et al (1996) Pex13p is an SH3 protein of the peroxisome membrane and a docking factor for the predominantly cytoplasmic PTs1 receptor. *J Cell Biol* 135:85–95
139. Gouveia AMM, Reguenga C, Oliveira MEM, et al (2000) Characterization of peroxisomal Pex5p from rat liver. Pex5p in the Pex5p-Pex14p membrane complex is a transmembrane protein. *J Biol Chem* 275:32444–51
140. Lorenz H, Hailey DW, and Lippincott-Schwartz J (2006) Fluorescence protease protection of GFP chimeras to reveal protein topology and subcellular localization. *Nat Methods* 3:205–10
141. Taylor DD and Shah S (2015) Methods of isolating extracellular vesicles impact down-stream analyses of their cargoes. *Methods* 87:3–10
142. Wheeler DC, Fernando RL, Gillett MP, et al (1991) Characterisation of the binding of low-density lipoproteins to cultured rat mesangial cells. *Nephrol Dial Transplant* 6:701–8
143. Goldstein JL and Brown MS (1974) Binding and degradation of low density lipoproteins by cultured human fibroblasts. Comparison of cells from a normal subject and from a patient with homozygous familial hypercholesterolemia. *J Biol Chem* 249:5153–62
144. Tian T, Zhu Y, Wang Y, et al (2013) Dynamics of Exosome Internalization and Trafficking. *J Cell Physiol* 228:1487–1495
145. Kuwert E, Wiktor TJ, Sokol F, et al (1968) Hemagglutination by rabies virus. *J Virol* 2:1381–92
146. Moore JP and Klasse PJ (1992) Thermodynamic and kinetic analysis of sCD4 binding to HIV-1 virions and of gp120 dissociation. *AIDS Res Hum Retroviruses* 8:443–50
147. Costa Verdera H, Gitz-Francois JJ, Schiffelers RM, et al (2017) Cellular uptake of extracellular vesicles is mediated by clathrin-independent endocytosis and macropinocytosis. *J Control Release* 266:100–108
148. Zech D, Rana S, Büchler MW, et al (2012) Tumor-exosomes and leukocyte activation: an ambivalent crosstalk. *Cell Commun Signal* 10:37
149. Yang K, Mesquita B, Horvatovich P, et al (2020) Tuning liposome composition to modulate corona formation in human serum and cellular uptake. *Acta Biomater* 106:314–327

150. Aiken C (1997) Pseudotyping human immunodeficiency virus type 1 (HIV-1) by the glycoprotein of vesicular stomatitis virus targets HIV-1 entry to an endocytic pathway and suppresses both the requirement for Nef and the sensitivity to cyclosporin A. *J Virol* 71:5871–7
151. Dudek T and Knipe DM (2006) Replication-defective viruses as vaccines and vaccine vectors. *Virology* 344:230–9
152. Versluis AJ, Geel PJ van, Oppelaar H, et al (1996) Receptor-mediated uptake of low-density lipoprotein by B16 melanoma cells in vitro and in vivo in mice. *Br J Cancer* 74:525–32
153. Osterloh K and Aisen P (1989) Pathways in the binding and uptake of ferritin by hepatocytes. *Biochim Biophys Acta* 1011:40–5
154. Feng D, Zhao W-L, Ye Y-Y, et al (2010) Cellular internalization of exosomes occurs through phagocytosis. *Traffic* 11:675–87
155. Lee H-J (2019) Microbe-Host Communication by Small RNAs in Extracellular Vesicles: Vehicles for Transkingdom RNA Transportation. *Int J Mol Sci* 20
156. Koumangoye RB, Sakwe AM, Goodwin JS, et al (2011) Detachment of breast tumor cells induces rapid secretion of exosomes which subsequently mediate cellular adhesion and spreading. *PLoS One* 6:e24234
157. Jia J, Claude-Taupin A, Gu Y, et al (2020) Galectin-3 Coordinates a Cellular System for Lysosomal Repair and Removal. *Dev Cell* 52:69–87.e8
158. Paz I, Sachse M, Dupont N, et al (2010) Galectin-3, a marker for vacuole lysis by invasive pathogens. *Cell Microbiol* 12:530–44
159. Kondow-McConaghy HM, Muthukrishnan N, Erazo-Oliveras A, et al (2020) Impact of the Endosomal Escape Activity of Cell-Penetrating Peptides on the Endocytic Pathway. *ACS Chem Biol* 15:2355–2363
160. Joshi BS, Beer MA de, Giepmans BNG, et al (2020) Endocytosis of Extracellular Vesicles and Release of Their Cargo from Endosomes. *ACS Nano* 14:4444–4455
161. Kim IS, Jenni S, Stanifer ML, et al (2017) Mechanism of membrane fusion induced by vesicular stomatitis virus G protein. *Proc Natl Acad Sci U S A* 114:E28–E36
162. Bailey CC, Zhong G, Huang I-C, et al (2014) IFITM-Family Proteins: The Cell’s First Line of Antiviral Defense. *Annu Rev Virol* 1:261
163. Feeley EM, Sims JS, John SP, et al (2011) IFITM3 inhibits influenza A virus infection by preventing cytosolic entry. *PLoS Pathog* 7:e1002337
164. Mudhasani R, Tran JP, Retterer C, et al (2013) IFITM-2 and IFITM-3 but not IFITM-1 restrict Rift Valley fever virus. *J Virol* 87:8451–64
165. Bailey CC, Kondur HR, Huang IC, et al (2013) Interferon-induced Transmembrane Protein 3 Is a Type II Transmembrane Protein. *J Biol Chem* 288:32184–32193
166. Li K, Markosyan RM, Zheng Y-M, et al (2013) IFITM Proteins Restrict Viral Membrane Hemifusion. *PLoS Pathog* 9:1003124
167. Lin TY, Chin CR, Everitt AR, et al (2013) Amphotericin B Increases Influenza A Virus Infection by Preventing IFITM3-Mediated Restriction. *Cell Rep* 5:895–908
168. John SP, Chin CR, Perreira JM, et al (2013) The CD225 Domain of IFITM3 Is Required for both IFITM Protein Association and Inhibition of Influenza A Virus and Dengue Virus Replication. *J Virol* 87:7837–7852
169. Buchrieser J, Degrelle SA, Couderc T, et al (2019) IFITM proteins inhibit placental syncytiotrophoblast formation and promote fetal demise. *Science* 365:176–180
170. Somiya M and Kuroda S (2021) Real-Time Luminescence Assay for Cytoplasmic Cargo Delivery of Extracellular Vesicles. *Anal Chem* 93:5612–5620

171. Perissinotto F, Rondelli V, Senigaglia B, et al (2021) Structural insights into fusion mechanisms of small extracellular vesicles with model plasma membranes. *Nanoscale* 13:5224–5233
172. Escrevente C, Keller S, Altevogt P, et al (2011) Interaction and uptake of exosomes by ovarian cancer cells. *BMC Cancer* 11:108
173. Izquierdo-Useros N, Naranjo-Gómez M, Archer J, et al (2009) Capture and transfer of HIV-1 particles by mature dendritic cells converges with the exosome-dissemination pathway. *Blood* 113:2732
174. Jong OG de, Murphy DE, Mäger I, et al (2020) A CRISPR-Cas9-based reporter system for single-cell detection of extracellular vesicle-mediated functional transfer of RNA. *Nat Commun* 11:1113
175. Dai S, Wei D, Wu Z, et al (2008) Phase I clinical trial of autologous ascites-derived exosomes combined with GM-CSF for colorectal cancer. *Mol Ther* 16:782–90
176. Escudier B, Dorval T, Chaput N, et al (2005) Vaccination of metastatic melanoma patients with autologous dendritic cell (DC) derived-exosomes: results of the first phase I clinical trial. *J Transl Med* 3:10
177. Morse MA, Garst J, Osada T, et al (2005) A phase I study of dexosome immunotherapy in patients with advanced non-small cell lung cancer. *J Transl Med* 3:9
178. Besse B, Charrier M, Lapierre V, et al (2016) Dendritic cell-derived exosomes as maintenance immunotherapy after first line chemotherapy in NSCLC. *Oncoimmunology* 5:e1071008
179. Nassar W, El-Ansary M, Sabry D, et al (2016) Umbilical cord mesenchymal stem cells derived extracellular vesicles can safely ameliorate the progression of chronic kidney diseases. *Biomater Res* 20:21
180. Vakhshiteh F, Atyabi F, and Ostad SN (2019) Mesenchymal stem cell exosomes: a two-edged sword in cancer therapy. *Int J Nanomedicine* 14:2847–2859
181. Xunian Z and Kalluri R (2020) Biology and therapeutic potential of mesenchymal stem cell-derived exosomes. *Cancer Sci* 111:3100–3110
182. Chen Y-S, Lin E-Y, Chiou T-W, et al (2019) Exosomes in clinical trial and their production in compliance with good manufacturing practice. *Ci ji yi xue za zhi = Tzu-chi Med J* 32:113–120
183. Kwon HH, Yang SH, Lee J, et al (2020) Combination Treatment with Human Adipose Tissue Stem Cell-derived Exosomes and Fractional CO₂ Laser for Acne Scars: A 12-week Prospective, Double-blind, Randomized, Split-face Study. *Acta Derm Venereol* 100:adv00310
184. Sengupta V, Sengupta S, Lazo A, et al (2020) Exosomes Derived from Bone Marrow Mesenchymal Stem Cells as Treatment for Severe COVID-19. *Stem Cells Dev* 29:747–754
185. Elsharkasy OM, Nordin JZ, Hagey DW, et al (2020) Extracellular vesicles as drug delivery systems: Why and how? *Adv Drug Deliv Rev* 159:332–343

ILLUSTRATION TABLE

FIGURE 1: FIRST EV OBSERVATIONS	16
FIGURE 2: EVs ARE MULTIMODAL INTERCELLULAR MESSENGERS.....	21
FIGURE 3: VIRAL INTERNALIZATION PATHWAYS LEADING TO THEIR CONTENT DELIVERY	29
FIGURE 4: FIRST REPRESENTATION OF THE ENDOCYTIC PATHWAY.	30
FIGURE 5: PRINCIPLE OF THE FIRST CELL-FREE IN VITRO CONTENT MIXING ASSAY.....	33
FIGURE 6: DESCRIBED FUSION SYSTEMS IN EUKARYOTIC CELLS.....	34
FIGURE 7: HOPS-MEDIATED TETHERING OF A LATE ENDOSOME AND A LYSOSOME	36
FIGURE 8: INITIAL SNARE HYPOTHESIS	37
FIGURE 9: SNARE-MEDIATED VESICLE MEMBRANE FUSION	38
FIGURE 10: HYPOTHETIC ROUTE FOR EV CONTENT RELEASE WITHIN ACCEPTOR CELLS.....	41
FIGURE 11: GRAPHICAL ABSTRACT OF EV CONTENT RELEASE QUANTIFICATION WITH IN CELL-FREE EXTRACT	43
FIGURE 12: GRAPHICAL ABSTRACT OF THE CELLULAR CHARACTERIZATION OF EV UPTAKE AND CONTENT DELIVERY WITHIN HeLA CELLS.	55
FIGURE 13: WORKING MODEL FOR EV UPTAKE AND CONTENT DELIVERY WITHIN ACCEPTOR CELLS.....	69
TABLE 1: SUMMARY OF METHODS USED TO STUDY EV UPTAKE	24

RÉSUMÉ

Les vésicules extracellulaires sont des particules lipidiques renfermant du contenu biologique (protéines, lipides et acides nucléiques) provenant de leur cellule sécrétrice (cellule donneuse). Elles ont été décrites pour la première fois en 1967, mais elles sont longtemps restées considérées comme des vésicules destinées à l'élimination de déchets cellulaires ; la cellule donneuse se séparant ainsi des molécules non nécessaires à son état physiologique. Il faut attendre 3 décennies pour réaliser que ces vésicules ne sont pas seulement libérées dans le milieu extracellulaire par les cellules sécrétrices. En effet, elles peuvent ensuite être prises en charge par des cellules receveuses. Aujourd'hui il a été établi que ces vésicules sont sécrétées par toutes les cellules et qu'elles peuvent être collectées dans tous les fluides corporels *in vivo* mais aussi dans le milieu de culture de cellules *in vitro*.

Ainsi, les vésicules extracellulaires sont des vecteurs impliqués dans la communication intercellulaire. Des études sur leur biologie ont permis de mettre en évidence deux voies de sécrétion, permettant de définir différentes populations de vésicules extracellulaires :

- Les vésicules extracellulaires peuvent être formées par bourgeonnement de la membrane plasmique, confinant une partie du cytoplasme dans leur membrane et étant directement sécrétées dans le milieu extracellulaire. Ces vésicules sont appelées ectosomes (du phénomène ectocytose), elles peuvent aussi être décrites comme microvésicules ou microparticules dans la littérature.
- D'autres vésicules extracellulaires sont formées par invagination de la membrane endosomale, formant ainsi des vésicules intraluminales à l'intérieur d'endosomes multivésiculaires. Ces derniers peuvent fusionner avec la membrane plasmique, entraînant la libération de vésicules intraluminales dans le milieu extracellulaire. Ces vésicules sont alors appelées exosomes.

D'autres nomenclatures ont été décrites pour essayer d'établir des sous-populations de vésicules extracellulaires. Leurs descriptions se basent soit sur leur méthode d'isolation ou de détection, soit sur le contexte physiologique de sécrétion. Cependant il reste aujourd'hui très complexe d'étudier un seul sous-type de vésicules. Cette étude vise à étudier la biologie de la population entière, et donc hétérogène, des vésicules extracellulaires.

Les vésicules extracellulaires soulèvent un grand intérêt scientifique, principalement de par leur propriété de vecteur intercellulaire. En effet, elles peuvent transmettre des informations via plusieurs modes d'action :

- Elles peuvent activer des voies de signalisation chez les cellules cibles en se liant à un de leurs récepteurs, à l'aide des protéines présentées à la membrane de ces vésicules extracellulaires.
- Elles peuvent délivrer un antigène à l'aide de complexes majeurs d'histocompatibilité, et ainsi permettre aux cellules présentatrices d'antigène receveuses d'activer des cellules T spécifiques.
- Elles peuvent enfin libérer leur contenu soluble dans le cytosol des cellules receveuses, leur permettant ainsi d'acquérir du contenu biologique provenant d'une autre cellule. Ici, le projet se focalise sur ce mécanisme, qui permet de transférer des molécules fonctionnelles d'une cellule donneuse au cytosol d'une cellule receveuse.

De nombreuses études ont décrit leurs implications dans de multiples processus physiologiques et pathologiques. L'une des plus décrites est l'interaction entre cellule tumorale et cellule immunitaire, où dépendant du contexte les vésicules peuvent avoir une activité pro-tumorale (favorisant l'apparition de métastases) ou anti-tumorale (transférant des antigènes tumoraux aux cellules dendritiques, qui peuvent ensuite déclencher une activation de lymphocytes T spécifiques d'antigènes tumoraux).

Ces propriétés font de ces vésicules des candidates prometteuses pour la fabrication de nouveaux vecteurs thérapeutiques. En effet, leur origine endogène leur confère une composition moins immunogène que les vecteurs utilisés de nos jours (viraux ou liposomes). Mais pour atteindre un tel niveau translationnel, il est important de comprendre les mécanismes biologiques impliqués dans la prise en charge de ces vésicules extracellulaires par les cellules receveuses. Malheureusement, la littérature à ce sujet reste pauvre, surtout en comparaison avec les mécanismes décrits pour l'entrée des virus dans les cellules cibles ou pour les transports des vésicules intracellulaires, qui partagent de nombreux paramètres physico-chimiques. La similarité morphologique entre les vésicules extracellulaires et ces deux types de vésicules (virus et vésicules intracellulaires) nous permet tout de même d'émettre des hypothèses quant aux mécanismes cellulaires et moléculaires impliqués dans la prise en charge des vésicules extracellulaires par les cellules receveuses.

Ainsi, leur entrée pourrait s'effectuer directement au niveau de la membrane plasmique, via sa fusion directe avec la membrane des vésicules. Le point d'entrée serait alors aussi le point de libération du contenu vésiculaire dans le cytosol accepteur. Les vésicules peuvent aussi entrer par différentes voies d'endocytoses, pour libérer leur contenu plus tard dans des compartiments intracellulaires tels que des endosomes. Cette seconde hypothèse est appuyée par plusieurs études montrant l'internalisation de contenu vésiculaire dans des compartiments intracellulaires des cellules receveuses. Cependant aucun consensus n'apparaît quant aux mécanismes impliqués dans cette internalisation.

Dans un second temps, la libération du contenu vésiculaire dans le cytosol de la cellule receveuse nécessite probablement un événement de fusion membranaire entre la membrane de la vésicule extracellulaire et la membrane du compartiment receveur. De tels évènements de fusion se produisent entre certaines cellules pendant le développement, grâce aux protéines myomaker ou syncytines par exemple, ou lors du transport intracellulaire entre différentes vésicules, impliquant principalement le complexe protéique SNARE. Dans ce dernier cas, il est important de garder à l'esprit que la topologie des membranes est inversée. Ainsi la machinerie de fusion ne peut pas être identique, mais des mécanismes similaires peuvent exister.

À partir de ces différents travaux dans les différents domaines du transport extra- et intra-cellulaire, cette thèse s'est concentrée sur la caractérisation cellulaire et moléculaire de la prise en charge des vésicules extracellulaires par les cellules receveuses, et de la libération cytosolique de leur contenu. Afin d'établir cette caractérisation, des approches basées sur le suivi du contenu des vésicules extracellulaires ont été générées *in vitro* et *in cellulo*. Pour cela, des lignées cellulaires ont été produites afin de sécréter des vésicules marquées. Une fois isolées, ces vésicules ont été incubées avec les compartiments receveurs : des membranes plasmiques purifiées (test *in vitro*) ou des cellules en culture (test *in cellulo*).

La première étude menée *in vitro* a montré que des vésicules extracellulaires pouvaient libérer leur contenu vésiculaire lorsqu'elles sont incubées avec des membranes plasmiques purifiées, si et seulement si le pH environnant est inférieur à 6. En effet, dans ces conditions le contenu marqué des vésicules extracellulaires pouvait être digéré par une enzyme ajoutée dans le milieu, ce qui ne serait pas possible si ce contenu restait à l'intérieur d'une vésicule. De plus, ce phénomène nécessite la présence de protéines sur les compartiments donneurs (vésicules) et accepteurs (membranes plasmiques).

Cette dépendance à un pH acide et aux protéines suggère que, dans un contexte cellulaire, la libération du contenu des vésicules extracellulaires pourrait s'effectuer après endocytose, dans des endosomes tardifs après acidification de leur contenu.

La seconde étude *in cellulo* a permis d'aller plus loin sur cette hypothèse. Ici, les vésicules marquées à l'aide de contenus fluorescent ou enzymatique ont été incubées avec des cellules non marquées. La haute sensibilité de l'enzyme NanoLuc luciférase a permis pour la première fois de quantifier au cours du temps la prise en charge des vésicules contenant cette enzyme par les cellules receveuses. Ainsi, une accumulation du contenu vésiculaire associée aux cellules receveuses est observée au cours du temps à 37°C, avec un taux spontané de 1% du contenu vésiculaire associé aux cellules receveuses après 1 heure d'incubation. Cette association n'est pas saturable et est fortement inhibée à 4°C, ce qui suggère l'absence d'un récepteur spécifique aux vésicules extracellulaires, du moins dans notre modèle d'étude que sont les cellules HeLa.

En utilisant les vésicules marquées à l'aide de contenu fluorescent, des colocalisations ont pu être identifiées avec deux types de compartiments intracellulaires : des endosomes précoces et des lysosomes. Ceci confirme qu'au moins une partie des vésicules extracellulaires peut être internalisée par les cellules receveuses et potentiellement atteindre des compartiments lysosomaux. L'étape suivante fut de quantifier le contenu vésiculaire qui peut être libéré dans le cytosol des cellules receveuses, permettant ainsi à ce contenu de pouvoir être fonctionnel (par exemple un ARNm pourrait y être traduit sans avoir été synthétisé dans la cellule receveuse).

Pour cela, une étape de fractionnement cellulaire a été réalisée sur les cellules receveuses après l'incubation avec les vésicules extracellulaires contenant la NanoLuc luciférase. Différents traitements mécaniques suivis de centrifugations différentielles ont permis d'isoler le cytosol des cellules receveuses de leurs membranes. Ceci a permis d'obtenir la première quantification de l'efficacité du transport de molécules par les vésicules extracellulaires : 30% du contenu vésiculaire associé aux cellules receveuses peut être détecté dans leur cytosol.

Cette libération cytosolique du contenu vésiculaire requiert une acidification des endosomes. En effet, si les cellules receveuses sont traitées avec de la Bafilomycine A1 (inhibiteur de l'acidification endosomale), alors le contenu vésiculaire n'est plus détecté dans leur cytosol et s'accumule dans leurs membranes. Cette inhibition de la libération cytosolique du contenu vésiculaire se traduit aussi en microscopie confocale par une

accumulation de ce contenu vésiculaire dans des compartiments intracellulaires des cellules receveuses. Cette libération semble donc s'effectuer au niveau des endosomes tardifs, et pourrait dépendre d'une fusion membranaire entre ces compartiments et les vésicules extracellulaires internalisées.

Pour adresser cette possibilité de fusion membranaire, des protéines IFITM (pour protéines TransMembranaires induites par InterFéron) ont été exprimées dans les cellules receveuses. Les IFITM sont connues pour leur capacité à inhiber l'entrée d'une grande variété de virus. Les études réalisées sur ce sujet suggèrent fortement que cette inhibition s'exerce par un changement de propriétés des membranes présentant les IFITM, qui ne peuvent plus fusionner pour libérer le contenu viral.

Ainsi, lorsque les cellules receveuses expriment ces protéines IFITM, une forte diminution de la libération du contenu vésiculaire dans le cytosol des cellules receveuses est observée. Ici aussi, la diminution de la libération cytosolique s'accompagne d'une accumulation du contenu des vésicules extracellulaires dans la fraction membranaire des cellules receveuses. Les images obtenues par microscopie confocale indiquent que ce contenu pourrait être séquestré dans des compartiments intracellulaires positifs aux IFITM. Ceci suggère qu'une fusion membranaire pourrait être impliquée dans l'étape finale, qui permet aux vésicules extracellulaires de délivrer leur contenu dans le cytosol de la cellule receveuse.

Ces deux études permettent d'obtenir un premier modèle sur la prise en charge des vésicules extracellulaires par les cellules receveuses, et la libération cytosolique de leur contenu :

1. La vésicule extracellulaire est tout d'abord internalisée, probablement par un processus tel que la macropinocytose, puisque nous n'avons pas pu mettre en évidence l'existence de récepteur spécifique aux vésicules extracellulaires sur les cellules receveuses. Les vésicules sont probablement internalisées en phase fluide par la cellule receveuse.
2. L'internalisation des vésicules extracellulaires dans les cellules receveuses se réalise avec une efficacité relativement faible, avec un taux spontané de 1% par heure. Bien que faible, ce taux peut être comparé à la prise en charge d'autres éléments extracellulaires tels que des virus.
3. Les vésicules internalisées peuvent être retrouvées dans les compartiments endocytiques tels que des endolysosomes.

4. Jusqu'à un tiers du contenu des vésicules extracellulaires associé aux cellules receveuses se situe dans le cytosol de ces dernières. La libération de ce contenu est conditionnée par l'acidification des endosomes contenant les vésicules internalisées, ainsi qu'une probable fusion membranaire qui est inhibée par la présence de protéines IFITM.

Cette description ouvre la voie pour une plus profonde caractérisation moléculaire, pour laquelle les expériences développées dans les deux études présentées peuvent être utilisées et adaptées, pour effectuer par exemple un criblage protéique qui permettrait d'identifier les acteurs moléculaires clés de la prise en charge des vésicules extracellulaires par les cellules receveuses.

En plus d'apporter des connaissances fondamentales encore manquantes dans le champ de recherche des vésicules extracellulaires, ces études pourraient à terme mener à l'optimisation de thérapies utilisant les vésicules extracellulaires comme vecteur. A ce sujet, il semble déjà qu'un des grands enjeux sera de pouvoir augmenter l'efficacité de la prise en charge globale des vésicules (de 1% seulement) plutôt que celle de l'étape finale de libération cytosolique du contenu vésiculaire (déjà de 30%). Ces vecteurs thérapeutiques pourraient alors s'avérer plus efficaces et plus sûrs que ceux actuellement utilisés.